To the Graduate Council:

I am submitting herewith a thesis written by Aaron Michael Williams entitled "Lean NOx Trap Catalysis for Lean Burn Natural Gas Engines." I have examined the final electronic copy of this thesis for form and content and recommend that it be accepted in partial fulfillment of the requirements for the degree of Masters of Science, with a major in Mechanical Engineering.

David Irick
Major Professor

We have read this thesis
and recommend its acceptance:

Ke Nguyen

Jeffrey Hodgson

Accepted for the Council:

Anne Mayhew
Vice Chancellor and
Dean of Graduate Studies

(Original signatures are on file with official student records.)

LEAN NOx TRAP CATALYSIS FOR LEAN BURN NATURAL GAS ENGINES

A Thesis

Presented for the

Master of Science

Degree

The University of Tennessee, Knoxville

Aaron Michael Williams

December 2004

This thesis is dedicated to my wife,

Sunny Iris.

Her genuine heart, relentless energy and strength of character

have provided the inspiration for all that I pursue.

ACKNOWLEDGEMENTS

I would like to thank my advisor, Dr. David Irick, for his time and guidance through the past three years. His direction on this project as well as through the FutureTruck program has helped me in the development of my interests as an engineer. I would also like to thank the rest of my graduate committee, Dr. Ke Nguyen and Dr. Jeffrey Hodgson and the rest of the professors for their support. I would like to express my appreciation to Danny Graham, Gary Hatmaker and Dennis Higdon and the staff of the Mechanical and Aerospace Engineering Department for their effort and time. Thanks to the U.S. Department of Energy and the Advanced Reciprocating Engine Systems (ARES) program for their financial support and to Dr. Ming Zheng who obtained the funding for this project.

Finally, I would like to express my debt of gratitude to the staff at the National Transportation Research Center for their continued support and for the use of their facilities. Thanks to Jim Parks, Norberto Domingo, Robert Wagner, Brian West, John Storey, Shean Huff, Jeff Chambers and Eric Nafziger, whose leadership and guidance provided for a great educational experience and whose constant friendship and personal character created a lasting impression.

ABSTRACT

As the nation's demand for energy grows along with concern for the environment, there is a pressing need for cleaner, more efficient forms of energy. The internal combustion engine is well established as one of the most reliable forms of power production. They are commercially available in power ranges from 0.5 kW to 6.5 MW, which make them suitable for a wide range of distributed power applications from small scale residential to large scale industrial. In addition, alternative fuels with domestic abundance, such as natural gas, can play a key role in weaning our nations dependence on foreign oil. Lean burn natural gas engines can achieve high efficiencies and can be conveniently placed anywhere natural gas supplies are available. However, the aftertreatment of NOx emissions presents a challenge in lean exhaust conditions. Unlike carbon monoxide and hydrocarbons, which can be catalytically reduced in lean exhaust, NOx emissions require a net reducing atmosphere for catalytic reduction. Unless this challenge of NOx reduction can be met, emissions regulations may restrict the implementation of highly efficient lean burn natural gas engines for stationary power applications.

While the typical three-way catalyst is ineffective for NOx reduction under lean exhaust conditions, several emerging catalyst technologies have demonstrated potential. The three leading contenders for lean burn engine de-NOx are the Lean NOx Catalyst (LNC), Selective Catalytic Reduction (SCR) and the Lean NOx Trap (LNT). Similar to the principles of SCR, an LNT catalyst has the ability to store NOx under lean engine operation. Then, an intermittent rich condition is created causing the stored NOx to be released and subsequently reduced. However, unlike SCR, which uses urea injection to create the reducing atmosphere, the LNT can use the same fuel supplied to the engine as the reductant. LNT technology has demonstrated high reduction efficiencies in diesel applications where diesel fuel is the reducing agent.

The premise of this research is to explore the application of Lean NOx Trap technology to a lean burn natural gas engine where natural gas is the reducing agent. Natural gas is primarily composed of methane, a highly stable hydrocarbon. The two primary challenges addressed by this research are the performance of the LNT in the temperature ranges experienced from lean natural gas combustion and the utilization of the highly stable methane as the reducing agent.

The project used an 8.3 liter lean burn natural gas engine on a dynamometer to generate the lean exhaust conditions. The catalysts were packaged in a dual path aftertreatment system, and a set of valves were used to control the flow of exhaust to either leg during adsorption and regeneration. The rich conditions for regeneration were created by injecting natural gas directly into the exhaust stream. An oxidation and reforming catalyst were placed upstream of the LNT to enhance the utilization of the methane.

The duration of time for catalyst adsorption (sorption period) and the amount of fuel for regeneration (injection rate) were the two primary variables used in developing the regeneration strategy. The goal of this study was to optimize the regeneration strategy for 5 modes of engine operation (10%, 25%, 50%, 75% and 100% load) at 1800 rpm. In optimizing this strategy, NOx reduction efficiencies greater than 90% were demonstrated for 25% and 50% engine load. Testing at 10%, 75% and 100% load revealed the temperature dependence of both the LNT and oxidation catalyst. Low temperatures at 10% load hindered the oxidation catalyst's ability to break down the methane, while the storage capacity of the LNT falls off at the higher temperatures of 75% and 100% load. This created a narrow temperature window in which the performance could be optimized.

TABLE OF CONTENTS

Chapter **Page**

1. INTRODUCTION……..……... 1
    - Oxides of Nitrogen ……2
    - Carbon Monoxide…… 7
    - Volatile Organic Compounds…….. 9
    - Particulate Matter……12
    - Natural Gas…….. 14
    - Lean Burn NOx Control…….. 15
    - Problem Statement…….. 18
2. EXPERIMENTAL TEST BED…….…… 19
    - Engine…….. 19
    - Emissions Analysis……..23
    - Exhaust Aftertreatment System…….….. 26
    - Controls and Data Acquisition…… 30
3. BASELINE TESTING…….. 38
    - LNT Capacity Estimations…….. 47
4. DEVELOPMENT OF REGENERATION PARAMETERS…… 50
    - Exhaust Flow Control…….. 50
    - Exhaust Composition Control……..54
    - Methane Oxidation…….. 55
5. LEAN NOx TRAP EVALUATION……..58
    - Lean NOx Trap Cycle……. 58
    - Optimizing Regeneration Parameters……..61
    - Adjusting Flow Rates for Regeneration…….. 68
    - NOx Storage Capacities……...71
    - Fixed Temperature Adsorption……73
    - Methane Utilization…….. 75

TABLE OF CONTENTS

Chapter **Page**

6. CONCLUSIONS……... 77

BIBLIOGRAPHY……..……..79

VITA……82

LIST OF TABLES

Table		Page
2.1	C Gas Plus Engine Specs	20
2.2	Emissions Analysis Instruments	23
2.3	Data Acquisition Temperatures	33
2.4	Data Acquisition Pressures	33
2.5	Data Acquisition Emissions	33
2.6	Data Acquisition Other	34
3.1	Baseline Test Matrix	39
3.2	Baseline Power Map	45
3.3	Baseline Throttle Map	45
3.4	Baseline Boost Pressure Map	45
3.5	Baseline Inlet Air Flow Map	45
3.6	Baseline Fuel Flow Map	45
3.7	Baseline Exhaust Flow Map	45
3.8	Baseline BSFC Map	46
3.9	Baseline BMEP Map	46
3.10	Baseline Exhaust Back Pressure Map	46
3.11	Baseline NOx Rating Map	46
3.12	Baseline Air to Fuel Ratio Map	46
3.13	Baseline Turbo Out Temperature Map	46
3.14	Weighting Factors 5 Mode Emissions Ratings	47
3.15	Conditions for Bench Flow Study	48
3.16	Results from Bench Flow Study	48
3.17	LNT Capacity Estimations	49
4.1	Exhaust Flow Rates During Adsorption and Regeneration	53
4.2	Exhaust Composition Control	55
4.3	Methane Oxidation Results	57

LIST OF FIGURES

Figure		Page
1.1	NOx Concentration vs. Equivalence Ratio	5
1.2	CO Concentration vs. Equivalence Ratio	9
1.3	Sources of Unburned Hydrocarbons	11
1.4	VOC Concentration vs. Equivalence Ratio	12
1.5	Lean NOx Trap Adsorption	17
1.6	Lean NOx Trap Regeneration with CO	17
1.7	Lean NOx Trap Regeneration with H_2	17
2.1	C Gas Plus Engine	20
2.2	Electronic Throttle Control	22
2.3	Emissions Analyzer Benches	24
2.4	Emissions Bench Schematic	25
2.5	Exhaust Aftertreatment System Picture	26
2.6	Exhaust Aftertreatment System Schematic	27
2.7	Natural Gas Injectors	28
2.8	Flow Control Valves	29
2.9	Dyne Systems Control Cabinet	31
2.10	National Instruments Control Cabinet	31
2.11	Dyne Systems Boom Box	32
2.12	Dyne Systems Companion Box	32
2.13	Cell Assistant Front VIP	34
2.14	Cell Assistant Analyzer Range Control VIP	35
2.15	Cell Assistant Safety Interlock VIP	36
2.16	LabView Front VIP	37
3.1	Engine Out CO Map	41
3.2	Engine Out NOx Map	42
3.3	Engine Out NO Map	42
3.4	Engine Out THC Map	43

LIST OF FIGURES

Figure		Page
3.5	Engine Out CH_4 Map	43
3.6	Engine Out CO_2 Map	44
3.7	Engine Out O_2 Map	44
4.1	Experimental Schematic for Slip Flow Estimations	52
4.2	Control Volume for Slip Flow Analysis	52
4.3	Exhaust Flow Rates During Adsorption and Regeneration	54
4.4	Sample Positions for Methane Oxidation Study	56
4.5	Methane Oxidation vs. Catalyst Temperature	57
5.1	Typical NOx Profiles	59
5.2	Fuel Flow and Exhaust Stoichiometry	59
5.3	Catalyst Temperatures	60
5.4	50% Load NOx Trapping Efficiencies	63
5.5	50% Load NOx Ratings and Fuel Penalties	63
5.6	50% Load NOx Profiles for Optimal Regen	64
5.7	25% Load NOx Trapping Efficiencies	65
5.8	25% Load NOx Ratings and Fuel Penalties	65
5.9	25% Load NOx Profiles for Optimal Regen	66
5.10	10% Load NOx Trapping Efficiencies	67
5.11	10% Load NOx Ratings and Fuel Penalties	67
5.12	10% Load NOx Profiles for Optimal Regen	68
5.13	10% Load NOx Trapping Efficiencies with Full Slip Flow	69
5.14	10% Load NOx Ratings with Full Slip Flow	70
5.15	10% Load Fuel Penalties with Full Slip Flow	71
5.16	LNT Storage Capacities vs. Temperature	72
5.17	NOx Ratings with Fixed Temperature Adsorption	74
5.18	50% Load CO Production and Consumption	76
5.19	25% Load CO Production and Consumption	76

CHAPTER 1 – INTRODUCTION

The internal combustion engine is a well-developed and reliable technology. Their relatively low cost, size and widespread availability make them a leading contender for stationary power generation. They are commercially available in power ranges from 0.5 kW to 6.5 MW, which make them suitable for a wide range of distributed power applications from small scale residential to large scale industrial. However, as the demand for energy grows along with worldwide concern for the environment, there is an ever-rising need for cleaner burning, more efficient energy production. Under the Department of Energy (DOE), the Advanced Reciprocating Engine Systems (ARES) program is leading a nationwide effort to advance the technology of the internal combustion engine for distributed energy applications. Through the development of natural gas fired engines and exhaust aftertreatment systems, the ARES program is targeting NOx emissions levels of 0.1 g/hp-hr and a fuel-to-electricity conversion efficiency of 50%.

To meet the targeted 50% efficiency it is most likely that a lean burn engine will be necessary. However, lean burn exhaust is rich in oxygen, which presents problems for the aftertreatment of NOx. Unlike hydrocarbons and carbon monoxide, which are removed through oxidation, oxides of nitrogen must be reduced in a fuel-rich environment. The three leading aftertreatment technologies for lean burn engine de-NOx are the Lean NOx Catalyst (LNC), Selective Catalytic Reduction (SCR) and the Lean NOx Trap (LNT).

In addition to exhaust aftertreatment systems, alternative fuels such as natural gas can play a role in reducing emissions. Natural gas, which is predominantly methane, offers several distinct environmental advantages compared with standard gasoline and diesel fuels. Methane is a very stable hydrocarbon, meaning that it is less likely to take part in photochemical reactions that lead to the production of photochemical smog. Furthermore, the low C/H ratio of

methane results in lower carbon dioxide emissions for a given engine efficiency [1].

This study will demonstrate the effectiveness of lean NOx trap technology when applied to a lean burn natural gas engine. The primary goal of the study was to manage the catalyst for maximum NOx reduction while minimizing the associated fuel penalty. Optimization of this catalyst management was focused on steady state conditions for 5 modes of engine operation (10%, 25%, 50%, 75% and 100% load) at 1800 rpm. Additional tests were conducted to investigate the storage capacity of the lean NOx traps and the methane oxidation efficiency of the oxidation catalyst under various engine conditions. The conditions for regeneration were created by injecting natural gas directly into the exhaust stream. An oxidation catalyst and reforming catalyst were used to convert the highly stable methane to a more useful source for regeneration. The catalysts were packaged in a dual path exhaust aftertreatment system and a set of valves were used to control the exhaust flow to either leg during catalyst adsorption and regeneration. The duration of time for catalyst adsorption (adsorption period) and the amount of fuel used for regeneration (injection rate) were the primary variables used to optimize the regeneration strategy.

OXIDES OF NITROGEN

Oxides of Nitrogen (NOx), primarily due to high combustion temperatures, are key contributors to global warming, photochemical smog and acid rain. There are seven different oxides of nitrogen, which form when a mixture containing oxygen and nitrogen (such as air) is heated to temperatures in excess of 1100° C [2]. These high combustion temperatures cause diatomic oxygen (O_2) and nitrogen (N_2) to disassociate and bond to form nitric oxide (NO). Over 90% of the NOx formed during combustion is NO, but as the exhaust gasses cool, NO is oxidized forming nitrogen dioxide (NO_2) [3]. Of the seven different oxides of nitrogen, NO and NO_2 are considered the major pollutants as they are a precursor to the

formation of photochemical smog. Nitrous oxide (N_2O) is also a concern because it is a greenhouse gas.

In the combustion of a fuel with no carbon bound nitrogen, there are three chemical mechanisms that lead to the formation of nitric oxide: the Fenimore or prompt mechanism, the N_2O intermediate mechanism and the thermal or Zeldovich mechanism. The Fenimore mechanism is important under rich combustion conditions while the N_2O intermediate mechanism plays an important role under lean, low temperature combustion. For high temperature combustion, the Zeldovich mechanism dominates in the production of NO over a wide range of equivalence ratios [4]. This third method is the most widely accepted form of NO formation. The Zeldovich mechanism shows that the formation of NO is governed by the pair of chain reactions:

$$O + N_2 \Leftrightarrow NO + N \quad (1)$$

$$N + O_2 \Leftrightarrow NO + O \quad (2)$$

Russian scientist Y. B. Zeldovich first proposed this reaction set in 1946. In 1970 Lavoie contributed a third equation [3]:

$$N + OH \Leftrightarrow NO + H \quad (3)$$

This set of reactions is referred to as the extended Zeldovich mechanism. The forward and reverse rate coefficients for these reactions are [4]:

$$k_{1f} = 1.8 \cdot 10^{11} \exp[-38{,}370/T]$$

$$k_{1r} = 3.8 \cdot 10^{10} \exp[-425/T]$$

$$k_{2f} = 1.8 \cdot 10^{7} \exp[-4680/T]$$

$$k_{2r} = 3.8 \cdot 10^{6} \exp[-20{,}820/T]$$

$$k_{3f} = 7.1 \cdot 10^{10} \exp[-450/T]$$

$$k_{3r} = 1.7 \cdot 10^{11} \exp[-24{,}560/T]$$

The concentration of O, O_2 and OH necessary for the Zeldovich mechanism directly couple this three-reaction set to the chemical mechanisms of the combustion process. However, if one assumes that fuel combustion is complete before NO formation begins, then the two processes can become uncoupled. This allows for the assumption that O, O_2, OH and N_2 concentrations are at equilibrium. If NO concentrations are assumed to be well below their equilibrium state, the reverse reactions can be neglected. These two assumptions yield the rather simple rate equation for the Zeldovich mechanism [4]:

$$d[NO]/dt = 2k_{1f}\,[O]_{eq}\,[N_2]_{eq}$$

As can be seen from the forward rate coefficient (k_{1f}), the formation of NO is highly dependent on temperature. However, as can be seen in Figure 1.1, the peak NOx formation does not occur for slightly rich mixtures where combustion temperatures are the highest. This is because in rich combustion the hydrogen and carbon atoms compete more favorably for the oxygen. Peak NOx formation occurs slightly lean of stoichiometric where there is excess oxygen and high enough flame temperatures. Time is also a factor in the formation of NOx. In diesel engines where flame speeds as well as engine speeds are typically slower, there is more time for NOx to form [3].

Nitrogen oxide emissions are a concern because they serve as a precursor to the formation of photochemical oxidants such as ozone. Oxides of nitrogen are responsible for the formation as well as the destruction of ozone as can be seen by the three-reaction set:

$$NO_2 + (\text{UV Sunlight}) \rightarrow NO + O \qquad (1)$$

$$O + O_2 \rightarrow O_3 \qquad (2)$$

$$NO + O_3 \rightarrow NO_2 + O_2 \qquad (3)$$

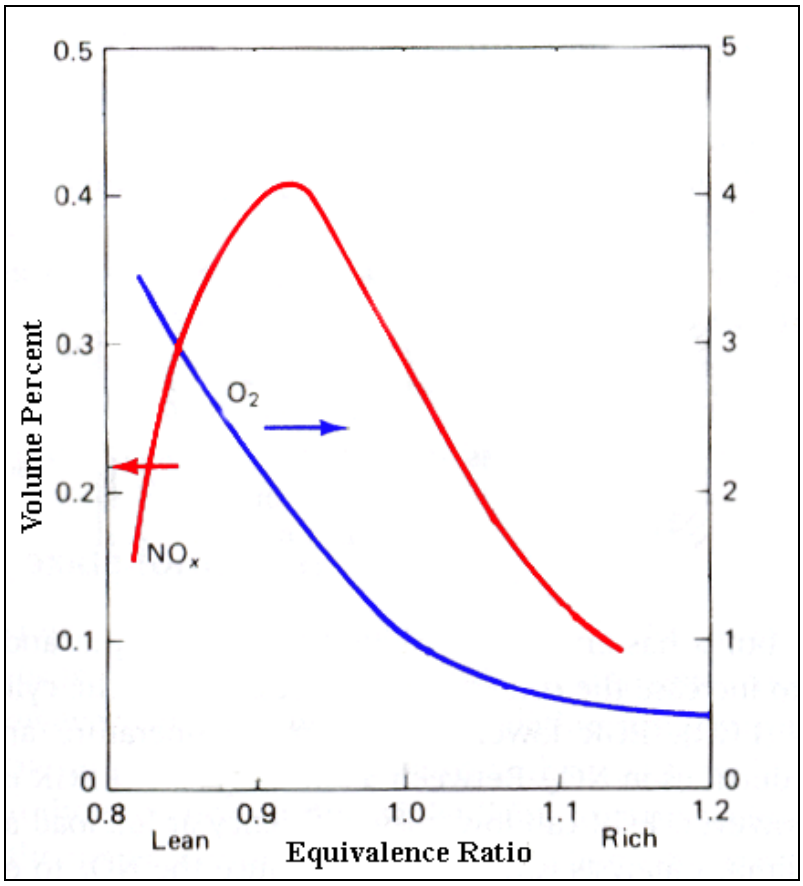


Figure 1.1 – NOx Concentration vs. Equivalence Ratio

The atomic structure of NO_2 allows it to absorb energy from ultraviolet sunlight. The extra energy causes the molecule to release an energized oxygen atom as shown in Equation 1. The highly reactive oxygen atom will subsequently react with an oxygen molecule to form ozone. The third equation shows how the presence of NO will naturally balance the ozone levels in the atmosphere by reacting to form NO_2 and O_2 [5]. In an atmosphere consisting of no volatile organic compounds (VOC's), the conversion of NO_2 and oxygen into ozone and NO is balanced by the subsequent conversion of NO and ozone back into NO_2 and oxygen. However, the presence of volatile organic compounds in the form of unburned hydrocarbons disrupts this balance. The hydrocarbons convert NO back to NO_2, eliminating the conversion of ozone back to oxygen, thus causing an accumulation of ground level ozone [6].

In addition to being a precursor to photochemical smog, nitrogen dioxide also contributes to the formation of acid rain. Nitrogen dioxide and sulfur dioxide react with atmospheric water to form the two major components of acid rain, nitric acid (HNO_3) and sulfuric acid (H_2SO_4). The nitric and sulfuric acid then return to the earth through precipitation of rain, snow or fog. Rain is naturally slightly acidic, but as acidity increases, it can cause damage to crops, wildlife, buildings and is indirectly harmful to humans. There is a direct relationship between the pH levels in lakes and the population of fish. At a pH level of 6.0, fish populations can naturally flourish. As the pH levels fall, the acid inhibits the production of an enzyme that allows trout larvae to escape their eggs. The acid also mobilizes toxic metals such as aluminum. The aluminum causes a buildup of mucus around the gills of certain fish preventing proper ventilation. At pH levels below 4.5, virtually no fish can survive. Acid rain also breaks down the waxy surface of leaves on trees, making them more susceptible to weather conditions, insects and parasites [7].

There are several strategies for controlling NOx in both the combustion process or with an exhaust aftertreatment system. In the combustion process the two most common control methods are to retard ignition timing or through the use of exhaust gas recirculation (EGR). Retarding the ignition will lower the peak temperature and pressure in the combustion chamber. Because NOx formation is highly temperature dependent this will consequently lower NOx emissions. However, retarding the ignition timing will have an adverse effect on power output and fuel economy [3]. Exhaust gas recirculation is an effective way to reduce NOx emissions at part load. As with ignition retard, increasing exhaust gas residuals in the combustion chamber also lowers peak temperatures [3].

The application of an exhaust aftertreatment system for NOx reduction depends on the stoichiometry of engine operation. For engines that run under stoichiometric air-fuel conditions, a typical three-way catalyst will reduce NOx

emissions. However, lean burn engines present challenges in the aftertreatment of NOx emissions. Unlike hydrocarbons and carbon monoxide, which are removed through oxidation, oxides of nitrogen must be reduced in a fuel-rich environment. The three leading aftertreatment technologies for lean burn engine de-NOx are the Lean NOx Catalyst (LNC), Selective Catalytic Reduction (SCR) and the Lean NOx Trap (LNT).

CARBON MONOXIDE

Carbon monoxide (CO), primarily due to incomplete combustion, is an odorless colorless gas that renders the blood incapable of transporting oxygen. This deprivation of oxygen can lead to headaches, dizziness, nausea and even death at high enough concentrations.

The combustion of a hydrocarbon fuel can be simplified into a two step process: the breakdown of the hydrocarbon, forming carbon monoxide, followed by the oxidation of carbon monoxide, forming carbon dioxide. The following four-reaction set describes carbon monoxide oxidation [4].

$$CO + O_2 = CO_2 + O \quad (1)$$

$$O + H_2O = OH + OH \quad (2)$$

$$CO + OH = CO_2 + H \quad (3)$$

$$H + O_2 = OH + O \quad (4)$$

The oxidation of carbon monoxide with oxygen (step 1) is much slower than the oxidation with the hydroxyl radical (step 3), however it serves as the initiator of the four-reaction set [4]. When this four-reaction set does not fully propagate, it results in high emissions of carbon monoxide. In other words, the exhaust of carbon monoxide emissions from an internal combustion engine is primarily due to the incomplete combustion of the fuel.

Carbon monoxide levels are a strong function of air-to-fuel ratio, where they are highest for rich combustion. Under normal operating conditions, rich mixtures are generally avoided. However, under cold start conditions or during wide open throttle operation, a rich mixture may be used to prevent stalling and maximize power output. Rich mixtures can also result from poor fuel metering or cylinder-to-cylinder mixture variations. As can be seen in Figure 1.2, carbon monoxide is still present in stoichiometric and lean combustion. This is mainly due to the dissociation of carbon dioxide [4]. High concentrations of carbon monoxide are also a consequence of the very rapid expansion and exhaust of the combustion products. As temperatures rapidly decrease, the reaction that oxidizes CO with OH (step 3) reaches equilibrium and CO levels are "frozen" in the exhaust stream. Other factors leading to incomplete combustion include flame quench layers by the cold cylinder walls, crevice volumes and valve leaks.

Carbon monoxide poisoning is the primary health concern associated with CO emissions. The hemoglobin in the blood plays a crucial role in the interaction between the respiratory and circulatory system. Oxygen is moved between the lungs and the cells by bonding to the hemoglobin molecules. Likewise, the waste product of biochemical oxidation, carbon dioxide, is transported out of the body by binding with the hemoglobin molecules. The bond between the hemoglobin and oxygen is sufficiently strong for transportation in the circulatory system. However, when inhaled, carbon monoxide bonds to the hemoglobin in the blood forming a much stronger bond than is formed with oxygen. As blood-CO levels increase the number of hemoglobin molecules necessary to maintain the transport of oxygen becomes reduced [8]. This eventually starves the body of oxygen, leading to headaches, dizziness, nausea and even death. People with circulatory or respiratory problems, fetuses, young infants and pregnant women are most susceptible to the dangers of carbon monoxide poisoning [2].

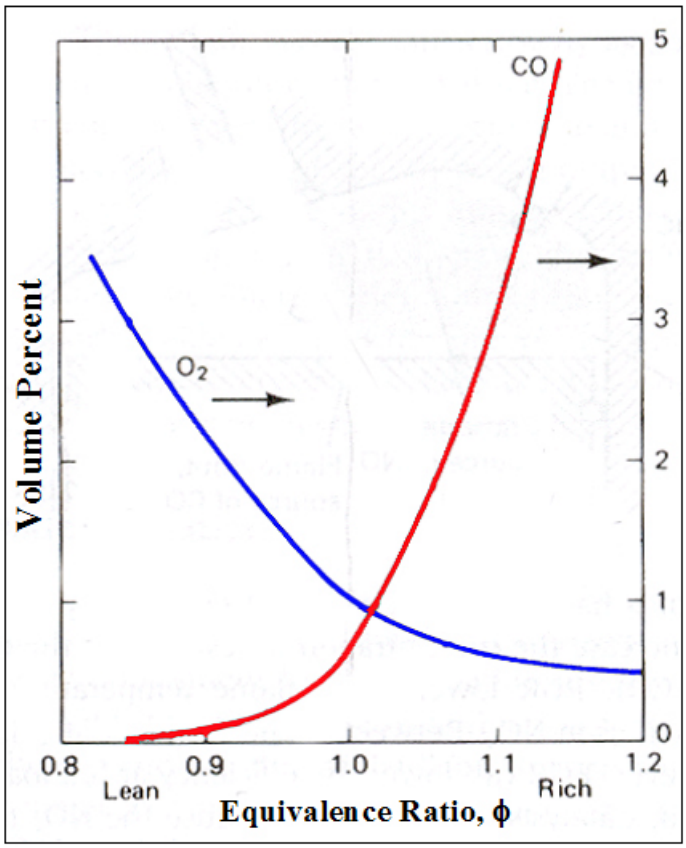


Figure 1.2 – CO Concentration vs. Equivalence Ratio

The formation of carbon monoxide emissions is primarily a function of the combustion air-to-fuel ratio. Thus, the primary way to prevent engine-out carbon monoxide emissions is to avoid fuel rich combustion. Reduction of CO through exhaust aftertreatment is achieved with an oxidizing or three-way catalyst. The three-way catalyst is effective in reducing carbon monoxide for stoichiometric and lean operation, but conversion efficiency falls off under rich operation.

VOLATILE ORGANIC COMPOUNDS

Volatile organic compounds (VOC) are the unburned hydrocarbons that result from evaporative emissions and incomplete combustion. A volatile organic compound is one that will evaporate under atmospheric conditions and is unstable enough to participate in photochemical reactions [2]. Because of its relative

stability in the atmosphere, methane is not considered a volatile organic compound. For this reason methane and non-methane hydrocarbons are distinguished in emissions testing [9].

There are six primary methods by which unburned hydrocarbons escape the combustion process. The first of these is flame quenching, whereby the cool walls of the combustion chamber extinguish the flame resulting in a thin layer of unburned fuel. Another source of unburned fuel is from crevice volumes in the combustion chamber. As the pressure in the combustion chamber builds, portions of the fuel-air mixture are forced into crevices that cannot be penetrated by the flame. The crevice mechanism is primarily a problem in the volume above the piston ring between the piston and the cylinder wall. The escape of hydrocarbons, as a consequence of quench layers and crevice volumes, is illustrated in Figure 1.3. A third source of unburned fuel is the absorption of the fuel into the oils and deposits formed on the combustion chamber walls during the intake and compression process. This is followed by desorption during the expansion and exhaust process. The final three methods by which unburned fuel escapes the combustion process are incomplete combustion due to poor mixing, leaking valves, and unevaporated fuel [2, 9].

Another source of hydrocarbon emissions includes the loss of fuel vapors from the fuel storage system into the atmosphere. There are four methods by which these vapors can escape: Refueling losses – when the fuel is introduced to the vehicle, Diurnal losses – when the fuel tank is heated and cooled as a result of fluctuations in the ambient temperature, Running losses – when the fuel tank is heated due to vehicle operation, Hot soak losses – when the vehicle is parked after operation.

The primary environmental and health concern for the emissions of VOCs is the formation of photochemical oxidants such as ozone (O3), peroxyacetyl nitrate and

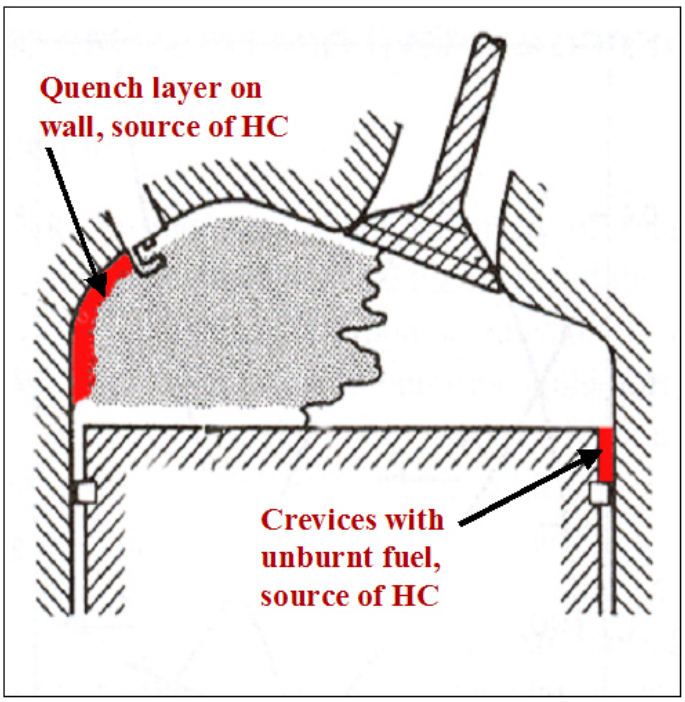


Figure 1.3 – Sources of Unburned Hydrocarbons

peroxybenzoyl nitrate [2]. These oxidants are a result of a complex chemical reaction caused when the unburned hydrocarbons and nitrous oxides emitted from vehicles and industrial processes are baked by the ultraviolet radiation from the sun. In high enough concentrations, they can irritate the lining of the nose, airways and lungs as well as inflame the eyes, cause chest constrictions and induce severe coughing. Photochemical oxidants are sometimes referred to as photochemical smog because they are responsible for the brownish-gray haze that commonly blankets densely populated urban areas. Because O_3 is the primary constituent of photochemical oxidants, ozone levels are used to estimate the level of photochemical smog.

The level of evaporative losses from a vehicle's storage tank is associated with the volatility of the fuel. Thus, control over evaporative emissions begins with controlling the volatility of the fuel. Fuels with lower vapor pressures (diesel fuels) and fuels already in a gaseous state (compressed natural gas) do not

produce significant levels of evaporative emissions. In addition, control devices can be implemented to help control fuel vapor losses [2].

As can be seen in Figure 1.4, the engine-out VOC emissions are dependent on air-fuel ratio. Maintaining an air-fuel ratio close to stoichiometric is a primary method for VOC control. An oxidizing or three-way catalyst can oxidize engine-out hydrocarbons to carbon dioxide and water under stoichiometric and lean operation. Engine designs that minimize crevice volumes and lower compression ratios can also help to reduce these emissions. The lower compression ratios reduce peak pressures, thus reducing the amount of fuel-air mixture that is forced into the crevice volumes.

PARTICULATE MATTER

Particulate matter is defined as any particle that cannot be collected by filtering exhaust at 325 K [3]. These dispersed airborne solid and liquid particles range in size from .0002 to 500 μm [2]. Those less than 2.5 μm ($PM_{2.5}$) in size are referred

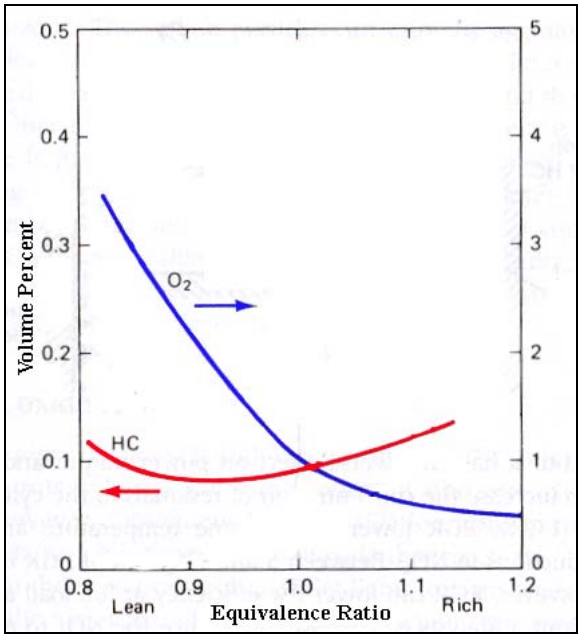


Figure 1.4 – VOC Concentration vs. Equivalence Ratio

to as fine particulates and pose the biggest threat to human health. Those larger than 2.5 μm are referred to as coarse particulates. While coarse particulates are of less concern, the EPA is maintaining an air quality standard on particulates less than 10 μm (PM_{10}). Particulates include condensed unburned hydrocarbons, soot from incomplete combustion, lubricating oil that migrates past the piston rings and oxidized sulfur from the fuel.

The formation of soot (black carbon particles) begins in the combustion chamber where large hydrocarbon molecules on the rich side of the reaction zone are split. Once the carbon particles reach the lean regions, they can become oxidized. Soot levels depend on the difference between the formation and oxidation of these carbon particles [3]. One way to reduce soot levels is to use higher injection pressures. This creates a finer fuel spray and minimizes the duration of diffusion combustion [3]. The combustion process also leads to the formation of sulfates from the oxidation of the sulfur found in fuels. The sulfur in the fuel is oxidized forming sulfur dioxide (SO_2) and smaller amounts of sulfur trioxide (SO_3), which is capable of combining with water vapor, yielding sulfuric acid (H_2SO_4) [10, 11].

Fine particulate matter ($PM_{2.5}$) pose a significant risk to human health as it is small enough to pass through the natural defenses of the respiratory system. These particulates then deposit themselves on the alveoli regions of the lungs. Once deposited the particulates can interfere with the normal respiratory function by blocking the gas exchange surface area of the alveoli. Furthermore, alveoli cells may die due to particulates which are intrinsically toxic or act as carriers for toxic substances. Particulates, which may contain mutagenic or possibly carcinogenic substances may be transported from the lungs to other vital organs via the bloodstream [12].

The most common form of aftertreatment for PM is the particulate trap. A particulate trap is a filter which removes the PM from the exhaust. The trapped

particles are then cleaned off through oxidation. The oxidation of soot typically requires temperatures of about 550-600° C. This is well out of the range of exhaust temperatures from diesel engines, thus the trap may be coated with a catalytic material capable of reducing ignition temperatures by as much as 200° C. Other solutions to this are the development of the electrically heated regenerative trap or additives to the fuel, which may be used to lower the oxidation temperatures [3, 13].

NATURAL GAS

Natural gas (85-95% methane) is a raw fuel extracted directly from the earth. In a gaseous state, it is typically found trapped between liquid petroleum and the capping rock in the earth's crust. Because of its domestic abundance, competitive price and exceptionally low levels of combustion pollution, natural gas is a prime alternative to other fossil fuels. There are several distinct mechanical and environmental advantages to the use of natural gas as an automotive fuel. Unlike liquid fuels, natural gas does not need to vaporize before ignition. This eliminates the need for cold start enrichment, a major source of VOC and CO emissions. Natural gas also has a wide flammability range (5-15%) allowing for more efficient lean burn operation. In addition, the high octane rating (>120) can be taken advantage of by increasing the compression ratio. The unburned hydrocarbon emissions from a natural gas engine are primarily methane. Because methane is a relatively stable organic gas when released into the environment, it does not take place in photochemical reactions and is not considered a volatile organic compound. Thus, the VOC emissions from a natural gas engine are significantly lower. The green house gas levels (carbon dioxide) will typically be lower than those of gasoline engines because methane has a lower carbon content per unit energy than gasoline. This carbon content can be seen in the carbon-to-hydrogen ratio of natural gas (C/H ~ .25) and gasoline (C/H ~ .45) [14, 15, 16]. Because of the unique advantages of natural gas its use is becoming more common in fleet vehicles and stationary power generators.

LEAN BURN NOx CONTROL

The aftertreatment of nitrogen oxide emissions from a lean burn engine presents a unique challenge. Unlike hydrocarbons and carbon monoxide which are reduced in an oxidizing environment, NOx are typically reduced in a fuel-rich environment. The three emerging technologies for the aftertreatment of lean burn NOx emissions are, selective catalytic reduction (SCR), the lean NOx catalyst (LNC) and the lean NOx trap (LNT).

The most mature of the three lean de-NOx technologies is Selective Catalytic Reduction. SCR is used worldwide for gas oil and coal fired power plants and has potential for on road applications as well. However, SCR requires secondary chemical storage and delivery systems which makes it more suited for stationary applications than for transportation engines. This technique uses a reducing agent ammonia, which is injected directly into the exhaust stream. The ammonia reacts with the nitrous oxides to form nitrogen and water vapor in accordance with the following chemical reactions:

$$4NO + 4NH_3 + O_2 \rightarrow 4N_2 + 6H_2O$$

$$2NO_2 + 4NH_3 + O_2 \rightarrow 3N_2 + 6H_2O$$

The ammonia that passes through the catalyst without reacting is referred to as ammonia slip. Controlling the ammonia slip requires tightly proportioning the ammonia dosing to the in-cylinder NOx generation. In addition to the formation of innocuous nitrogen and water, the catalytic reaction can also produce the undesirable byproducts ammonium sulfate $(NH_4)SO_4$ and ammonium bisulfate (NH_4HSO_4) [3, 17, 18].

$$SO_2 + 1/2O_2 \rightarrow SO_3$$

$$2NH_3 + SO_3 + H_2O \rightarrow (NH_4)SO_4$$

$$NH_3 + SO_3 + H_2O \rightarrow NH_4HSO_4$$

These corrosive byproducts, which can plug the catalyst, are a function of exhaust temperature and the sulfur content of the fuel. SCR systems are typically the most effective when operated in a temperature window between 350–400° C. At temperatures above 450° C a reverse reaction can occur in which ammonia is converted back into NOx and below 200° C high levels of ammonium sulfate are formed. Conversion efficiencies as high as 80% with less than 20 ppm ammonia slip have been demonstrated with SCR [18].

Lean NOx Catalysts, which can be managed actively or passively, are able to continuously reduce NOx emissions. Active de-NOx is able to continuously reduce NOx emissions by the use of a supplemental hydrocarbon reducing agent. The reducing agent is typically injected directly into the exhaust stream, creating the necessary fuel-rich environment. The reducing agent can also be added through late in-cylinder injection. The drawback to active de-NOx is the fuel penalty associated with the reducing agent. A passive lean NOx catalyst uses the hydrocarbons present in the lean-burn exhaust to chemically reduce the nitrous oxides. However, there is a narrow temperature window within which the competition for hydrocarbons between oxygen and NOx will favor the NOx reduction mechanism. For platinum catalysts, this temperature window is limited to very low temperatures, 160-220° C [3]. In a copper-exchange zeolite catalyst, up to 60% NOx conversion has been demonstrated for temperatures as high as 400° C [19].

The Lean NOx Trap is a catalyst, which temporarily stores the nitrogen oxides during lean burn operation. Before the LNT becomes saturated, a fuel-rich environment is created allowing the stored NOx to be released and reduced. This type of catalyst employs a precious metal group material (typically platinum) for oxidation and an alkali/alkaline earth material (typically barium oxide) for storing the NOx [3, 17, 20]. As can be seen in Figure 1.5, in the sorption stage, the nitric oxide is oxidized and stored as barium nitrate ($Ba(NO_3)_2$). Before all of the

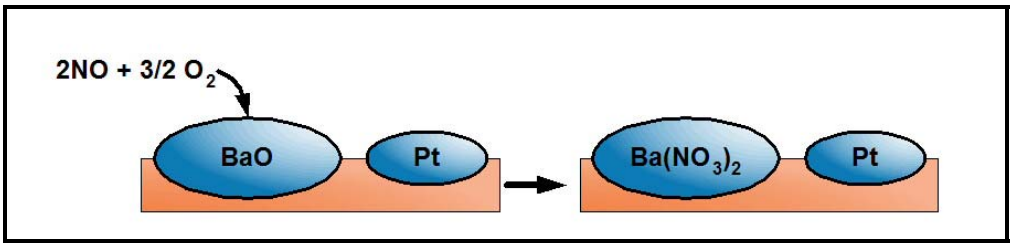


Figure 1.5 – Lean NOx Trap Adsorption

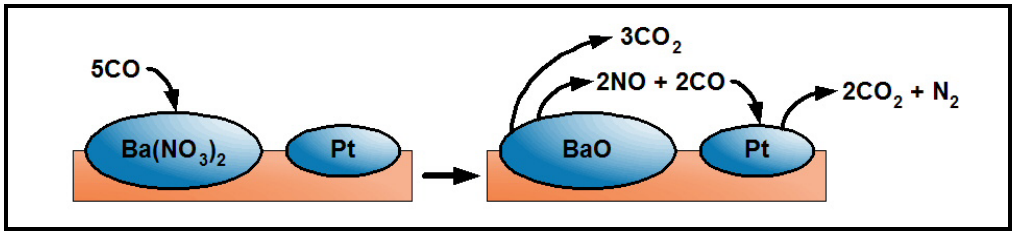


Figure 1.6 – Lean NOx Trap Regeneration with CO

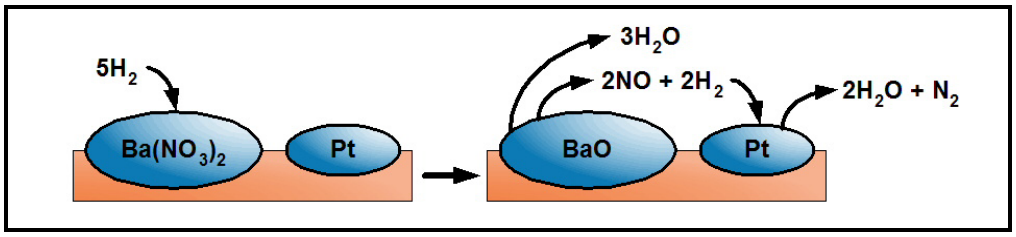


Figure 1.7 – Lean NOx Trap Regeneration with H_2

barium oxide (BaO) sites are utilized, a fuel-rich transient is achieved by running the engine rich or by injecting a reducing agent directly into the exhaust stream. The carbon monoxide and hydrocarbons then prompt the release of the NOx from the storage sites, which are consequently oxidized by the platinum sites as shown in Figures 1.6 and 1.7. This fuel rich transient is called the regeneration stage. Lean NOx Traps have shown high conversion efficiencies but require complex control. The timing and dosing of the reducing agent must be closely controlled in order to avoid a high fuel penalty.

PROBLEM STATEMENT

This study served to investigate the effectiveness of lean NOx trap technology applied to a lean burn natural gas engine. The objective was to demonstrate the NOx conversion efficiency and associated fuel penalty through the use of an open loop regeneration schedule and a methane reducing agent. A reforming catalyst was used upstream of the LNT to convert methane to H_2 and CO. The key technical issues addressed by the research are as follows:

1. Will open loop control of LNT regeneration be sufficient to reach the 0.1 g/hp-hr NOx target?
2. What fuel penalties can be expected from regenerating the LNT?
3. Will the reforming catalyst successfully convert enough methane for LNT regeneration?
4. How will exhaust temperatures affect the storage capacity of the LNT catalysts?

CHAPTER 2 - EXPERIMENTAL TEST BED

The first step of the research was to develop the experimental test bed for the aftertreatment of lean-burn natural gas exhaust. The test bed was designed to facilitate research for the ARES projects at the University of Tennessee and Oak Ridge National Lab. Furthermore, the exhaust aftertreatment system for the national lab was implemented and served as the subject of this research. Development of the test bed included the following four steps, each of which is detailed in this chapter; installation of the natural gas engine onto the dynamometer, development of the emissions sampling system, implementation of the exhaust aftertreatment system and setup of the data acquisition and controls.

ENGINE

The engine selected for the research, shown in Figure 2.1, was the 8.3-liter C Gas Plus (Model CG-280). It is a lean-burn, spark-ignited, natural gas engine developed by Cummins-Westport. The engine produces a peak 280 hp at 2400 rpm and a peak torque of 850 ft-lbs at 1400 rpm. With several upgrades over the C8.3G it represents the latest in lean burn natural gas engine technology including a third generation electronic control module with increased memory and speed. The engine management system offers advanced diagnostics and engine protection. Newly incorporated diagnostic features include engine back pressure, fuel supply pressure, intake manifold temperature and engine knock sensing and control. The C Gas Plus also features a coil-on-plug ignition system with multiple spark discharge for improved operation and maintenance [21, 22]. Table 2.1 lists general engine specifications as well as performance data for the rated torque and power points.

A study conducted by West Virginia University has shown that the C Gas Plus engine, equipped with an oxidation catalyst, achieves a NOx rating of 1.52 g/hp-hr over a transient test cycle and 1.35 g/hp-hr for the Supplemental Emissions



Figure 2.1 – C Gas Plus Engine

Table 2.1 – C Gas Plus Engine Specs

C Gas Plus General Engine Data		
Name	C Gas Plus	
Model	CG-280	
Type	4 Cycle; In-Line 6 Cylinder	
Bore x Stroke (mm)	114 x 135	
Displacement (L)	8.3	
General Performance Data	**Peak Power**	**Peak Torque**
Engine Speed (rpm)	2400	1400
Engine Power (kW)	209	169
Engine Torque (N-m)	831	1153
Inlet Air Flow (L/sec)	293	205
Exhaust Gas Flow (L/sec)	817	539
Exhaust Gas Temperature (C)	643	587
Nominal Fuel Consumption (kg/hr)	47	34
Inlet Air Restriction (mm H2O)	445	
Exhaust Restriction (mm Hg)	102	

Tests (SET). The objective of the study was to compare in-use exhaust emissions, fuel consumption and cost of four tractor-trailers (two natural gas and two diesel) from Viking Freight. A test cycle which simulated the Viking Freight in-service driving cycle was developed for transient testing. The C Gas Plus engine not only demonstrated significant reductions in carbon monoxide, oxides of nitrogen and particulate matter, it also met the California Air Resources Board (CARB) low-NOx emissions standards (2.0 g/hp-hr) for automotive and urban busses [22].

This engine which is typically used in heavy duty transportation applications was used here to simulate exhaust gasses from a large scale genset, consistent with the goals of the ARES program. The engine was coupled to a 500 hp DC motoring dynamometer. The dynamometer was controlled with DyneSystem's Dyne-Loc IV. Dyne-Loc IV is a digital dynamometer control system that allows for both speed and torque control modes.

The advanced electronic management system maintains full control over the air/fuel handling and allows for engine operation over a wide range of natural gas compositions. Methane numbers as low 65 are acceptable compared to 80 for the C8.3G. The engine is capable of operating on compressed or liquefied natural gas. For this research, a set of Copeland scroll compressors (Model SZM22C1A-ABS-XXX) supplied compressed natural gas (CNG) to the engine at 115 psia. The mass fuel flow to the engine was metered with a Micro Motion Coriolis mass flow meter (Model CMF025M009NU).

The C Gas Plus engine features an electronically controlled throttle. The engine control module reads an input signal from the accelerator pedal, interprets driver intent and sends an output signal to the throttle actuator. For the purpose of the experimental test bed, a linear 10 kΩ potentiometer was used to simulate the accelerator pedal. The position of the potentiometer was controlled from within the control room with DyneSystem's DTC-1. The DTC-1 is a digital throttle

control system which allows the user to enter precise throttle set points through a digital keypad from within the control room. As part of the DTC-1 system a gear head DC motor, located in the test cell, is used to adjust the potentiometer (accelerator pedal) position, as shown in Figure 2.2.

The intake air to the engine is preconditioned for control of temperature and humidity. The air is controlled to a dry bulb temperature of 75° F with 55.9% relative humidity and a dew point of 58.2° F. A Meriam Instruments laminar flow element (Model 50MC2-6F) is used to measure the inlet air flow rate, and a manual throttle, placed just before the turbocharger, is used to set the specified inlet restriction. The C Gas Plus has a waste gated turbocharger and creates a maximum 24 psig boost pressure at 1400 rpm. An intercooler was used to control the boosted air temperature entering the engine. The boost air temperature was set to 37° C at the peak load point (WOT at 1400 rpm) by controlling the flow of coolant through the intercooler with a ball valve.

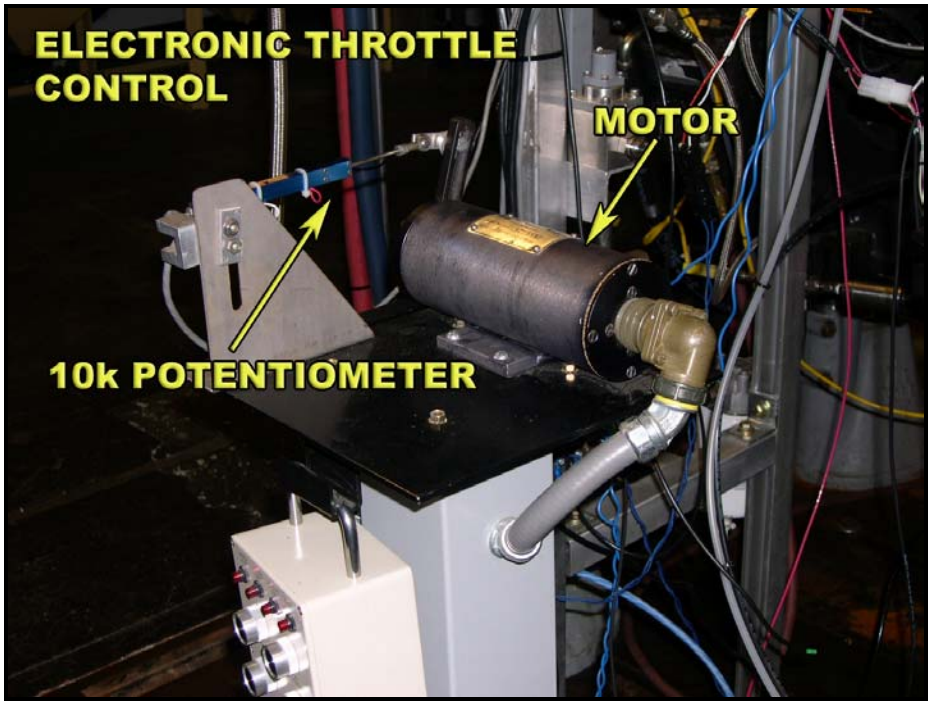


Figure 2.2 – Electronic Throttle Control

EMISSIONS ANALYSIS

The emissions analysis system consists of two separate analyzer benches, each capable of continuous exhaust gas sampling. Shown in Figure 2.3, one bench is for measuring emissions directly out of the engine and the other is for sampling emissions downstream of the catalyst. The engine out bench is capable of measuring CO, O_2, CO_2, HC and NOx, and the catalyst out bench has instruments for measuring CO_2 and NOx. Nondispersive infrared (NDIR) analysis measures CO and CO_2 concentrations. A magneto-pneumatic detector measures the O_2 concentrations. Flame ionization detection (FID) is used for HC measurement, and NOx are measured through photochemiluminescence. The manufacturer, analyzer ranges and principles of measurement for each instrument are summarized in Table 2.2. The analyzers are incorporated into a continuous exhaust gas sampling system which controls moisture, temperature, pressure and flow rate of the sampled gas.

A vacuum pump is used to pull the sample from the exhaust stream to the analyzer benches. The sample, once extracted from the exhaust, is first filtered to

Table 2.2 – Emission Analysis Instruments

Engine Out Bench				
Gas	**Manufacturer**	**Principle of Measure**	**Model**	**Ranges**
CO (Low)	Horiba	Nondispersive Infrared	AIA-220	100, 300, 1000, 3000 ppm
CO (High)	Horiba	Nondispersive Infrared	AIA-220	.5, 2, 5, 10%
O2	Horiba	Magneto-Pneumatic	MPA-220	5, 10, 25%
CO2	Horiba	Nondispersive Infrared	AIA-210	1, 5, 10, 20%
THC/CH4	California Analytical	Flame Ionization	300M	10, 30, 100, 300, 1000, 3000, 10000, 30000 ppm
NOx/NO	California Analytical	Photochemiluminescence	400	30, 100, 300, 1000, 3000 ppm
Catalyst Out Bench				
Gas	**Manufacturer**	**Principle of Measure**	**Model**	**Ranges**
CO2 (High)	California Analytical	Nondispersive Infrared	200	1, 5, 10%
CO2 (Low)	California Analytical	Nondispersive Infrared	200	.5, 1, 2%
NOx/NO	California Analytical	Photochemiluminescence	400	30, 100, 300, 1000, 3000 ppm

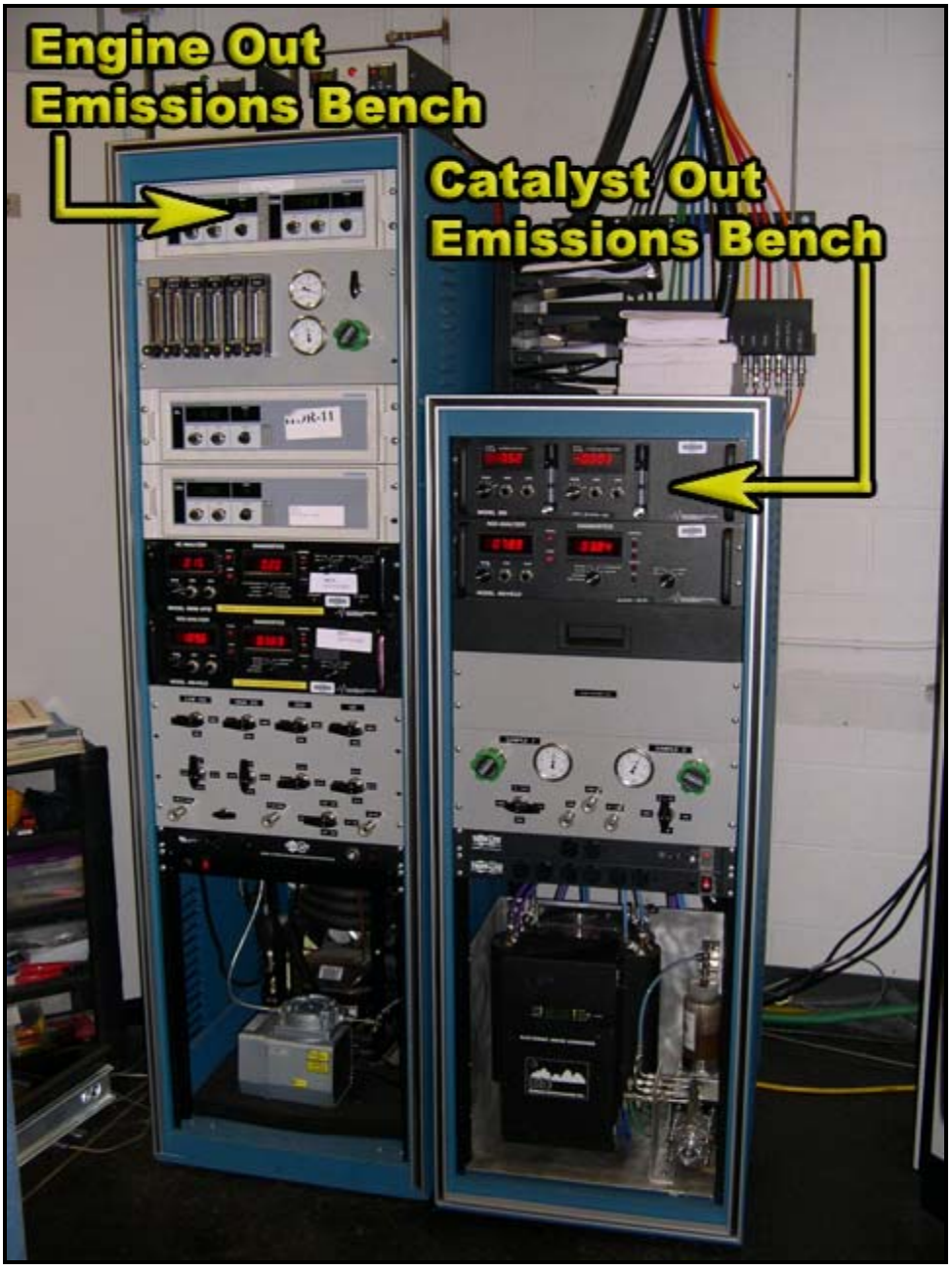


Figure 2.3 – Emissions Analyzer Benches

remove solid and liquid particulate matter larger than .01 µm. This inert, fibrous filter made by Balston is contained in a stainless steel housing. After filtration, the sample is then pulled to the emissions bench through a heated Teflon line. A set of heater controllers are used to maintain the filter housing and sample line at a temperature well above the dew point of the exhaust gas (375° F) to prevent the formation of condensate.

The flow path of span gasses, purge air and the exhaust gas sample to each instrument in the emissions bench are illustrated in Figure 2.4. Once the sample reaches the emissions bench it passes through a chiller which is used to condense and remove water vapor. This is not necessary for the HC and NOx analyzers, as they are both heated instruments with internal pumps. Thus, the sample reaches them before passing through the pump and chiller. After passing through the chiller, the sample is once again filtered to remove any remaining solid or liquid particulates. A set of four way valves allows the operator to choose between flowing sample gas, span gas or purge air to the instruments and flow meters with needle valves allow for control of flow rates. The instruments were calibrated each day before conducting experiments using purge air for zeroing and bottled gasses for spanning.

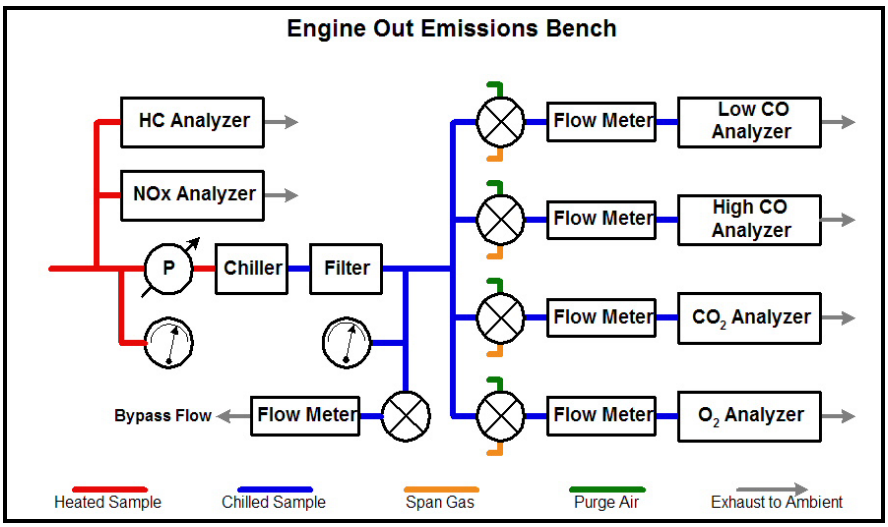


Figure 2.4 – Emissions Bench Schematic

EXHAUST AFTERTREATMENT SYSTEM

Aftertreatment of lean burn natural gas NOx was achieved through implementation of a dual path NOx adsorbing catalyst system as shown in Figures 2.5 and 2.6. The dual path system allows for NOx reduction by managing the LNT catalyst on a time-shared schedule. By periodically alternating the flow, the catalyst leg can flow the majority of the exhaust while in its adsorption mode. When it is time to regenerate the catalyst, the majority of the flow is diverted through the bypass leg. Restricting the flow across the catalyst during regenerating serves two purposes. The lower catalyst space velocity allows enough time for the release and reduction of stored NOx. In addition, the lower mass flow rate of lean exhaust gasses reduces the amount of reductant needed to create the correct stoichiometry for regeneration. This consequently reduces the fuel penalty.

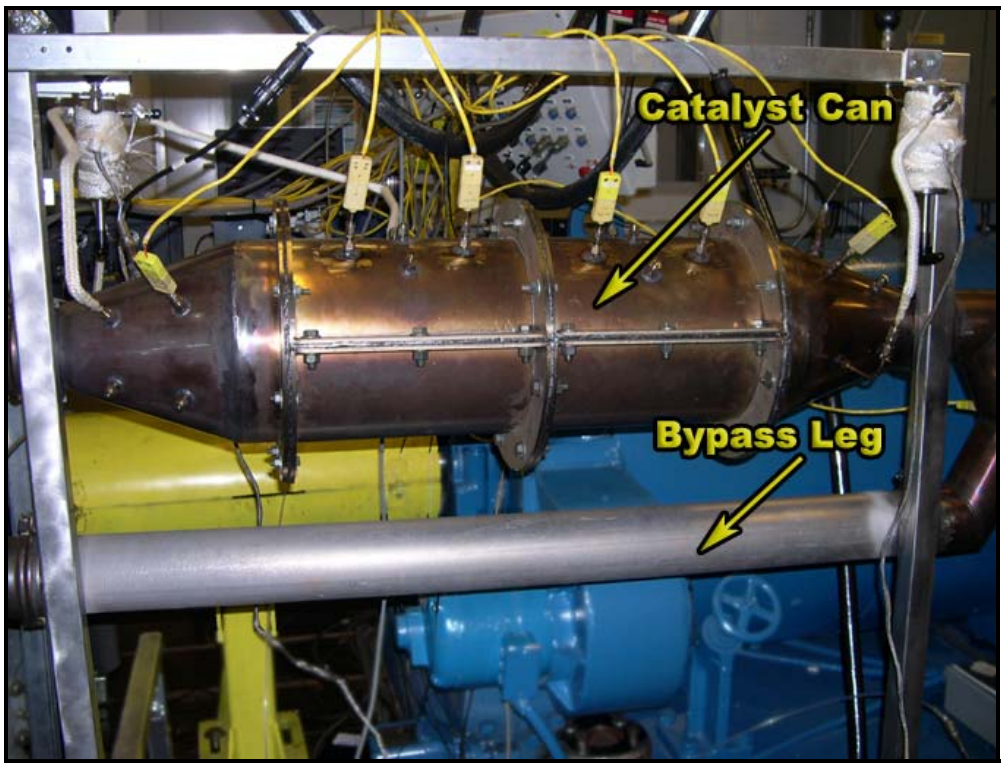


Figure 2.5 – Exhaust Aftertreatment System Picture

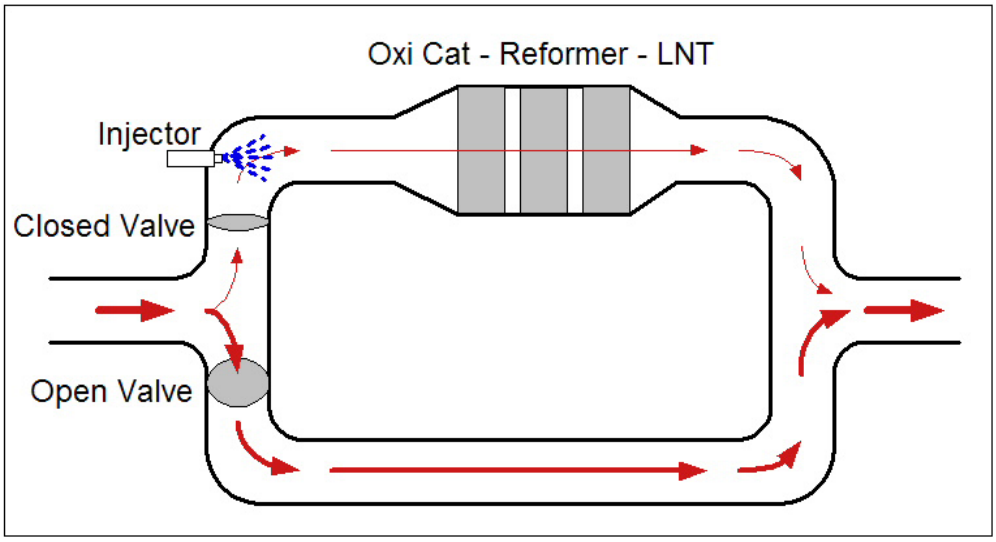


Figure 2.6 – Exhaust Aftertreatment System Schematic

For the purpose of simplifying the experiment, only one leg of the system contains catalyst bricks. In an actual application, both legs of the system would contain catalysts. However, the single chamber system was used here to evaluate the lean NOx trap's ability to store and reduce NOx as well as the reforming catalyst's ability to break down methane into a usable source for regeneration. Projections of the conversion efficiencies and fuel penalties for a two chamber system were made from measurements of the one chamber system.

For this research, the same compressed natural gas supplied to the engine was used as the reducing agent. Shown in Figure 2.7, a pair of automotive injectors introduced the reductant directly upstream of the catalyst can. The injectors were actuated by a 75 Hz square wave signal. The amount of reducing agent introduced was controlled by adjusting the duty cycle of this signal. The natural gas supplied was primarily methane. However, efficient regeneration of an LNT requires hydrogen or carbon monoxide in an oxygen free environment. Thus, an oxidation catalyst and reforming catalyst, placed upstream of the LNT, served to burn out the excess oxygen from the lean exhaust and reform the methane to a usable source for regeneration.

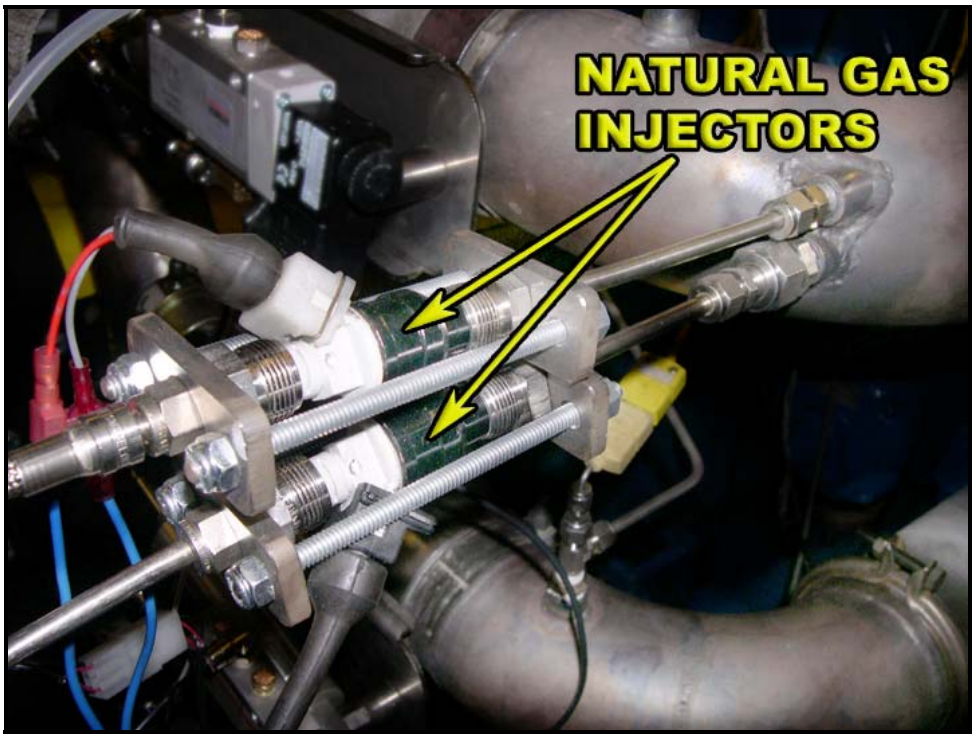


Figure 2.7 – Natural Gas Injectors

The oxidation catalyst, reforming catalyst and two lean NOx trap catalyst bricks were each 9.5" in diameter by 6" in length. Each of the catalysts, developed by EmeraChem, were deposited on a cordierite honeycomb with 300 cells/in^2. The LNT catalyst contained a loading of 1.6 g/in^3 Al_2O_3, 100 g/ft^3 of Platinum and 0.14 g/in^3 of barium oxide. The oxidation catalyst had a coating of 1.8 g/in^3 alumina and 50 g/ft^3 of palladium metal. The reformer catalyst was prepared with a 1.59 g/in^3 6:1 Platinum-Rhodium washcoat with a precious metal loading of 40 g/ft^3 and 3.9% cerium oxide on alumina. An additional 20 g/ft^3 of Rhodium was deposited on the surface.

A set of pneumatically actuated exhaust brake valves designed by US Gear were used to control the flow of the exhaust gasses. Used here as flow control valves, these butterfly valves are designed as a brake assist for heavy duty highway vehicles. Shown in Figure 2.8, one valve is mounted in each leg of the exhaust system and are alternately opened and closed to redirect the exhaust flow. These

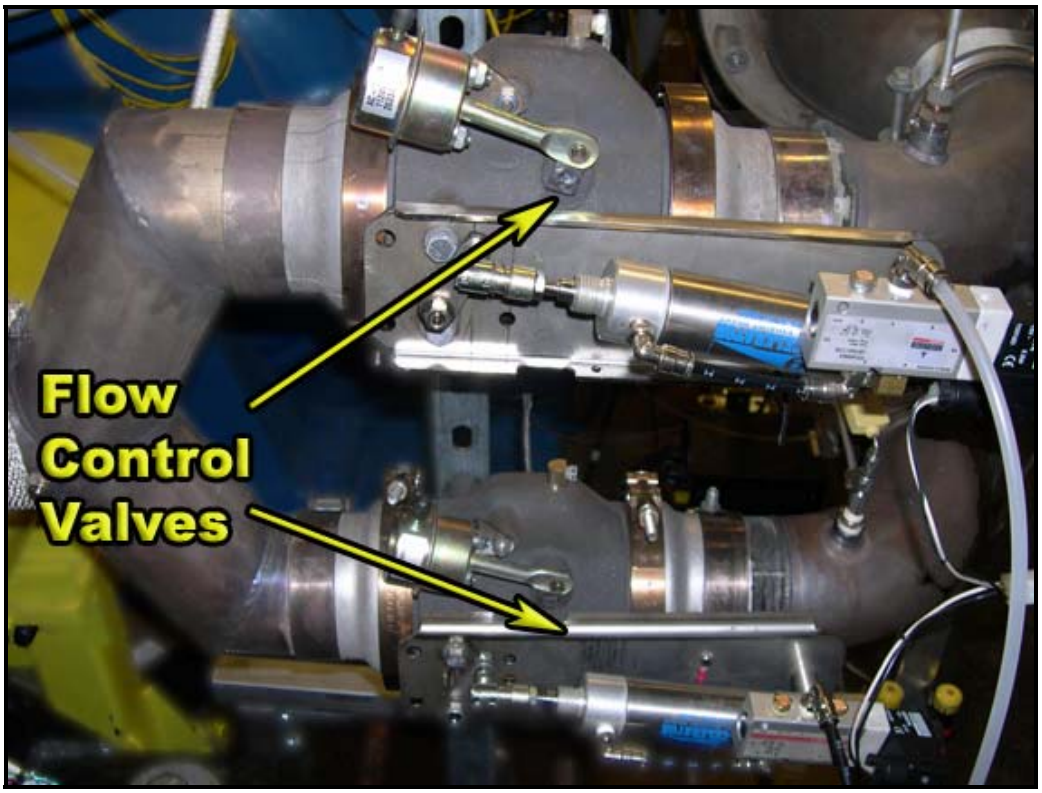


Figure 2.8 – Flow Control Valves

normally open butterfly valves are designed to be fully closed with a pneumatic piston and thus, are either fully open or fully closed. Even in the fully closed position, the valves are designed to allow a portion of the exhaust to pass. However, it was desired to have more control over the exhaust flow rate, thus a mechanical stop was designed which could be positioned to hold the arm of the pneumatic piston from fully closing. This design consisted of a mechanical screw jack turned by a stepping motor. This allowed the flow control valve to be precisely positioned, giving the operator control over the exhaust flow rate. Exhaust flow control experiments later proved this design to be unnecessary, as the amount of flow across the valve even in the fully closed position was already sufficiently high. Thus, the remainder of the research was conducted with the valves operated as either fully open or fully closed.

CONTROLS AND DATA ACQUISITION

There were two primary control systems for the experimental setup. The first system, developed with DyneSystem's hardware and software (Figure 2.9), controls dynamometer operation, the engine's electronic throttle, a safety interlock system and logs pertinent data. The second control system, developed with National Instrument's hardware and software (Figure 2.10), is responsible for all controls pertaining to LNT management.

As mentioned previously, the DyneSystem's control hardware includes the Dyne-Loc IV for dynamometer control and the DTC-1 for engine throttle control. The hardware also includes Companion II, which acquires and conditions all analog data signals from the test cell. The Companion II, consisting of the boom box and companion box shown in Figures 2.11 and 2.12, is capable of measuring most types of analog signals, including voltages, currents and frequencies. All data signals are gathered through the boom box, which includes thermocouple connections and a series of pressure transducers. The signals are then routed to the companion box where they are conditioned and communicated to the test cell's central data acquisition PC.

DyneSystem's Cell Assistant, a PC based controls and data acquisition software, acquires, logs and displays all of these data signals. All pertinent data was displayed on a series of virtual instrument panels shown in Figures 2.13 through 2.15. A complete data acquisition list is given in Tables 2.3 through 2.6. These tables include the name of the channel as defined in Cell Assistant, type of channel, range and units of measure, type and position of signal conditioner in the companion box, position of measurement on the boom box and calibration values if applicable.

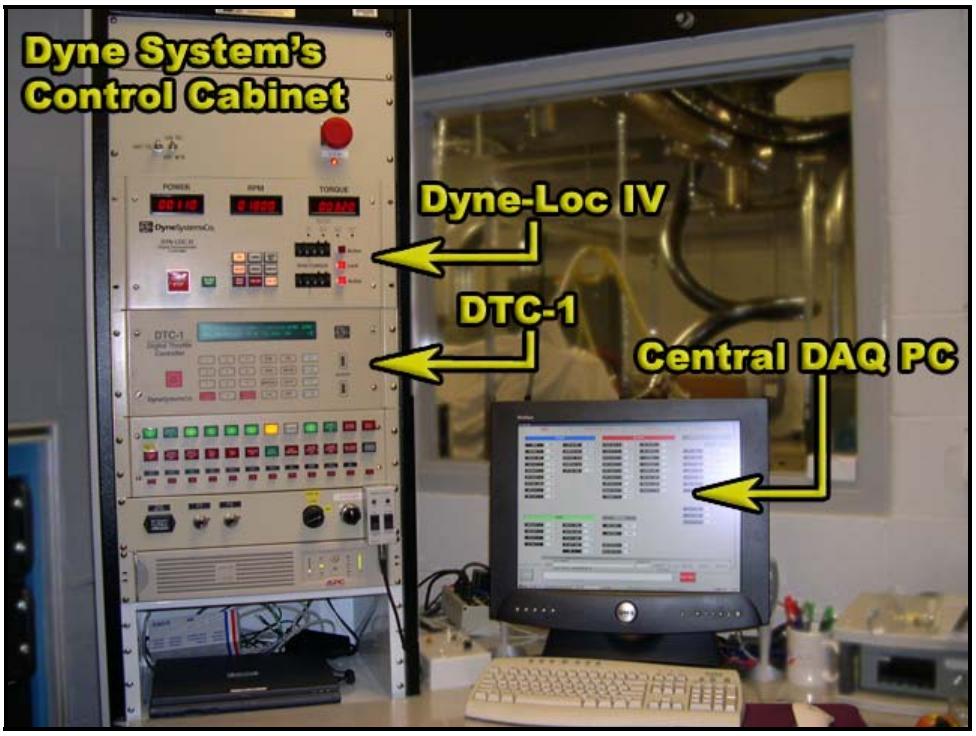


Figure 2.9 – Dyne Systems Control Cabinet

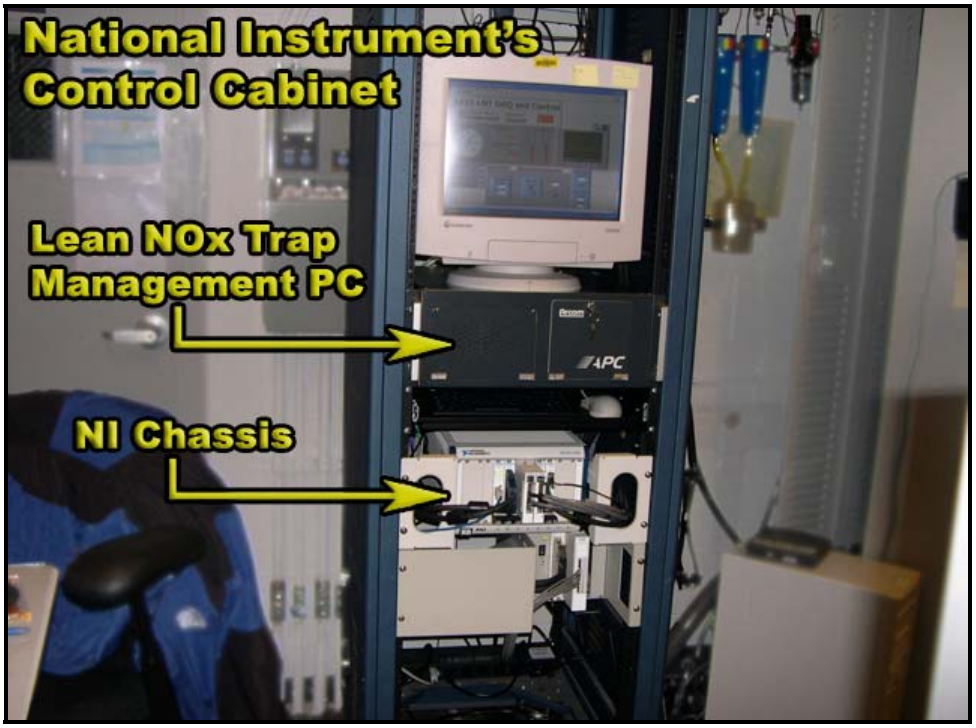


Figure 2.10 – National Instruments Control Cabinet

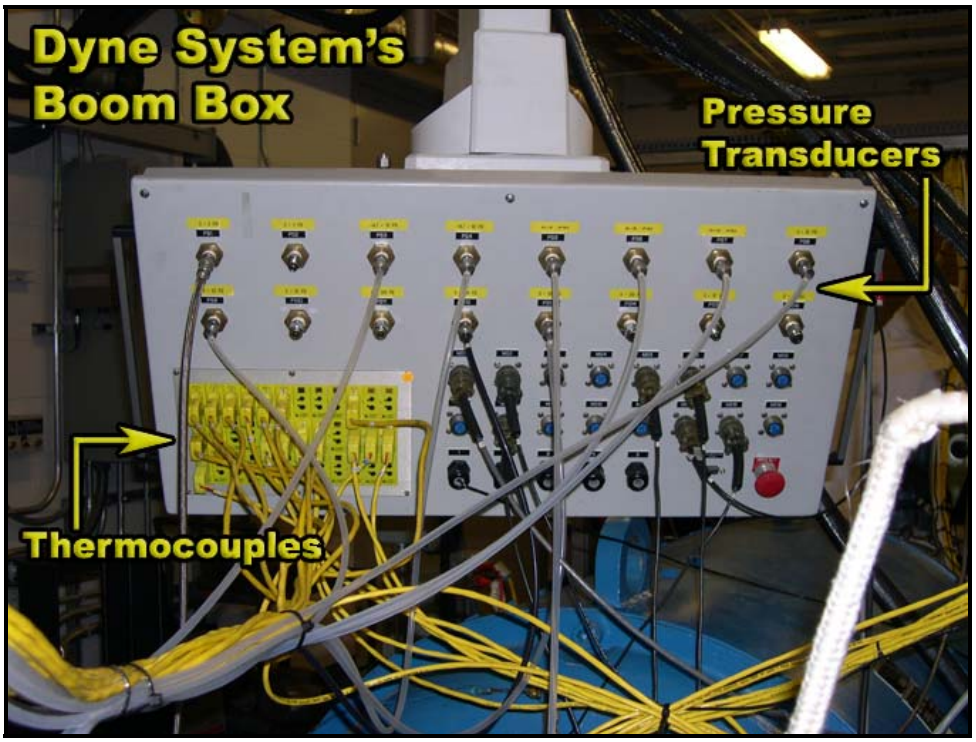


Figure 2.11 – Dyne Systems Boom Box

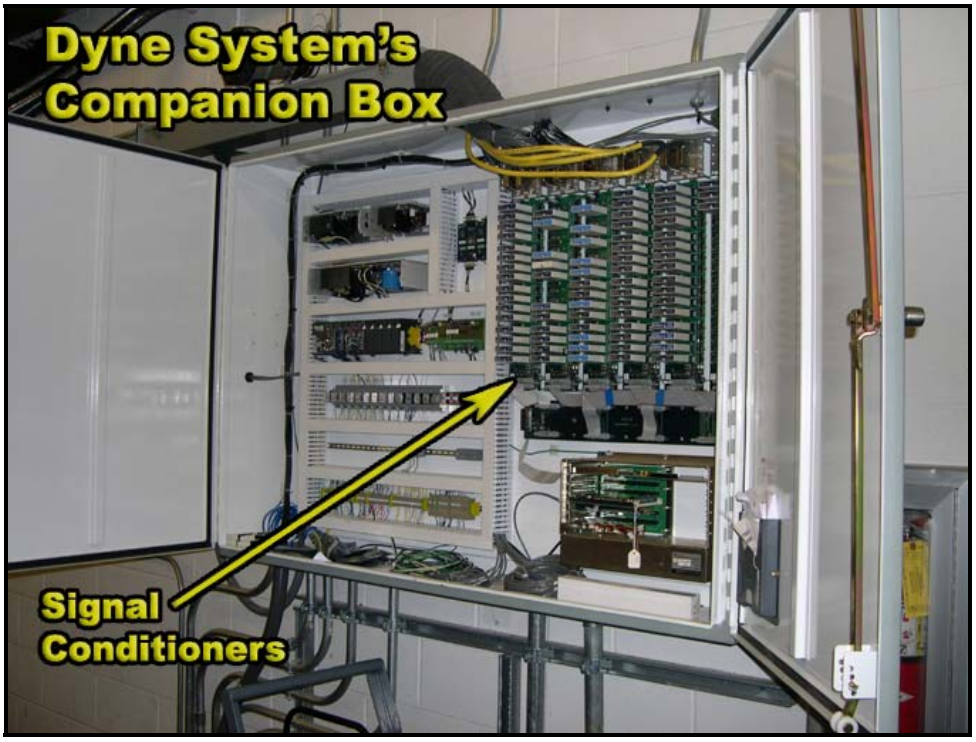


Figure 2.12 – Dyne Systems Companion Box

Table 2.3 – Data Acquisition Temperatures

DESCRIPTION	CHANNEL NAME	RANGE	BACKPLANE	MODULE	BOOM	m	b
Ambient air	aicAmbientT	0-500 C	7	16	-	-	-
Inlet air	aicInletAirT	0-500 C	4	5	T-5	-	-
IC in	aicIntCoolerAirInT	0-500 C	4	13	T-13	-	-
IC out	aicIntCoolerAirOutT	0-500 C	4	14	T-14	-	-
Turbo out	aicTurboEOT	0-1000 C	4	6	T-6	-	-
LNT in	aicNOxCat_InT	0-1000 C	6	6	T-22	-	-
Oxi Cat mid	aicOxiCat_CoreT	0-1000 C	6	3	T-19	-	-
Reformer Cat mid	aicReformerCat_CoreT	0-1000 C	6	4	T-20	-	-
LNT mid 1	aicNOxCat_CoreT	0-1000 C	6	7	T-23	-	-
LNT mid 2	aicNOxCat_Core2T	0-1000 C	6	1	T-17	-	-
LNT out	aicNOxCat_OutT	0-1000 C	6	8	T-24	-	-
Bypass leg	aicBypassLegT	0-1000 C	6	2	T-18	-	-
End of system	aicTailpipeT	0-1000 C	6	9	T-25	-	-
Engine coolant in	aicH2OinT	0-500 C	4	1	T-1	-	-
Engine coolant out	aicH2OoutT	0-500 C	4	2	T-2	-	-
Fuel	aicFuel_InT	0-500 C	4	10	T-10	-	-
Oil sump	aicOilCrankT	0-500 C	4	4	T-4	-	-
Oil block	aicOilBlockT	0-500 C	4	3	T-3	-	-

Table 2.4 – Data Acquisition Pressures

DESCRIPTION	CHANNEL NAME	RANGE	BACKPLANE	MODULE	BOOM	m	b
Ambient air	aicBarokPa	kPa	7	14	-	10	59
Inlet air	aicInletAirP	-14.7 - 30 psi	1	4	P-4	8.9238	-15.716
Boost before IC	aicIntCoolerAirInP	-14.7 - 30 psi	1	8	P-8	10.036	-1.1553
Boost after IC	aicIntCoolerAirOutP	-14.7 - 30 psi	1	9	P-9	9.9687	-1.2469
Turbo out	aicExhBP	0 - 5 psi	1	1	P-1	1.1067	-0.5133
LNT in	aicNOxCat_InP	0 - 5 psi	1	6	P-6	1.0006	-0.49
Bypass Leg	aicBypassP	0 - 5 psi	1	7	P-7	1.0025	-0.5228
End of system	aicTailpipeP	0 - 2 psi	1	5	P-5	0.4	-0.1926
Oil	aicOil_Press	0 - 200 psi	1	12	P-12	40	-20
LFE inlet	aicLFE_Pin_gage	0 - 10" H20	1	15	P-15	1.9349	1.3033
LFE dP	aicLFE_R1	dP	2	1	MS-1	2.247	0.13
Backpressure in Hg	clcExhBP_inHG	in-Hg	-	-	-	-	-

Table 2.5 – Data Acquisition Emissions

DESCRIPTION	CHANNEL NAME	RANGE	BACKPLANE	MODULE	BOOM	m	b
NOx engine out	clcNOx_EngOut	0-3000ppm	-	-	-	-	
O2 engine out	clcO2_EngOut	0-25%	-	-	-	-	-
Low CO engine out	clcLowCO_EngOut	0-3000ppm	-	-	-	-	-
High CO engine out	clcHighCO_EngOut	0-5%	-	-	-	-	
High CO2 engine out	clcHighCO2_EngOut	0-20%	-	-	-	-	-
THC engine out	clcHC_Eng_Out	0-10000ppm	-	-	-	-	-
Low CO2 Tailpipe	clcLowCO2_Tailpipe	0-1%	-	-	-	-	
High CO2 Tailpipe	clcHighCO2_Tailpipe	0-15%	-	-	-	-	-
NOx Tailpipe	clcNOx_Tailpipe	0-3000ppm	-	-	-	-	-

Table 2.6 – Data Acquisition Other

DESCRIPTION	CHANNEL NAME	RANGE	BACKPLANE	MODULE	BOOM	m	b
Engine Speed	aicDynoSpeed	rpm	-	-	-	-	-
Engine Torque	aicDynoTorque	ft-lbs	-	-	-	-	
Engine Power	aicDynoPower	hp	-	-	-	-	-
% Throttle	aicThrottlePosition	%	-	-	-	-	-
% Humidity	aicHumidity	%	7	15	-	-	-
BMEP	clcBMEP_bar	bar	-	-	-	-	-
UEGO engine out	aicUEGO1	A/F	2	14	MS-14	30	6
UEGO cat out	aicUEGO2	A/F	2	15	MS-15	30	6
Lambda engine out	clcLambda	Lambda	-	-	-	-	-
Lambda cat out	clcLambda2	Lambda	-	-	-	-	-
ACFM	clcACFM	acfm	-	-	-	-	-
SCFM	clcSCFM	scfm	-	-	-	-	-
Mass inlet air flow	clcAirMFlow	g/sec	-	-	-	-	-
Mass fuel flow	aicGaseous_FuelFlow	0-150 lb/hr	2	2	MS-2	9.332	-36.953
Mass exhuast flow	clcExhMFlowNG	g/sec	-	-	-	-	-
Injector Frequency	aicInjectorFreq	0 - 500 Hz	2	10	MS-10	-	-
Upper Valve	aicUpperValve	0-20 V	2	5	MS-5	-	-
Lower Valve	aicLowerValve	0-20 V	2	6	MS-6	-	-

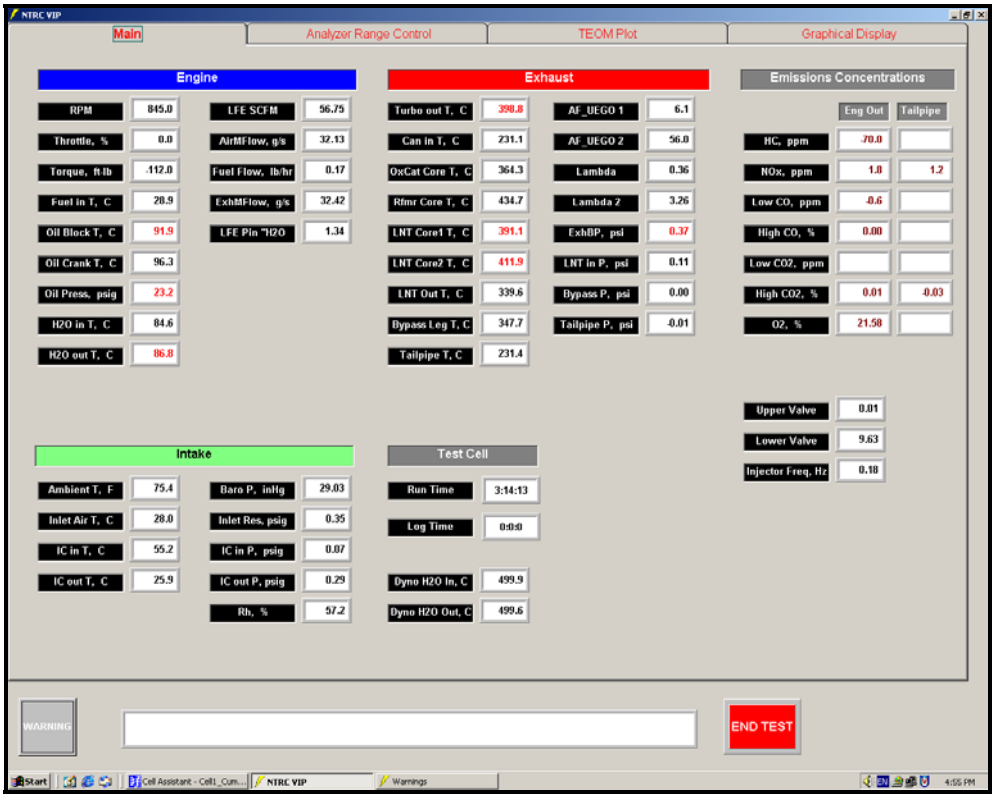


Figure 2.13 – Cell Assistant Front VIP

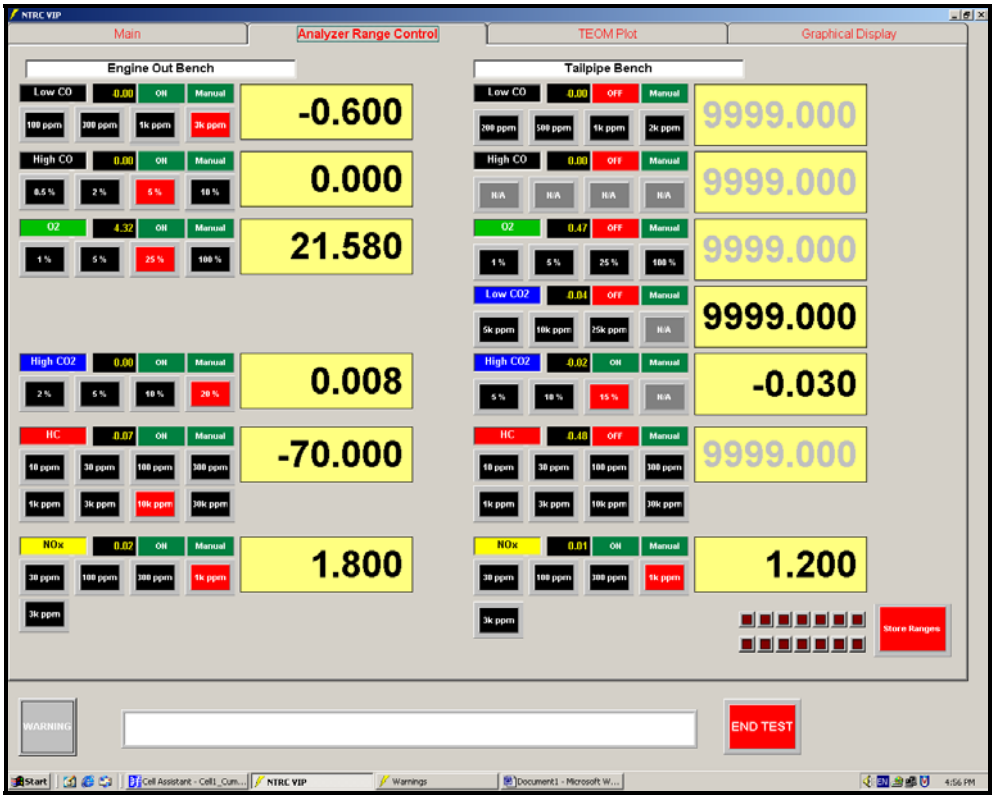


Figure 2.14 – Cell Assistant Analyzer Range Control VIP

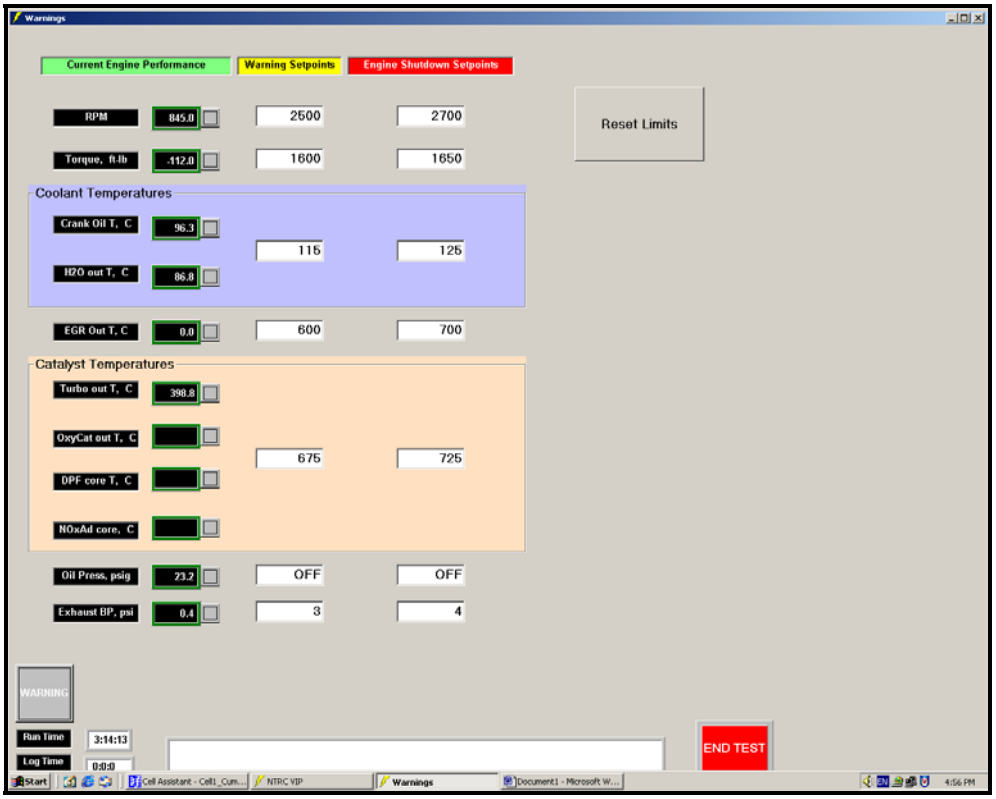


Figure 2.15 – Cell Assistant Safety Interlock VIP

In addition to control and data acquisition, the DyneSystem's controls cabinet also included a safety interlock system. The safety interlocks ensured that the engine ignition and fuel were shut off if the test cell ventilation system or engine coolant were lost. Other safety measures were also incorporated into the Cell Assistant code. This included monitoring and safety shutdown procedures for excess engine temperature, backpressure or over speed.

The second of the two control systems was developed with National Instruments hardware and software. This system was used primarily for management of the LNT adsorption and regeneration modes, which included control of the exhaust flow control valves as well as the frequency and duty cycle of the injectors. The signal to the injectors and valves was produced with a National Instruments PXI-66025 counter timer module and PXI-6052E digital I/O module. The controls for the system was written in LabView 7.0 for which the virtual instrument panel is shown in Figure 2.16.

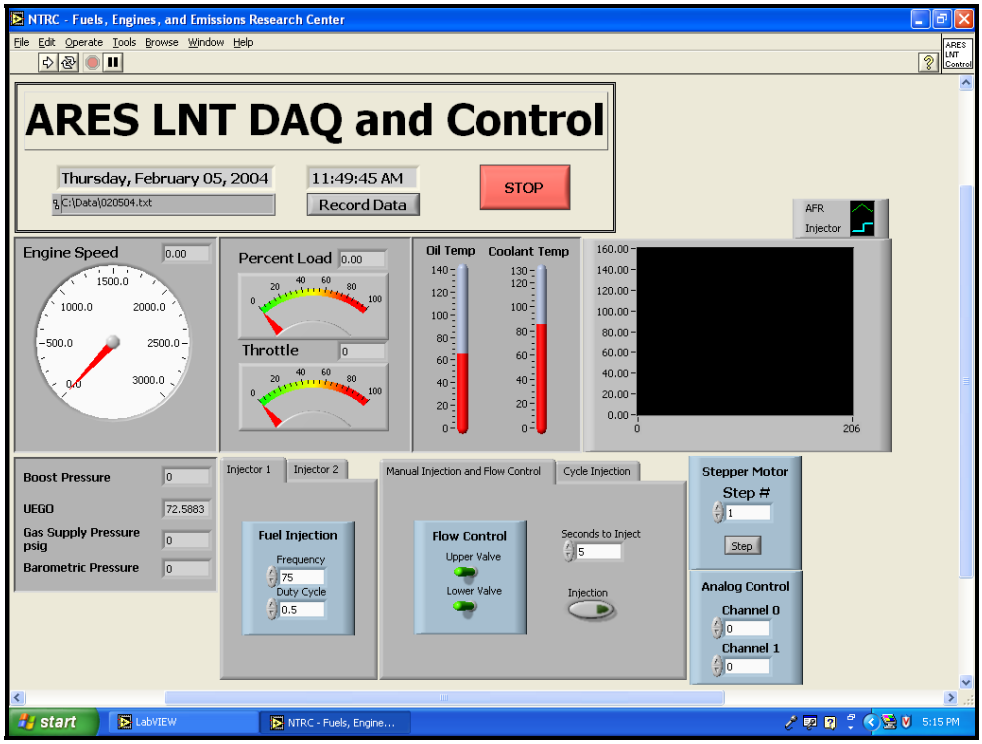


Figure 2.16 – LabView Front VIP

CHAPTER 3 – BASELINE TESTING

Following the development of the experimental test bed, the first objective was to characterize the engine through a series of baseline tests. These tests would serve to provide pertinent performance and emissions data necessary for the development of the exhaust aftertreatment system. While the 210 kW engine does not fall into the .5 to 6.5 MW range of interest to the ARES program, it serves as a practical starting point for assessing the catalyst technology. Thus, baseline testing not only evaluates the performance and emissions characteristics, but it was also necessary to determine the scalability of the 8.3 liter engine compared to larger gensets of interest to ARES. A complete set of baseline data also serves to support further experimental results and aids in the comparison to other published data. In accordance with ARES goals, baseline testing was focused on a fixed speed of 1800 rpm. The baseline map was then extended to include a full load torque curve from 800 to 2400 rpm as well as a 45-point test matrix. This chapter serves to outline the details and present the results of all baseline testing. In addition, estimations of the catalyst's performance are made for certain test modes.

Before conducting baseline tests, a procedure was followed for engine warm up and calibration of the emissions analyzers. The same engine warm up procedure was followed throughout the research to maintain consistency and to ensure repeatability of results. Following engine warm up, the inlet and exhaust restrictions at rated conditions were set at 17.5" H_2O and 4" Hg. The following list outlines the standard engine warm up procedure as specified in CFR 40, Part 89, Subpart E (89.407), for constant speed engines:

1. For constant-speed engines
    (a) Operate the engine at minimum load for 2 to 3 minutes.
    (b) Operate the engine at 50 percent load for 5 to 7 minutes.
    (c) Operate the engine at maximum load for 25 to 30 minutes.

2. Start test cycle within 20 minutes of the end of the warm up. A mode begins when the speed and load are stabilized within ±2%. A mode ends when valid emission sampling for that mode ends. For a mode to be valid, the speed and load requirements must be maintained continuously during the mode.

3. Calculate the torque for any mode with operation at rated speed.

4. Record all data during a minimum of the last 60 seconds of each mode.

The emissions instruments were turned on at least one hour before calibration. Each analyzer was first zeroed with purge air, then calibrated with bottled span gasses. The span drift was checked at the end of testing to ensure zero and span difference did not exceed ±3% of full scale as specified by CFR 40, Part 89, Subpart E (89.408).

The first step in the baseline test procedure was to generate a 9 point full load torque curve from 800 rpm to 2400 rpm. This full load curve was then used to determine the 45-point test matrix for baseline testing. Modes for the test matrix included 10%, 25%, 50%, 75% and 100% load for each of the 9 speeds used to develop the full load torque curve. After warm up, testing began at the highest speed and load point then moved through each of the 5 load points at this fixed speed. Data was collected at five minute intervals between each mode to allow temperatures and engine out emissions to stabilize. Each mode in the test matrix was logged for 120 seconds at a sampling frequency of 10 Hz. The full test matrix is shown in Table 3.1.

Table 3.1 – Baseline Test Matrix

	Torque (ft-lbs)								
	800 rpm	1000 rpm	1200 rpm	1400 rpm	1600 rpm	1800 rpm	2000 rpm	2200 rpm	2400 rpm
100%	468	546	665	841	809	753	712	630	580
75%	351	410	499	631	607	565	534	473	435
50%	234	273	333	421	405	377	356	315	290
25%	117	137	166	210	202	188	178	158	145
10%	47	55	67	84	81	75	71	63	58

The exhaust flow, brake specific fuel consumption (BSFC), brake mean effective pressure (BMEP) and the NOx rating were calculated using the experimental data. The equations and assumptions used for calculating each of these are described below.

$$\dot{V}_{exh} = \dot{V}_{fuel} + \dot{V}_{air}$$

$$\dot{V}_{fuel} = \frac{\dot{m}_{fuel} * SV}{MW_{fuel}}$$

Where:

$\dot{V}_{exh}$ = *calculated volumetric exhaust flow* $(\frac{Liters}{\min})$

$\dot{V}_{fuel}$ = *calculated volumetric fuel flow* $(\frac{Liters}{\min})$

$\dot{V}_{air}$ = *measured volumetric inlet air flow* $(\frac{Liters}{\min})$

$\dot{m}_{fuel}$ = *measured mass fuel flow* $(\frac{lb}{\min})$

SV = *standard volume* $(22.414 \frac{Liters}{mole})$

MW_{fuel} = *molecular weight* $(16.499 \frac{g}{mole})$

$$NOx\ Rating = \frac{\dot{m}_{NOx}}{P}$$

$$\dot{m}_{NOx} = \frac{X_{NOx} * \dot{V}_{exh} * MW_{NO_2}}{SV}$$

Where:

NOx Rating = *calculated NOx rating* $(\frac{g}{hp-hr})$

$\dot{m}_{NOx}$ = *calculated mass NOx flow* $(\frac{g}{hr})$

P = *measured power* (HP)

X_{NOx} = *measured NOx concentration* (ppm)

MW_{NO_2} = *molecular weight* $(46 \frac{g}{mole})$

$$BMEP = \frac{2 * P}{N * V_{swept}}$$

Where:

$BMEP$ = *calculated brake mean effective pressure* (bar)

P = *measured power* (kW)

N = *measured engine speed* $\left(\frac{rev}{sec}\right)$

V_{swept} = *engine swept volume* $(.0083\, m^3)$

$$BSFC = \frac{\dot{m}_{fuel}}{P}$$

Where:

$BSFC$ = *calculated brake specific fuel consumption* $\left(\frac{lb}{hp-hr}\right)$

$\dot{m}_{fuel}$ = *measured mass fuel flow* $\left(\frac{lb}{hr}\right)$

P = *measured power* (HP)

Emissions maps of the engine are represented by the bubble plots in Figures 3.1 through 3.7. All other pertinent data collected during baseline testing is summarized in Tables 3.2 through 3.13.

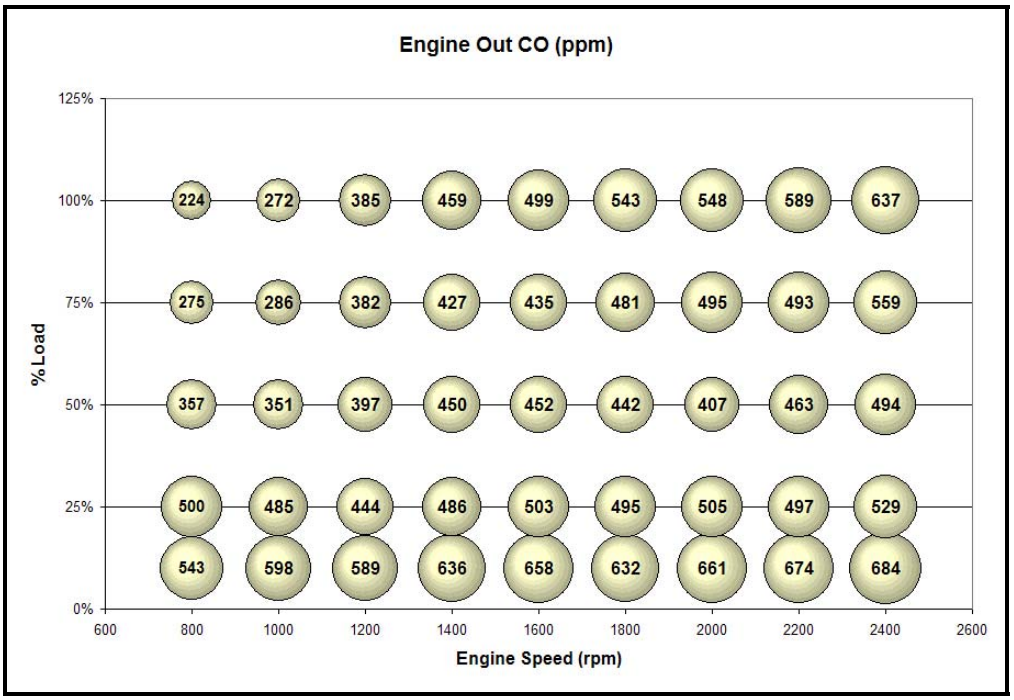


Figure 3.1 – Engine Out CO Map

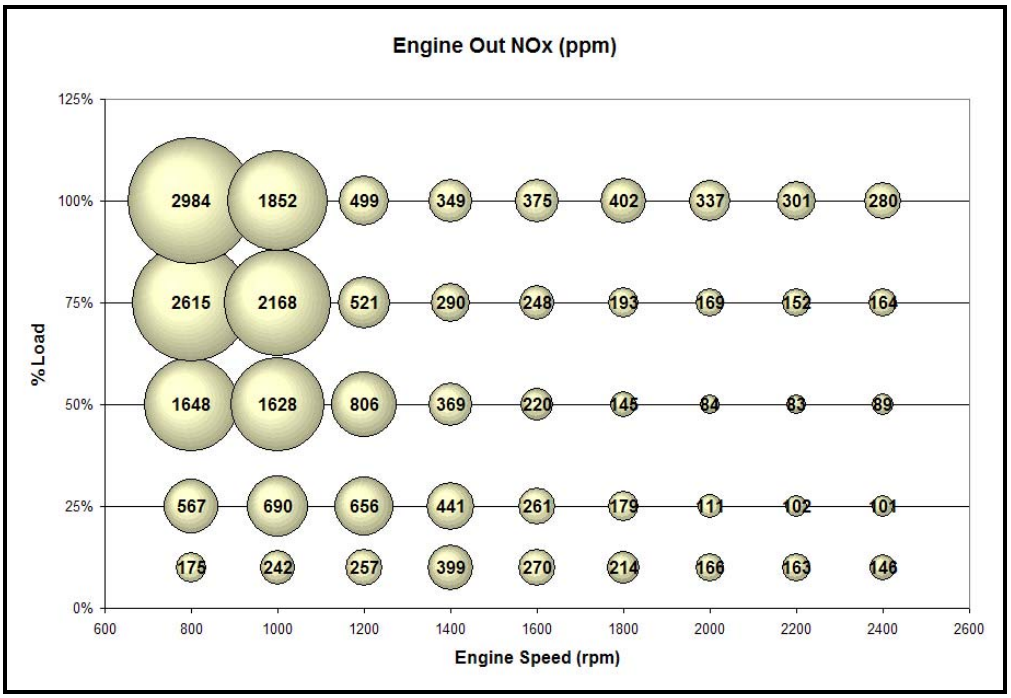


Figure 3.2 – Engine Out NOx Map

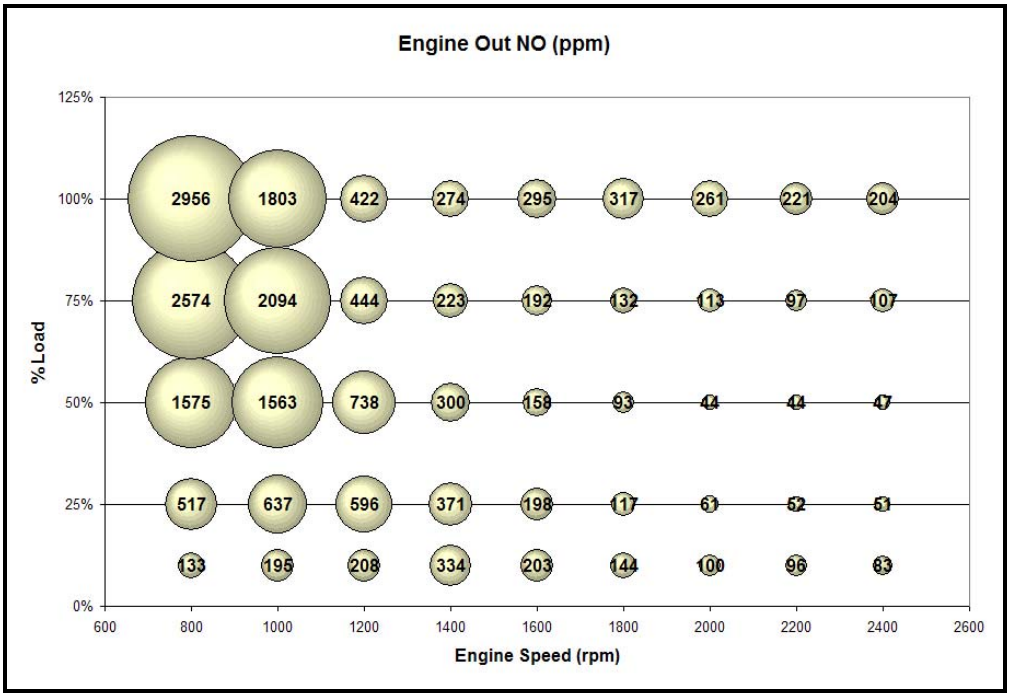


Figure 3.3 – Engine Out NO Map

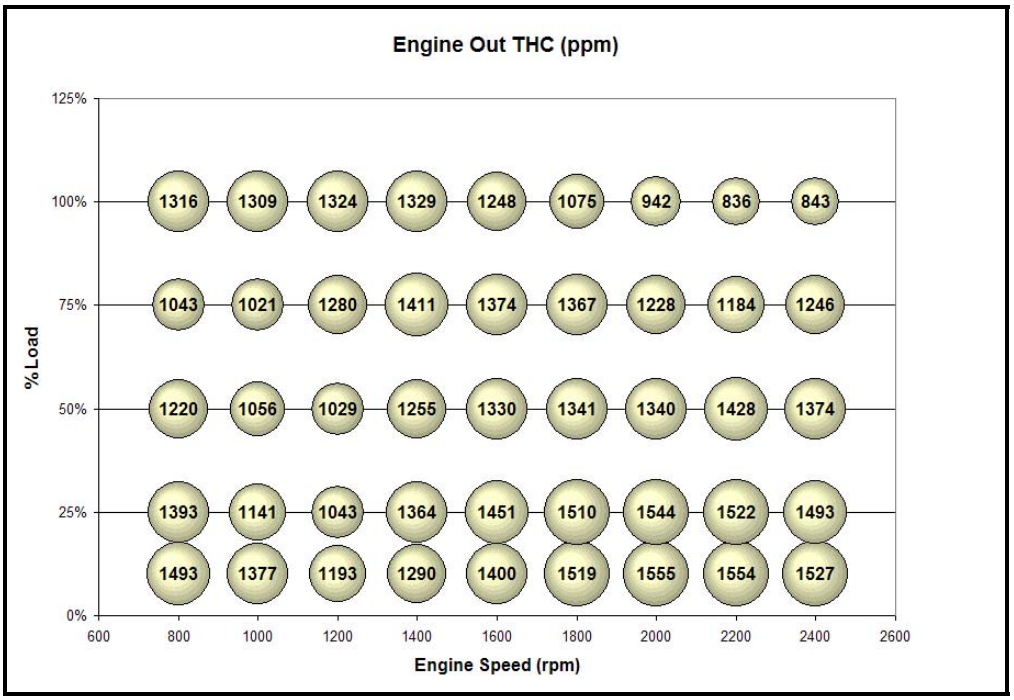


Figure 3.4 – Engine Out THC Map

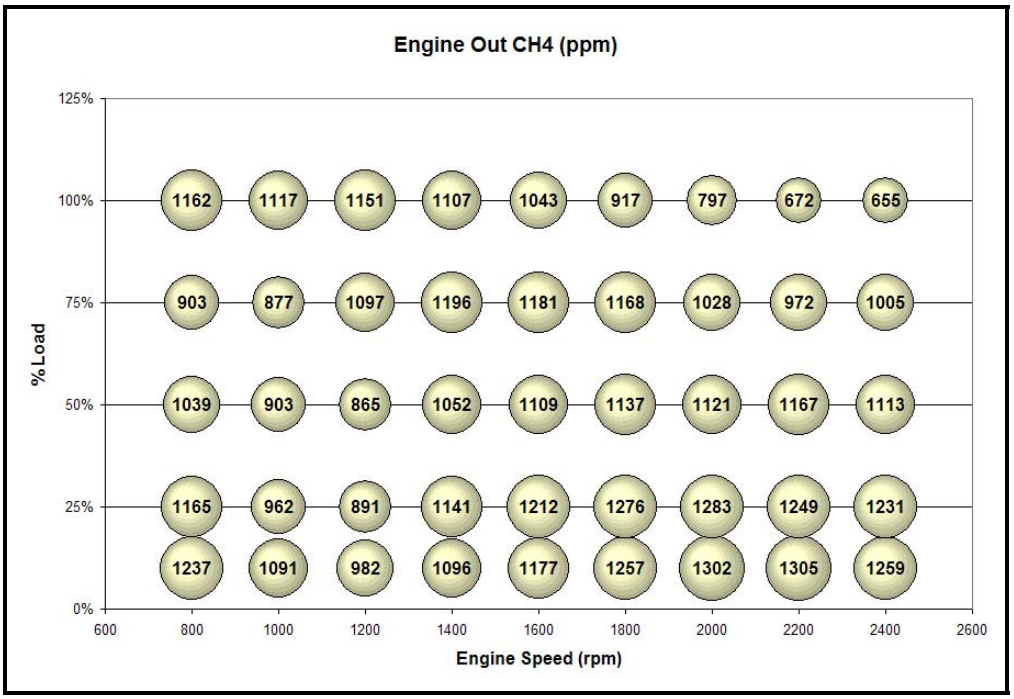


Figure 3.5 – Engine Out CH_4 Map

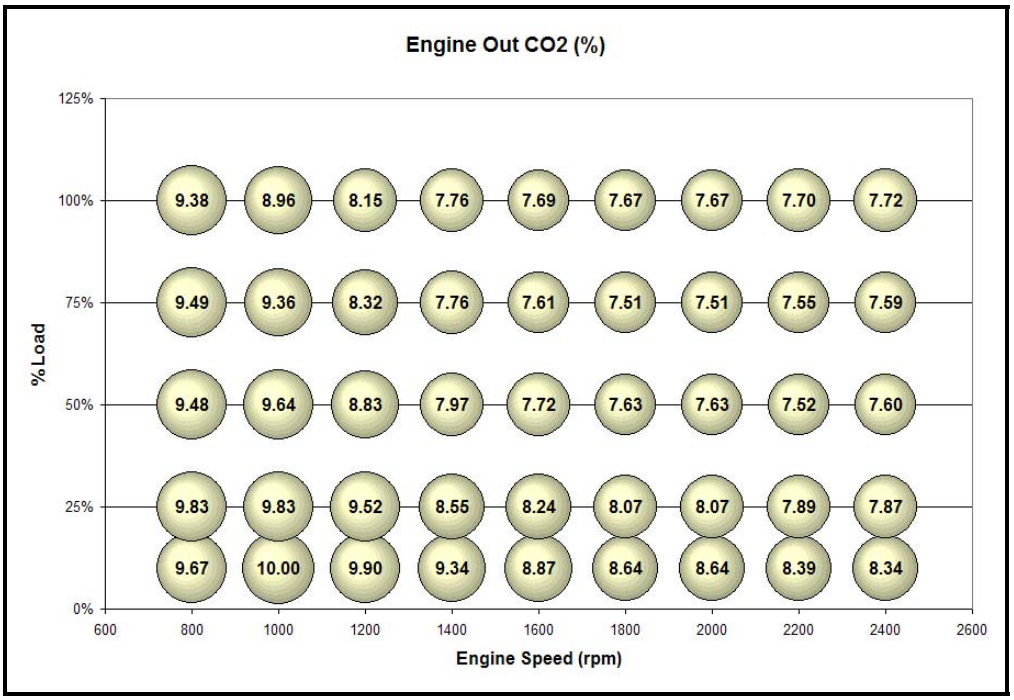


Figure 3.6 – Engine Out CO_2 Map

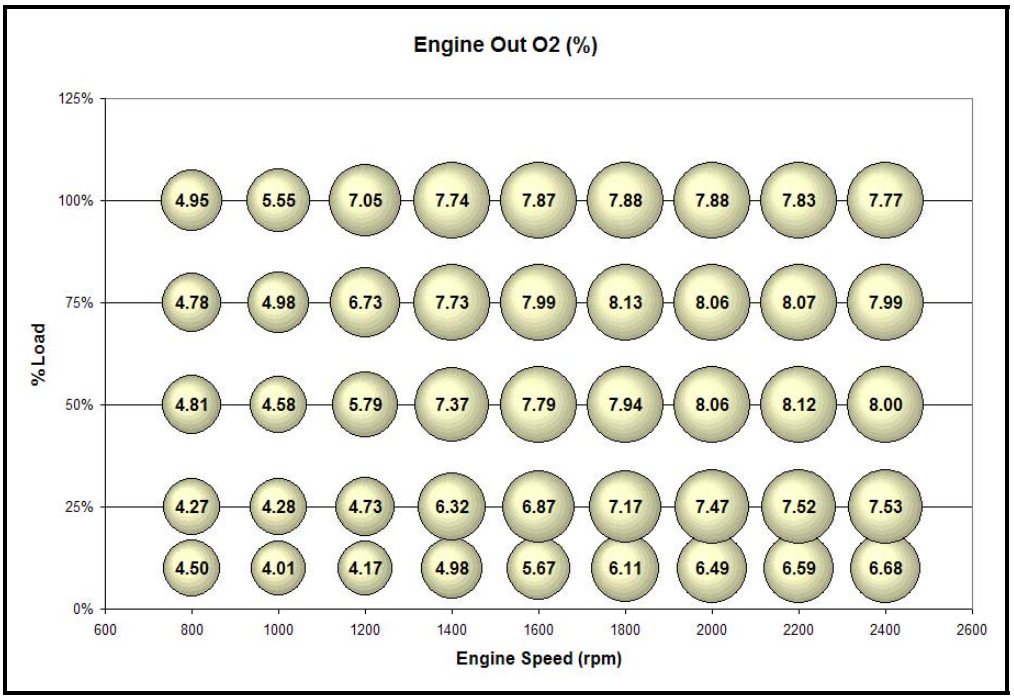


Figure 3.7 – Engine Out O_2 Map

Table 3.2 – Baseline Power Map

Power (hp)									
	800 rpm	1000 rpm	1200 rpm	1400 rpm	1600 rpm	1800 rpm	2000 rpm	2200 rpm	2400 rpm
100%	66	95	137	213	239	252	264	276	276
75%	50	71	103	161	179	188	198	209	208
50%	33	48	69	106	121	126	131	138	138
25%	16	24	34	53	59	61	65	67	68
10%	7	10	13	22	24	25	26	27	27

Table 3.3 – Baseline Throttle Map

Throttle (%)									
	800 rpm	1000 rpm	1200 rpm	1400 rpm	1600 rpm	1800 rpm	2000 rpm	2200 rpm	2400 rpm
100%	100	100	100	100	100	100	100	100	100
75%	30.4	38.5	51.2	75.9	78.4	77.8	77.2	77.1	76.7
50%	24.3	28.5	36.2	49.4	56.2	58.5	60.7	60.6	59.4
25%	20.5	22.3	25.8	32.6	37.3	38.5	39.9	41.1	41.7
10%	16.3	19.8	20.9	24	26.5	28.2	30.6	32.5	33.8

Table 3.4 – Baseline Boost Pressure Map

Boost Pressure (psig)									
	800 rpm	1000 rpm	1200 rpm	1400 rpm	1600 rpm	1800 rpm	2000 rpm	2200 rpm	2400 rpm
100%	2.79	5.70	11.63	21.21	21.34	20.04	19.65	19.49	18.09
75%	1.61	3.24	7.33	13.91	14.13	13.99	14.21	14.73	14.35
50%	0.63	1.50	3.47	7.58	9.38	9.74	10.85	11.80	12.44
25%	0.01	0.28	0.88	2.38	3.27	4.23	5.60	6.70	7.68
10%	-0.16	-0.05	0.12	0.52	0.87	1.31	1.87	2.42	3.27

Table 3.5 – Baseline Inlet Air Flow Map

Inlet Air Flow (scfm)									
	800 rpm	1000 rpm	1200 rpm	1400 rpm	1600 rpm	1800 rpm	2000 rpm	2200 rpm	2400 rpm
100%	112	158	268	446	498	524	563	602	615
75%	95	122	191	338	377	403	437	477	491
50%	81	97	130	207	252	282	324	356	372
25%	70	78	91	119	137	153	176	194	211
10%	64	69	75	85	95	103	113	123	136

Table 3.6 – Baseline Fuel Flow Map

Fuel Flow (lb/hr)									
	800 rpm	1000 rpm	1200 rpm	1400 rpm	1600 rpm	1800 rpm	2000 rpm	2200 rpm	2400 rpm
100%	23.5	33.2	47.8	72.4	81.0	86.5	93.4	100.5	103.7
75%	18.5	25.7	37.1	56.2	62.7	67.7	73.8	80.3	83.2
50%	13.7	19.0	26.5	38.4	44.6	49.0	54.7	59.1	62.3
25%	8.8	12.2	16.6	22.8	26.1	28.8	32.6	35.7	38.5
10%	6.2	8.5	10.8	14.1	16.3	18.2	20.5	22.8	25.4

Table 3.7 – Baseline Exhaust Flow Map

Exhaust Flow (L/min)									
	800 rpm	1000 rpm	1200 rpm	1400 rpm	1600 rpm	1800 rpm	2000 rpm	2200 rpm	2400 rpm
100%	3421	4826	8066	13367	14921	15739	16901	18070	18481
75%	2882	3709	5798	10159	11320	12101	13130	14338	14749
50%	2439	2938	3960	6245	7600	8483	9740	10685	11160
25%	2061	2326	2741	3594	4144	4619	5313	5871	6382
10%	1875	2040	2227	2562	2844	3094	3416	3728	4113

Table 3.8 – Baseline BSFC Map

BSFC (lb/hp-hr)									
	800 rpm	1000 rpm	1200 rpm	1400 rpm	1600 rpm	1800 rpm	2000 rpm	2200 rpm	2400 rpm
100%	0.355	0.349	0.349	0.341	0.338	0.343	0.354	0.364	0.376
75%	0.371	0.362	0.361	0.348	0.350	0.360	0.373	0.385	0.400
50%	0.414	0.398	0.384	0.362	0.370	0.389	0.417	0.429	0.450
25%	0.553	0.514	0.486	0.430	0.445	0.472	0.502	0.533	0.570
10%	0.954	0.849	0.814	0.646	0.680	0.740	0.778	0.847	0.929

Table 3.9 – Baseline BMEP Map

BMEP (bar)									
	800 rpm	1000 rpm	1200 rpm	1400 rpm	1600 rpm	1800 rpm	2000 rpm	2200 rpm	2400 rpm
100%	8.90	10.25	12.31	16.37	16.12	15.09	14.23	13.52	12.38
75%	6.73	7.65	9.23	12.43	12.07	11.25	10.67	10.22	9.34
50%	4.44	5.14	6.20	8.16	8.12	7.55	7.07	6.76	6.22
25%	2.16	2.57	3.06	4.07	3.95	3.65	3.49	3.29	3.04
10%	0.88	1.08	1.20	1.69	1.62	1.47	1.42	1.32	1.23

Table 3.10 – Baseline Exhaust Back Pressure Map

Exhaust Back Pressure (psig)									
	800 rpm	1000 rpm	1200 rpm	1400 rpm	1600 rpm	1800 rpm	2000 rpm	2200 rpm	2400 rpm
100%	0.67	0.78	1.03	1.57	1.80	1.99	2.23	2.52	2.59
75%	0.64	0.72	0.88	1.23	1.38	1.54	1.71	1.94	1.98
50%	0.62	0.67	0.75	0.91	1.01	1.12	1.26	1.37	1.42
25%	0.60	0.63	0.67	0.72	0.76	0.79	0.85	0.90	0.93
10%	0.58	0.60	0.63	0.66	0.66	0.69	0.71	0.73	0.75

Table 3.11 – Baseline NOx Rating Map

NOx Rating (g/hp-hr)									
	800 rpm	1000 rpm	1200 rpm	1400 rpm	1600 rpm	1800 rpm	2000 rpm	2200 rpm	2400 rpm
100%	19.02	11.57	3.62	2.70	2.88	3.09	2.66	2.43	2.31
75%	18.58	13.96	3.62	2.24	1.93	1.53	1.38	1.29	1.43
50%	15.01	12.36	5.70	2.67	1.71	1.20	0.76	0.79	0.89
25%	9.00	8.29	6.49	3.69	2.27	1.67	1.12	1.10	1.18
10%	6.22	6.06	5.30	5.75	3.94	3.32	2.65	2.78	2.69

Table 3.12 – Baseline Air to Fuel Ratio Map

Air to Fuel Ratio									
	800 rpm	1000 rpm	1200 rpm	1400 rpm	1600 rpm	1800 rpm	2000 rpm	2200 rpm	2400 rpm
100%	20.5	21.4	23.1	24.3	24.6	24.8	24.9	25.0	25.3
75%	20.1	20.8	22.9	24.1	24.6	24.7	24.8	24.9	24.8
50%	19.9	20.2	21.0	23.6	24.1	24.4	24.6	24.6	24.5
25%	19.7	19.9	20.5	20.7	20.6	21.9	22.8	23.6	23.6
10%	19.3	19.5	19.8	20.5	21.3	21.5	21.4	20.9	20.7

Table 3.13 – Baseline Turbo Out Temperature Map

Turbo Out Temp (C)									
	800 rpm	1000 rpm	1200 rpm	1400 rpm	1600 rpm	1800 rpm	2000 rpm	2200 rpm	2400 rpm
100%	527	579	604	586	590	604	621	638	656
75%	519	573	599	598	600	614	630	645	655
50%	489	543	580	585	590	606	636	640	649
25%	453	506	553	564	574	586	604	615	624
10%	411	455	507	539	549	569	586	595	614

The overall NOx rating for an engine is calculated in accordance with CFR 40, Part 89, Subpart E, where the NOx rating for each of five modes is weighted and summed per the weighting factors shown in Table 3.14. Using the NOx rating data for 1800 rpm from Table 3.11, the engine's rating is 1.73 g/hp-hr. The goal for the ARES program is to achieve a NOx rating of 0.1 g/hp-hr. Thus, the exhaust aftertreatment system must reduce the NOx levels by greater than 94% to meet this goal.

LNT CAPACITY ESTIMATION

Baseline data is useful in predicting the performance of the lean NOx trap system at particular engine modes. Using baseline engine data along with bench flow reactor data provided by EmeraChem, estimates of the NOx storage capacity were made. The trapping capacity of the catalyst is highly dependent on temperature as was demonstrated by the bench flow reactor studies. Data from these studies gives the capacity of the catalyst after 10% and 50% NOx breakthrough (τ_{10} and τ_{50}) over a range of temperatures. The conditions of the experiment along with bench flow data are listed in Tables 3.15 and 3.16.

Unfortunately, the catalyst temperatures on the engine test stand exceed the range of temperatures demonstrated in the bench flow study, thus the data was extrapolated to estimate capacities above 550 °C. The storage capacity was estimated, as a function of temperature, for 10%, 25%, 50%, 75% and 100% engine load at 1800 rpm. With knowledge of the catalyst's storage capacity

Table 3.14 – Weighting Factors 5 Mode Emissions Ratings

Mode #	% of Full Load	Time in Mode (min)	Weighting Factors
1	100%	5	0.05
2	75%	5	0.25
3	50%	5	0.30
4	25%	5	0.30
5	10%	5	0.10

Table 3.15 – Conditions for Bench Flow Study

Parameter	Bench Flow Value
LNT catalyst space velocity	30,000 /hr
Oxidation catalyst space velocity	60,000 /hr
Reformer catalyst space velocity	60,000 /hr
Temperature	400, 450, 500, 550° C
NOx	500ppm
CO	500ppm
H2O	13.5%
CO2	6.7%
O2	6.0%
N2	balance

Table 3.16 – Results from Bench Flow Study

Temperature (C)	Capacity @ t10 (g/L)	Capacity @ t50 (g/L)
400	2.1	3.5
450	1.4	2.5
500	0.6	1.3
550	0.3	0.4

(grams) and the engine's NOx flow rate (grams/sec), the 10% and 50% breakthrough times were estimated. Table 3.17 shows the results of these estimates based on a 14 liter LNT catalyst volume. Estimates for the 75% and 100% load points were not made, as interpolations of bench flow data showed trapping capacities falling off to zero at these temperatures.

Table 3.17 – LNT Capacity Estimations

% Load	100%	75%	50%	25%	10%
Temperature (C)	600	580	560	510	440
NOx flow (g/sec)	0.192	0.067	0.037	0.030	0.018
t10 Capacity (g)	-	-	1.96	7.56	21.56
t50 Capacity (g)	-	-	3.08	15.68	37.8
t10 Time (sec)	-	-	53	252	1198
t50 Time (sec)	-	-	83	523	2100

CHAPTER 4 – DEVELOPMENT OF REGENERATION PARAMETERS

As discussed in Chapter 2, NOx are trapped on the barium oxide storage sites in a lean (excess oxygen) environment, forming barium nitrate. In a rich (oxygen depleted) environment, the stored NOx are released by reactions with excess CO and H_2 and is subsequently reduced over the catalyst's platinum loading. The conditions for the rich mode, termed "regeneration", are created by injecting natural gas into the exhaust. The natural gas, which is primarily methane, reacts across an oxidation catalyst to burn out the excess oxygen. A reforming catalyst is then used to further promote the combustion of the highly stable methane into CO and H_2. In addition to controlling the exhaust composition during regeneration, it was also necessary to control the exhaust flow rate across the catalyst. This was done by redirecting the majority of the exhaust through the bypass leg with a set of flow control valves. The ability to control both the exhaust composition and flow rate is critical to successful regeneration of the lean NOx trap. Therefore, a series of experiments were conducted to help gain insight into exhaust flow rates and compositions under various engine conditions and injection parameters. The first of these experiments was designed to determine the flow rate across the catalyst, during regeneration, for a range of engine conditions. The second experiment was to map out the exhaust composition for a range of engine conditions and injection parameters. The final experiment was to determine the oxidation efficiency of methane across the catalysts for a range of exhaust temperatures. This chapter serves to outline the methods and results for each of these experiments.

EXHAUST FLOW CONTROL

Controlling flow through the dual leg exhaust system was crucial for management of the catalyst. When the NOx trap is in the adsorption stage the bypass leg must be closed off, thus directing most of the exhaust across the catalysts. Once the LNT begins to saturate, the majority of the lean exhaust gases must be redirected

through the bypass leg and the reductant is injected. Diverting the majority of the exhaust for regeneration is crucial to LNT management for two reasons. It reduces the oxygen mass flow, thereby minimizing the amount of reductant needed, and consequently reducing the fuel penalty. It also reduces the space velocity across the catalyst, allowing enough time for release of the stored NOx and their subsequent reduction. In bench flow reactor studies conducted at EmeraChem, a space velocity of 5,000 /hr was used during regeneration. Based on a total LNT volume of 14 liters the exhaust flow rate would have to be throttled to 1167 liters/min to achieve similar conditions. The following experiment was used to map out the exhaust flow rate across the catalyst, while the flow control valve was used to restrict the flow.

With the flow control valve in the closed position, the portion of the exhaust that is allowed to pass is termed "slip flow". It was desired to know the rate of this slip flow under various engine conditions. Thus, an experiment was designed to estimate the volumetric slip flow rate by diluting the flow with nitrogen and measuring the change in the exhaust composition.

As shown in Figure 4.1, with the flow control valve partially closed, nitrogen was injected into the throttled exhaust stream at a fixed flow rate. The fraction of the exhaust flow, which crosses the flow control valve, was diluted by the injected nitrogen flow. The dilution ratio could be determined by taking exhaust samples upstream and downstream of the injection. The slip flow rate could then be calculated from the known nitrogen flow rate and the measured dilution ratio. The following control volume analysis (Figure 4.2) was used to derive an equation for the volumetric slip flow rate.

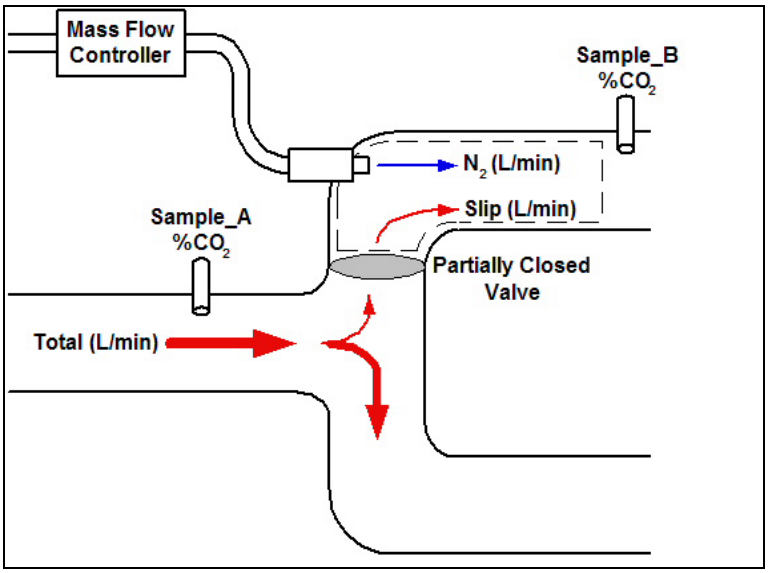


Figure 4.1 – Experimental Schematic for Slip Flow Estimations

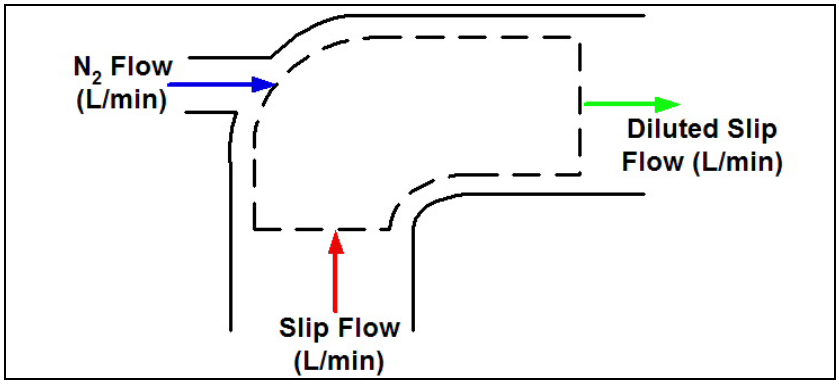


Figure 4.2 – Control Volume for Slip Flow Analysis

The volumetric flow rate of CO_2 into and out of the control volume can be calculated as follows.

$$CO_2_In\left(\tfrac{L}{\min}\right)=\%CO_2_A\times\left[Slip\ Flow\left(\tfrac{L}{\min}\right)\right]$$

$$CO_2_Out\left(\tfrac{L}{\min}\right)=\%CO_2_B\times\left[Diluted\ Slip\ Flow\left(\tfrac{L}{\min}\right)\right]$$

$$=\%CO_2_B\times\left[Slip\ Flow\left(\tfrac{L}{\min}\right)+N_2\ Flow\left(\tfrac{L}{\min}\right)\right]$$

Then an equation for the slip flow rate can be derived by equating the volumetric flow of CO_2 into and out of the control volume.

$$CO_2_In\left(\tfrac{L}{\min}\right)=CO_2_Out\left(\tfrac{L}{\min}\right)$$

$$\%CO_2_A\times\left[Slip\ Flow\left(\tfrac{L}{\min}\right)\right]=\%CO_2_B\times\left[Slip\ Flow\left(\tfrac{L}{\min}\right)+N_2\ Flow\left(\tfrac{L}{\min}\right)\right]$$

$$Slip\ Flow\ \left(\tfrac{L}{\min}\right)=N_2\ Flow\left(\tfrac{L}{\min}\right)\times\left[\frac{\%CO_2_B}{\%CO_2_A-\%CO_2_B}\right]$$

These exhaust flow control experiments were used to determine the slip flow at 10%, 25%, 50%, 75% and 100% load for 1800 rpm. Measurements were taken at various nitrogen flow rates to verify repeatability of the test. Nitrogen flows were controlled with a Hastings mass flow controller. Bottled ultra high purity nitrogen was supplied to the mass flow controller at a constant 80 psi. The results of these tests are presented in Table 4.1 and Figure 4.3. Experimental results for estimating slip flow rates at 10% load are not presented, as they were highly inconsistent.

Table 4.1 – Exhaust Flow Rates During Adsorption and Regeneration

% Load	Slip Flow During Adsorption (L/min)	Slip Flow During Regeneration (L/min)
100	14418	1298
75	11069	905
50	7814	603
25	4419	250

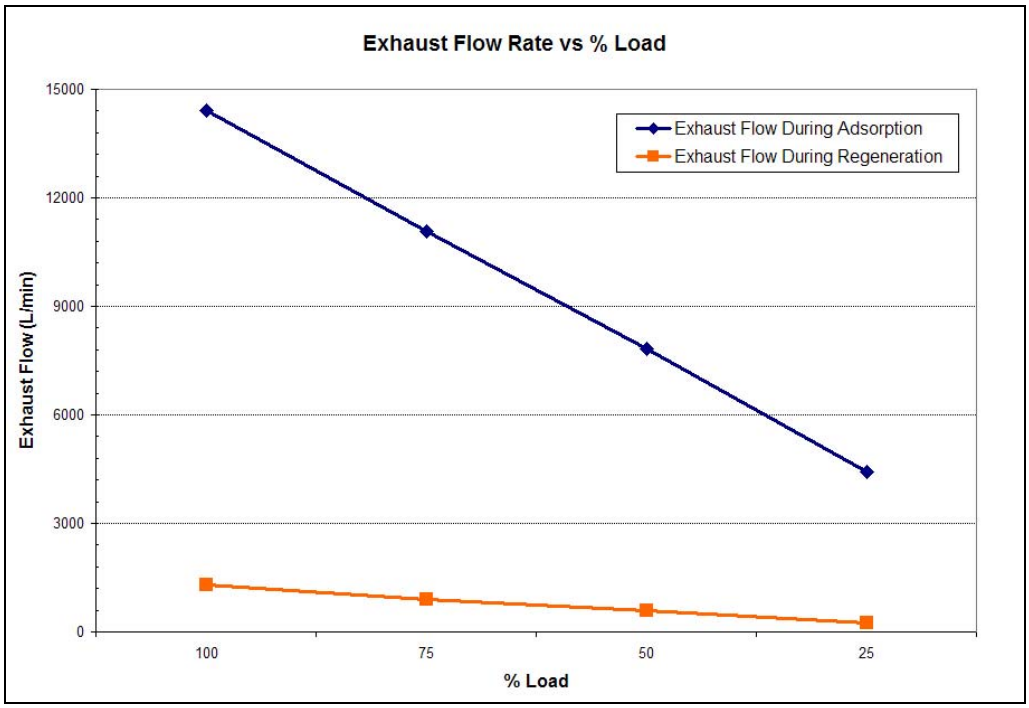


Figure 4.3 – Exhaust Flow Rates During Adsorption and Regeneration

EXHAUST COMPOSITION CONTROL

As with controlling the flow rate across the catalyst, controlling the exhaust composition is also critical to regeneration. Enough reducing agent must be injected to fully burn out the excess oxygen and create the CO and H_2 necessary for regeneration. A universal exhaust gas oxygen sensor (UEGO) placed down stream of the injectors was used to determine the stoichiometry of the exhaust gasses entering the catalyst can. A stoichiometric air-fuel mixture for natural gas combustion has an A/F ratio of 17.2 while the lean burning C Gas Plus engine operates between 21.5 to 24.8 at 1800 rpm. In terms of lambda values, this is 1.25 to 1.44, where 1.00 represents a stoichiometric mixture and less than 1.00 would be rich. The goal of this experiment was to map out the injection parameters necessary to achieve lambda values of 0.5, 0.7 and 0.9 for each of the five load points at 1800 rpm. A 75Hz, 12 volt square wave signal was used to excite the injectors. The signal's duty cycle was the variable used to adjust the overall flow rate, thus controlling the exhaust composition. The following results

present the number of injectors and the duty cycle used to achieve the desired equivalence ratio. As can be seen in Table 4.2, the two injectors at maximum duty cycle could not inject enough reductant to achieve the targeted equivalence ratio of 0.5 at 100% and 75% load. In addition, the fuel penalty was calculated, based on a cycling period of 25 second adsorption (lean operation) followed by a 5 second regeneration (rich operation) with a 3 second injection.

METHANE OXIDATION

Successful regeneration of the LNT depends on the ability of the oxidation and reforming catalyst to combust methane with the excess oxygen present in the lean exhaust. The ability of the catalysts to combust the highly stable methane is partially dependent on the catalyst temperatures. Thus, at lower loads (i.e. lower temperatures), regeneration of the lean NOx trap may become more difficult. The following experiment was intended to assess the dependence of methane oxidation on catalyst temperatures. Exhaust methane concentrations were

Table 4.2 – Exhaust Composition Control

1800 rpm - 25 sec lean - 5 sec regen - 3 sec injection					
% Load	Number of Injectors	Duty Cycle %	Target Lambda	Actual Lambda	Fuel Penalty %
100	2	95	0.5	0.70	2.22%
100	2	95	0.7	0.70	2.22%
100	2	35	0.9	0.90	0.80%
75	2	95	0.5	0.57	3.17%
75	2	65	0.7	0.70	2.09%
75	2	25	0.9	0.90	0.82%
50	2	72	0.5	0.49	3.29%
50	2	38	0.7	0.70	1.71%
50	2	18	0.9	0.90	0.70%
25	2	27	0.5	0.48	2.32%
25	2	16	0.7	0.70	1.29%
25	1	8	0.9	0.91	0.53%
10	1	13	0.5	0.50	1.58%
10	1	8	0.7	0.72	0.80%
10	1	6	0.9	0.90	0.42%

sampled at three locations as depicted in Figure 4.4, Oxi Cat In, Oxi Cat Out and LNT Out. These samples were taken at 8 different load points for 1800 rpm. This gave a range of catalyst temperatures from 550° to 413° C. Table 4.3 gives the reduction efficiencies through the oxidation catalyst and through the end of the aftertreatment system for this range of temperatures. Also shown in the table are the engine out methane concentrations in parts per million. As can be seen in Figure 4.5, the reduction efficiency begins to fall off below 500° C, and the oxidation catalyst becomes nearly ineffective below 450° C. The inability to regenerate the catalyst at lower temperatures presents a challenge for the application of the lean NOx trap aftertreatment system. This poor performance at lower temperatures coupled with the lower NOx storage capacity at higher temperatures creates a narrow temperature window for optimizing system performance. These temperature issues are further illustrated with testing presented in the next chapter.

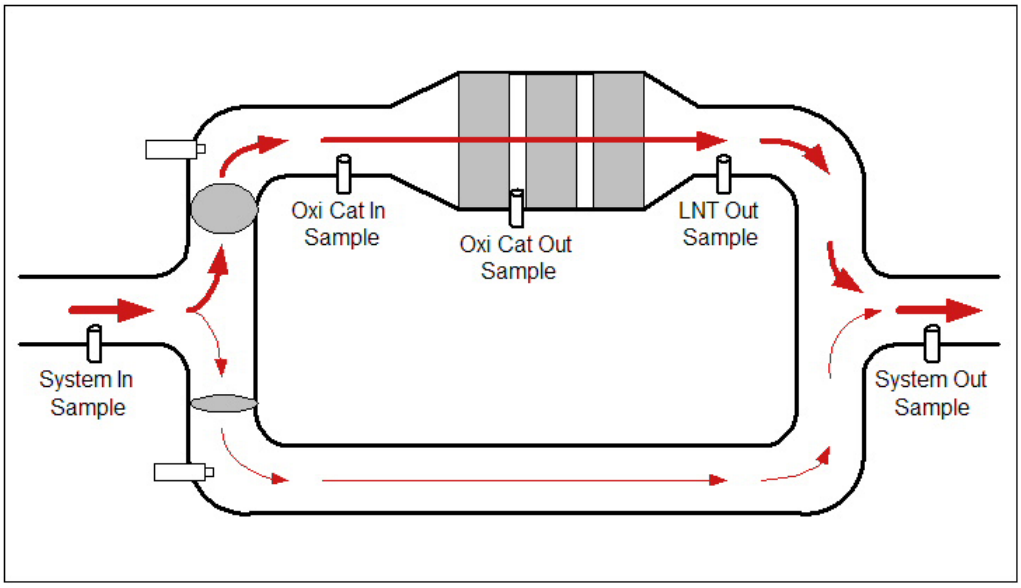


Figure 4.4 – Sample Positions for Methane Oxidation Study

Temp (C)	Oxi Cat Out CH4 Reduction	LNT Out CH4 Reduction	Engine Out CH4 (ppm)
413	0.4%	19.5%	1180
452	6.7%	26.9%	1242
482	18.7%	34.6%	1212
508	26.7%	35.3%	1171
522	27.3%	33.3%	1219
538	26.0%	35.3%	1162
548	27.1%	34.6%	1134
550	28.8%	33.2%	1103

Table 4.3 – Methane Oxidation Results

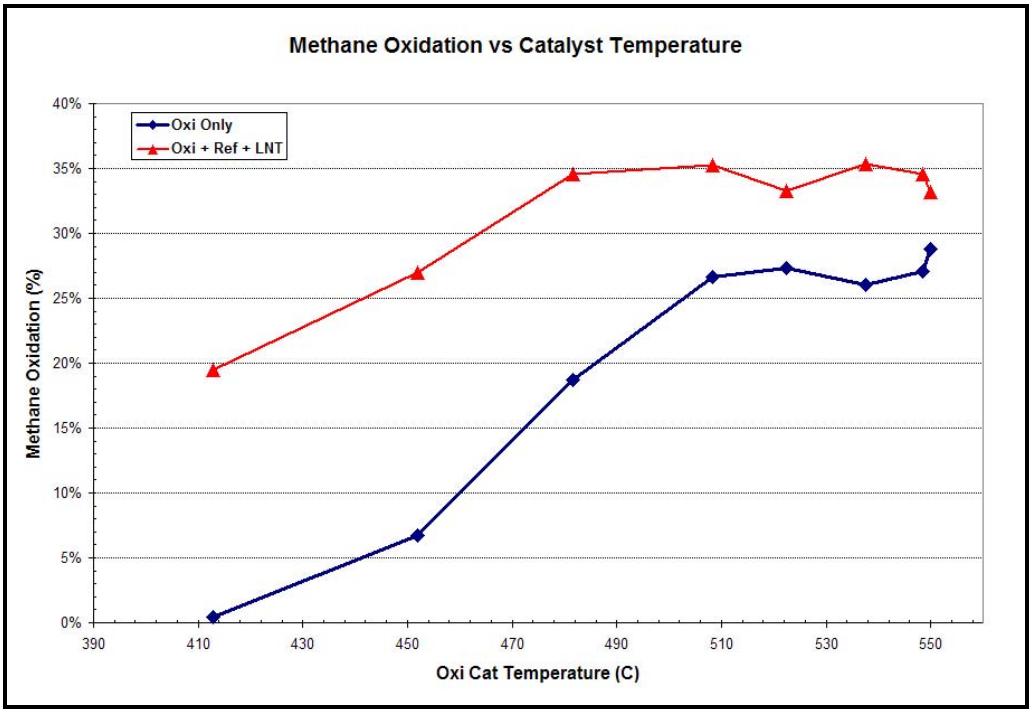


Figure 4.5 – Methane Oxidation vs. Catalyst Temperature

CHAPTER 5 – LEAN NOx TRAP EVALUATION

The primary focus of this research was to evaluate the application of lean NOx trap catalysis to a lean burn natural gas engine. The key technical issues to be addressed were the utilization of natural gas for regeneration, as methane is difficult to catalytically combust, and the storage capacity of the catalyst under the high exhaust temperatures of natural gas combustion. As will be demonstrated in the following experiments, methane more readily reacts at higher temperatures, yielding better results for regeneration, while the LNT has higher storage capacities at lower temperatures. This leads to a narrow temperature window where the system will exhibit maximum performance. Testing of the aftertreatment system was conducted under steady state conditions at 1800 rpm with 10%, 25% and 50% engine loads; the catalyst temperatures under these conditions were 440, 510 and 560° C, respectively. Testing at 75% and 100% engine loads was avoided because high temperatures could potentially damage the catalysts. The remainder of this chapter serves to describe the procedures and results for these tests and concludes with an evaluation of the exhaust aftertreatment system.

LEAN NOx TRAP CYCLE

Results of a typical test with the lean NOx trap system are shown in Figures 5.1 through 5.3. During this test, the engine was operated at 1800 rpm and 50% load. The catalyst was managed with 120 second sorption periods and 20 second regenerations. The exhaust flow rates were 297 scfm during sorption periods and 21 scfm during regeneration periods. This correlates to LNT space velocities of 36,042/hr and 2,550/hr based on 14 liters of catalyst. The 140 second catalyst management cycle, for which three periods are shown in the following figures, was repeated under steady state engine conditions. The first of these figures shows the NOx levels measured into and out of the dual leg system. Locations of the “system in” and “system out” sample points are shown in Figure 4.4.

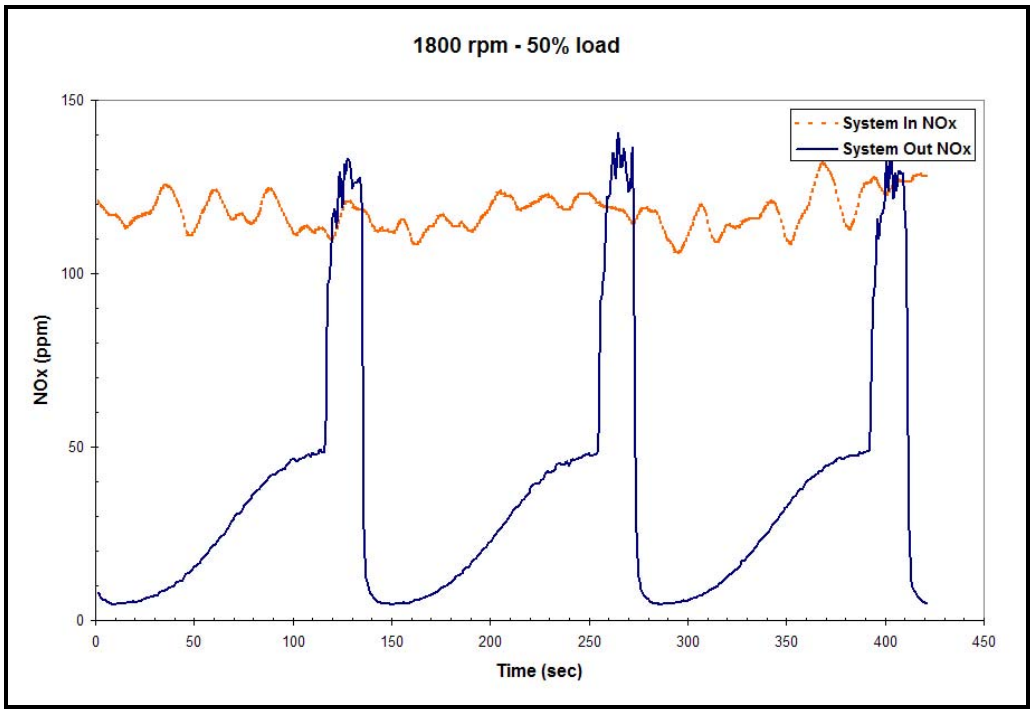


Figure 5.1 – Typical NOx Profiles

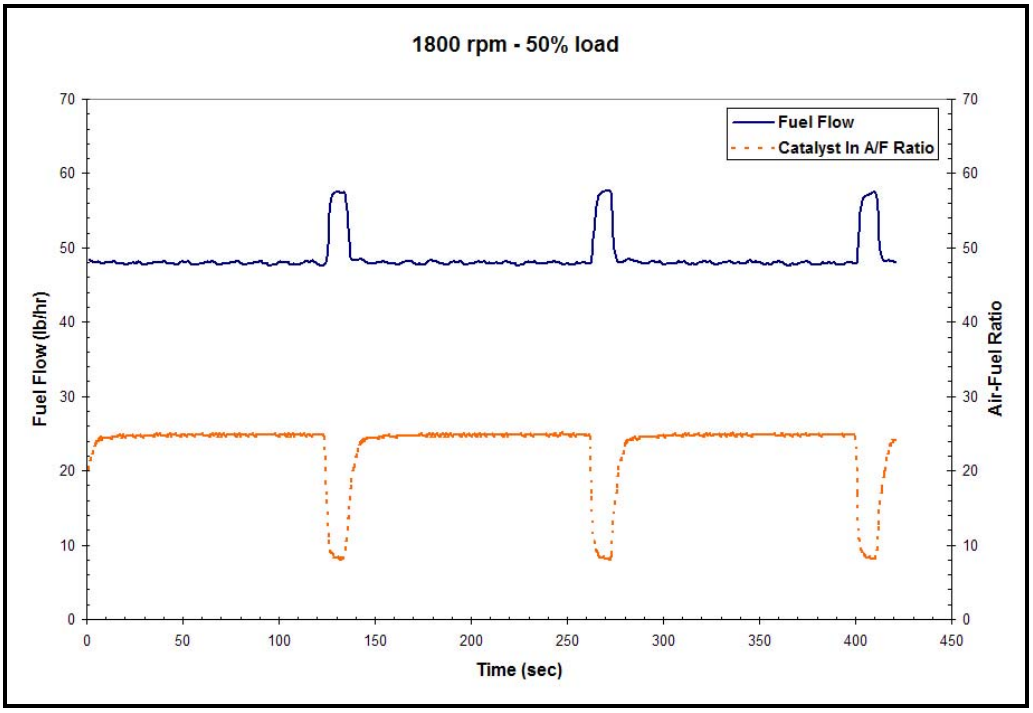


Figure 5.2 – Fuel Flow and Exhaust Stoichiometry

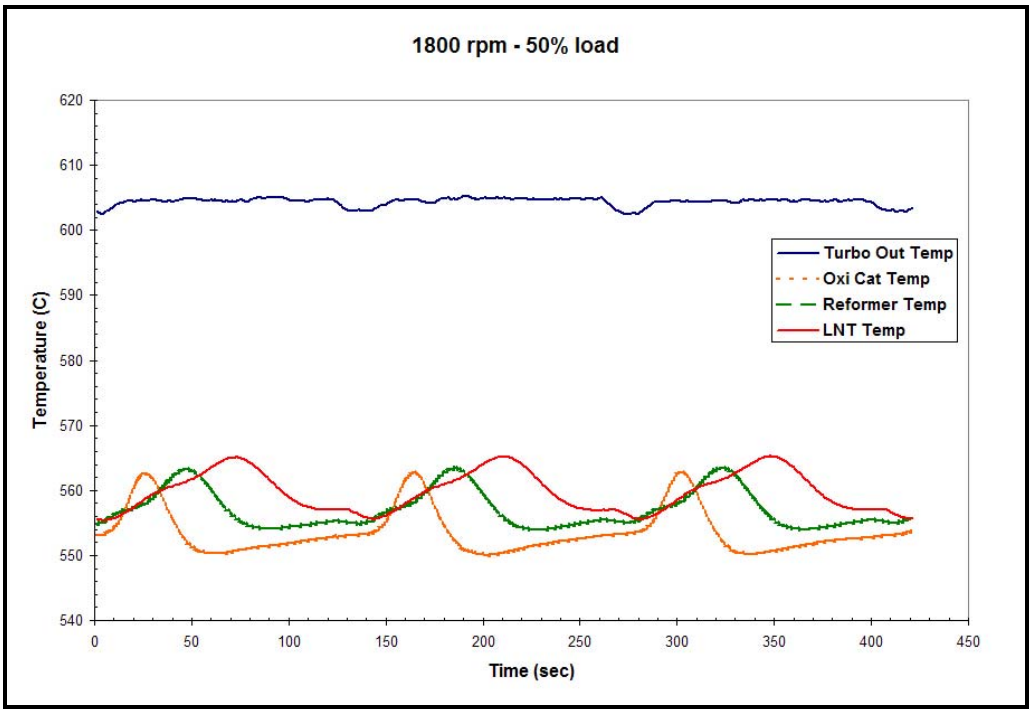


Figure 5.3 – Catalyst Temperatures

The system in NOx levels average 120 ppm, while the system out NOx levels vary through the management cycle. Directly following the regeneration sequence, system out NOx levels reach their lowest levels of 5 ppm. This represents an instantaneous trapping efficiency of 96%. As the sorption period continues, and storage sites on the catalyst become occupied, NOx slip begins to occur. By the end of the 120 second sorption, the catalyst is only trapping 58%, with system out NOx levels reaching 50 ppm. This is followed by the 20 second regeneration period. Of the 20 second regeneration period, fuel was injected for the first 10 seconds. The remaining 10 seconds was a delay in switching the valves. This valve delay throttles the exhaust flow across catalyst long enough for the reductant to completely pass through the catalysts. The geometry of the exhaust aftertreatment system is a dual leg system with one leg serving as a bypass during catalyst regeneration. This single chamber system allows all of the engine out NOx to circumvent the LNT during the 20 second regeneration. In a single chamber system, this fraction of exhaust which goes untreated inevitably

leads to a lower overall NOx reduction efficiency. However, in an actual application this single chamber system could be expanded into a two chamber system by adding a catalyst to the bypass leg.

For the purpose of this study the catalysts are evaluated by their trapping efficiencies. The trapping efficiency is defined as the percentage of NOx stored by the catalyst during the sorption period. The catalyst's trapping efficiency varies with changes in engine conditions and catalyst management parameters.

Figure 5.2 shows the air-fuel ratio measured directly upstream of the oxidation catalyst and the fuel flow to both the engine and injectors. With an air-fuel ratio of 17.1 representing stoichiometric conditions, it can be seen here that lean conditions exist through the sorption period. Following the injection and closing of the valve, an oxygen depleted, reductant rich exhaust condition is created in which the stored NOx can be released and reduced. Another crucial parameter for system evaluation is the amount of fuel required for regeneration. As the energy from this fuel supplies no power to the end user, it is considered a fuel penalty and is defined as the percentage of fuel injected to that which is supplied to the engine. During the injection, an instantaneous fuel penalty of 20% is measured. However, over a full cycle, this is only a 1.7% fuel penalty.

Figure 5.3 shows temperatures at the cores of the oxidation, reformer and lean NOx trap catalysts as well as the exhaust temperature at the turbo outlet. The temperature oscillations of the catalyst bricks are due to the exothermic oxidation of the methane. The wide temperature difference between the turbo outlet and the catalyst bricks is due to heat loss along the exhaust pipe.

OPTIMIZING REGENERATION PARAMETERS

The trapping efficiency as well as the associated fuel penalty are primary parameters for evaluating the aftertreatment system. These evaluation parameters

are highly dependent on engine conditions (i.e. exhaust temperatures and NOx flow rates) as well as the conditions used for catalyst management (i.e. injection rates and sorption period). The system was evaluated at a matrix of injection rates and sorption periods for 10%, 25% and 50% engine loads. The results from this test matrix revealed the optimal conditions for catalyst management at a given engine condition. The injection rate was used to control the exhaust stoichiometry during regeneration. Oxygen depleted exhaust with lambda values of 0.5, 0.6, 0.7 and 0.8 were targeted for the test matrix. A 10 second injection duration was used for all testing. After the injection sequence, switching of the valves was delayed until the stoichiometry downstream of the catalyst reached lean conditions (lambda > 1.0). This ensured enough time for the reductant to pass through the catalysts. The performance was allowed to stabilize with sorption periods of 30, 60, 120 and 240 seconds for each targeted lambda value.

Figures 5.4 through 5.6 below show the results of the test matrix for engine conditions at 50% load. The four sorption periods are shown across the x-axis and each curve represents a different injection rate. A 60 second sorption period yields greater than 90% trapping efficiencies for all lambda values. Beyond this period the trapping efficiencies begin to drastically fall off. A shorter sorption period of 30 seconds yields modest gains in trapping efficiencies, yet results in markedly higher fuel penalties. In optimizing the regeneration strategy it is often necessary to compromise one performance parameter for gains in another. Because the ARES program targets NOx ratings of 0.1 g/hp-hr, this was the deciding factor in determining the optimal parameters for regeneration. Figure 5.6 shows that injecting for 0.6 lambda with a sorption period of 60 seconds achieves a 0.088 g/hp-hr NOx rating. This was just within the ARES target, thus it was chosen as the optimal regeneration scheme. This optimal scheme for steady state conditions at 50% engine load results in a 2.84% fuel penalty. Figure 5.6 shows the NOx profiles through 5 cycles for this optimal regeneration scheme.

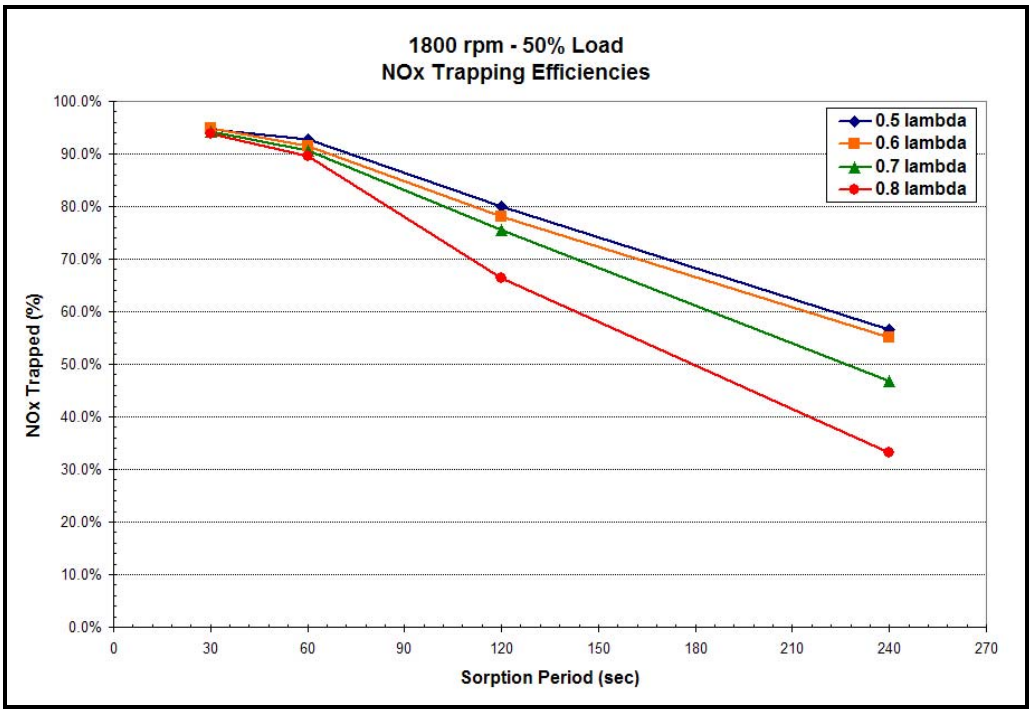


Figure 5.4 – 50% Load NOx Trapping Efficiencies

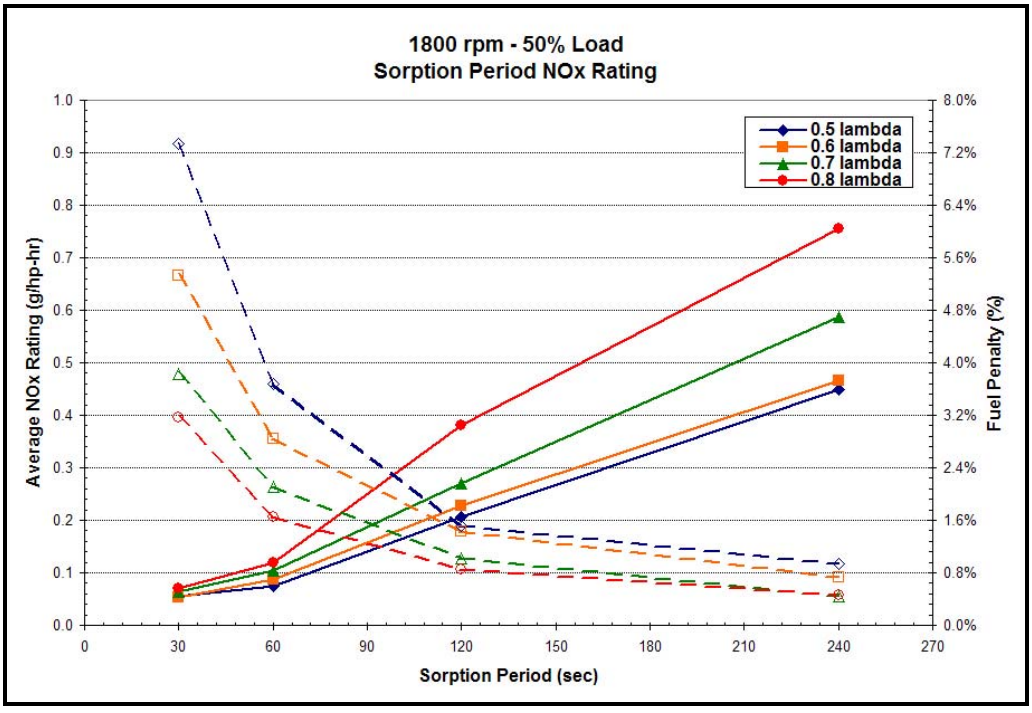


Figure 5.5 – 50% Load NOx Ratings and Fuel Penalties

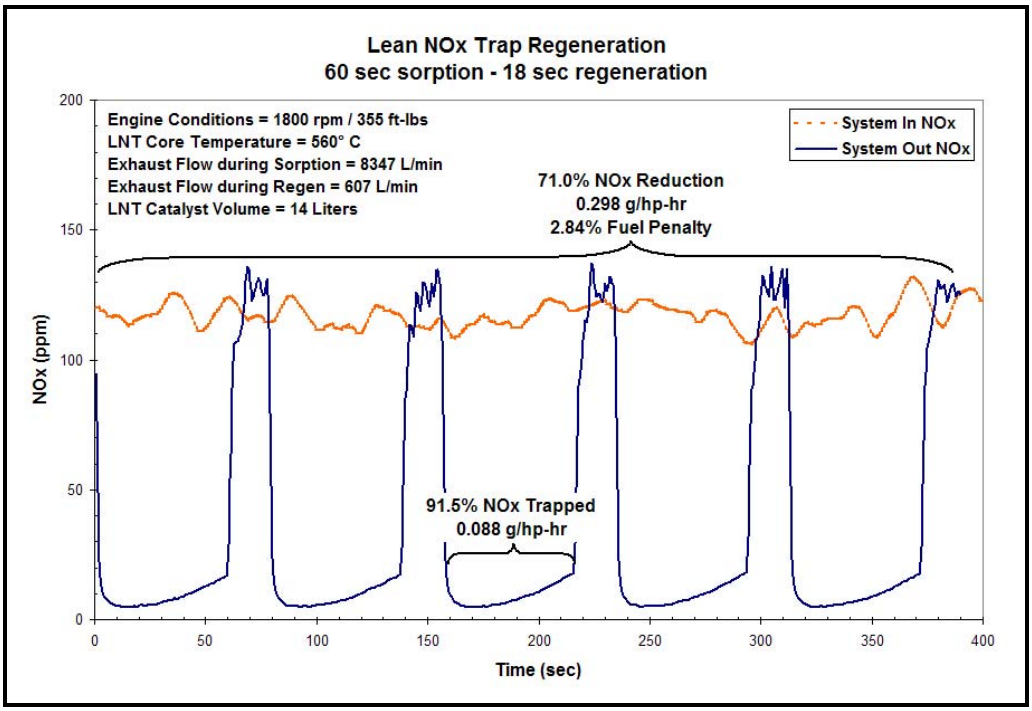


Figure 5.6 – 50% Load NOx Profiles for Optimal Regen

Figures 5.7 through 5.9 below show the results of the test matrix for engine conditions at 25% load. A 120 second sorption period with injections for 0.5 lambda yields trapping efficiencies higher than 97% and NOx ratings as low as 0.05 g/hp-hr. These optimal regeneration conditions for steady state conditions at 25% engine load lead to a 1.62% fuel penalty. NOx profiles through 5 regeneration cycles for these optimal conditions is shown in Figure 5.9. It is important to note that the optimal adsorption period for 25% load (120 seconds) is twice what it was for 50% load (60 seconds). This is in part due to the lower catalyst temperatures at 25% load. The storage capacity of the lean NOx trap is a function of its temperature. Thus, as the exhaust temperatures increase with increasing load, the catalyst's storage capacity will decrease as will the effective adsorption period. This concept is explored in more detail later in this chapter.

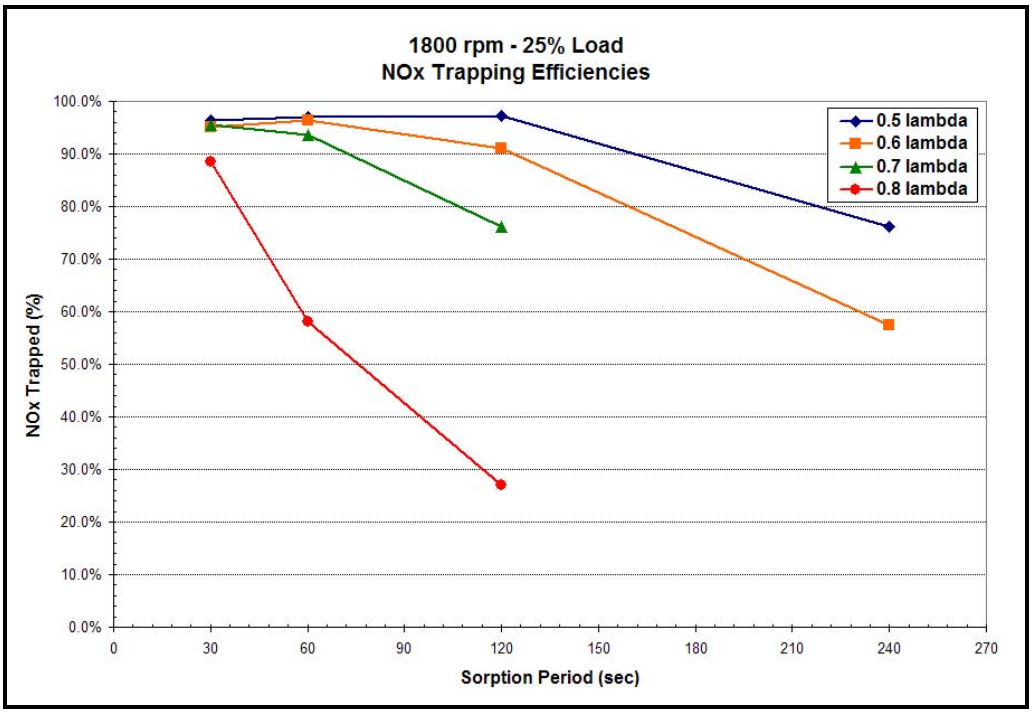


Figure 5.7 – 25% Load NOx Trapping Efficiencies

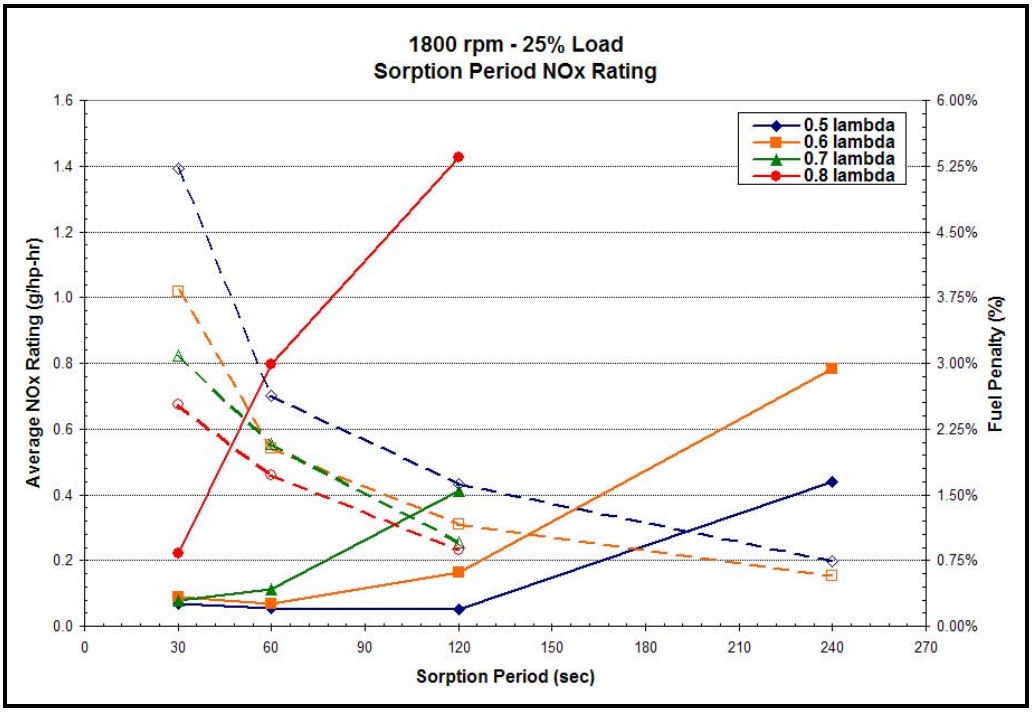


Figure 5.8 – 25% Load NOx Ratings and Fuel Penalties

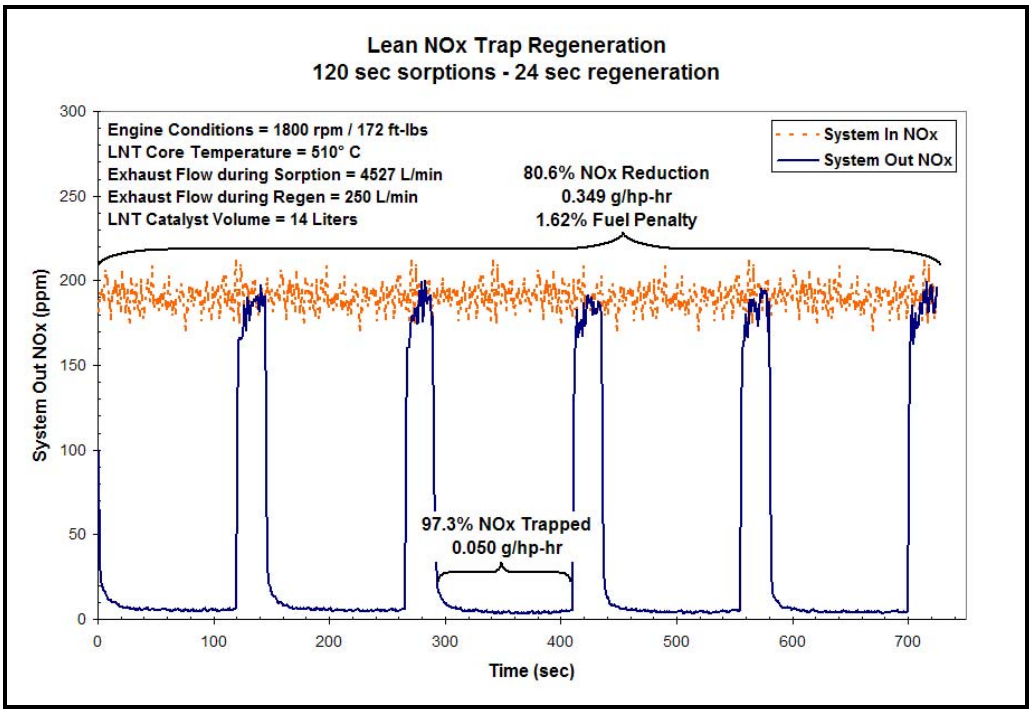


Figure 5.9 – 25% Load NOx Profiles for Optimal Regen

Figures 5.10 through 5.12 below show the results of the test matrix for engine conditions at 10% load. A 30 second sorption period with 0.5 lambda yields a 91% trapping efficiency. With an engine out NOx rating of 5.00 g/hp-hr, this trapping efficiency achieves an average rating of 0.47 g/hp-hr and instantaneous ratings of 0.36 g/hp-hr. These results fall well short of the ARES goal. These conditions resulted in a 3.66% fuel penalty. Besides not achieving high enough trapping efficiencies at 0.5 lambda, the catalyst would not regenerate beyond 120 second sorption periods. Trapping efficiencies dropped off to zero, thus the data is not presented in the following figures. Similar results occurred beyond 60 second sorptions for 0.6 lambda and beyond 30 second sorptions for 0.7 and 0.8 lambda. There are two explanations for this inability to regenerate the catalyst at 10% engine load. The first, is that low catalyst temperatures hinder the reforming of methane into the H_2 and CO necessary for regeneration. This was demonstrated by the methane oxidation study presented in Chapter 4.

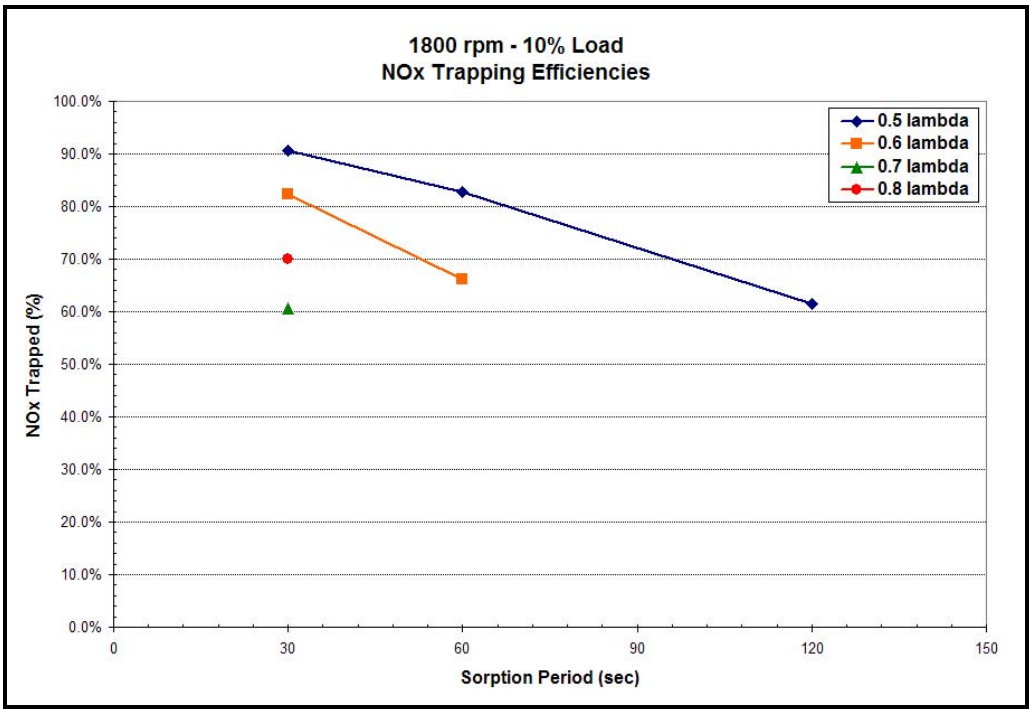


Figure 5.10 – 10% Load NOx Trapping Efficiencies

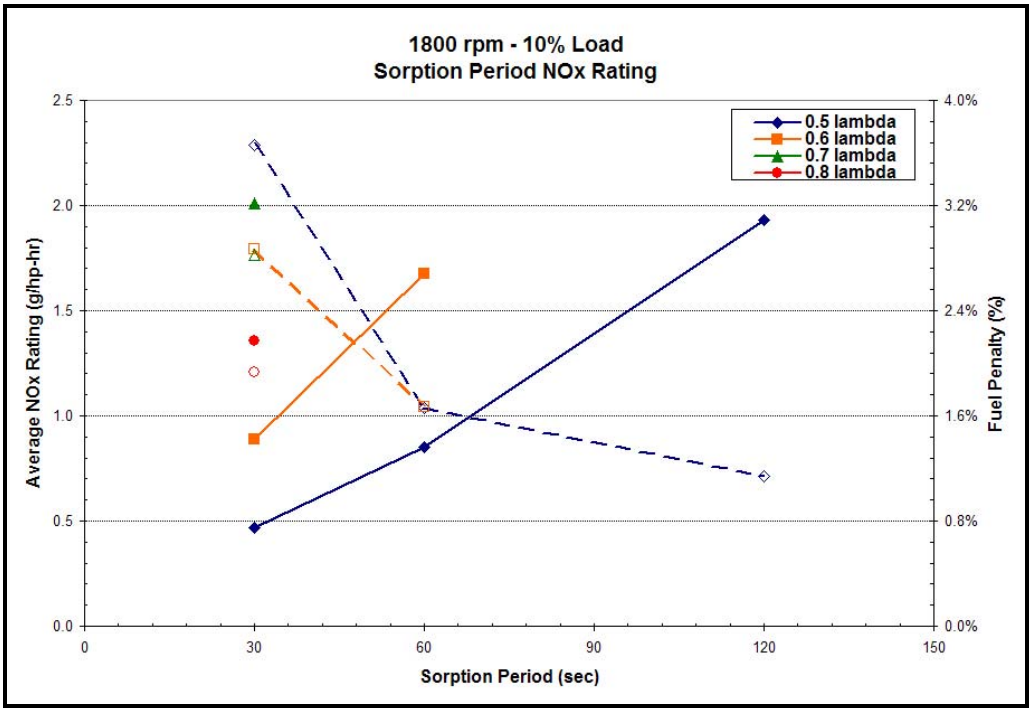


Figure 5.11 – 10% Load NOx Ratings and Fuel Penalties

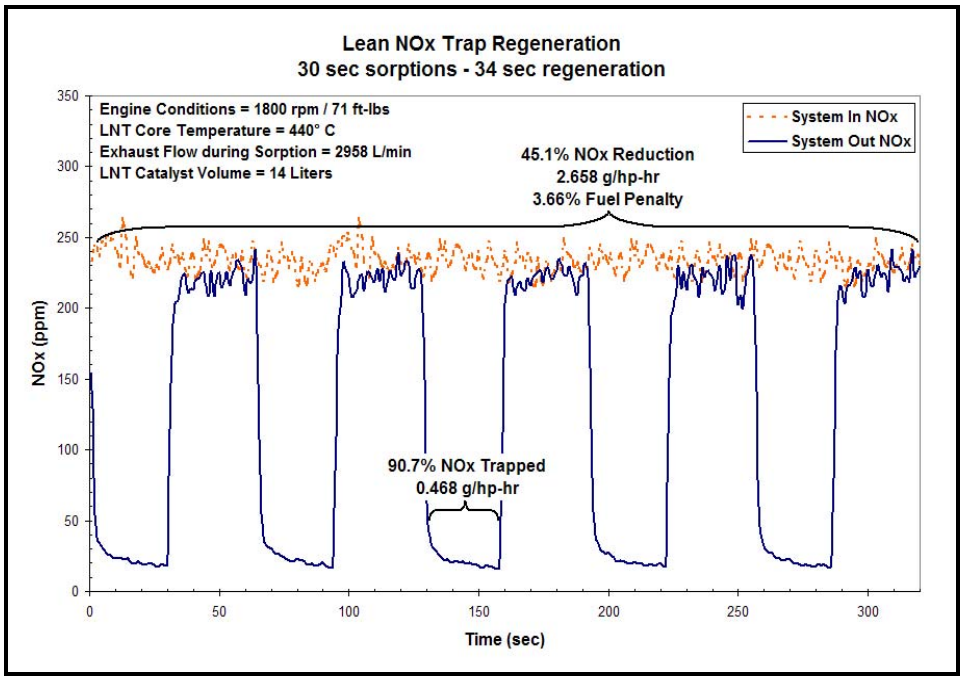


Figure 5.12 – 10% Load NOx Profiles for Optimal Regen

At 10% load catalyst temperatures are 440° C. At these low temperatures, the oxidation catalyst has not reached its light off temperature as indicated in Figure 4.5. Thus, not enough of the injected methane is being catalytically combusted to create the conditions necessary for regeneration. The second explanation for poor performance is that the mass flow of exhaust, which must slip past the closed valve for regeneration, becomes too low. Although the targeted lambda values are met, the mass of fuel injected is simply not enough to fully regenerate a saturated catalyst. This second explanation is explored with further testing and the results are presented in the following section.

ADJUSTING FLOW RATES FOR REGENERATION

The exhaust flow that slips past the valve during regeneration becomes very low at 10% load. This results in a low injection of reductant to attain the desired stoichiometry. The poor catalyst performance at 10% load could result from an insufficient mass of fuel injection to regenerate the catalyst. A potential solution to this problem would be to prevent the valve from fully closing, thus allowing

higher mass flow rates of exhaust during regeneration. This would result in higher injection rates of fuel necessary to attain the desired stoichiometry. Segments of the test matrix were repeated for this scenario, in which the valve was left wide open during regenerations. Fuel injection rates were set to achieve 0.7 lambda for 60, 120 and 240 second sorption periods. Figures 5.13 through 5.15 show results from these tests.

As can be seen in Figure 5.13, the trapping efficiency reached 97.4% for 0.7 lambda and 120 second sorptions. As the original test matrix revealed the catalyst would not even regenerate under these conditions with the valve fully closed during regeneration. The 97.4% trapping efficiency achieved a 0.129 g/hp-hr NOx rating and instantaneous ratings as low as 0.10 g/hp-hr. These conditions resulted in a 2.62% fuel penalty. The catalysts trapping efficiency is maintained at 95.6% with 240 second sorptions. These conditions yielded fuel penalties as low as 1.05%. These results prove that the position of the flow control valve during regeneration can play a role in further optimizing the system. This is particularly true for lower loads, and is recommended as a next step in LNT evaluation studies.

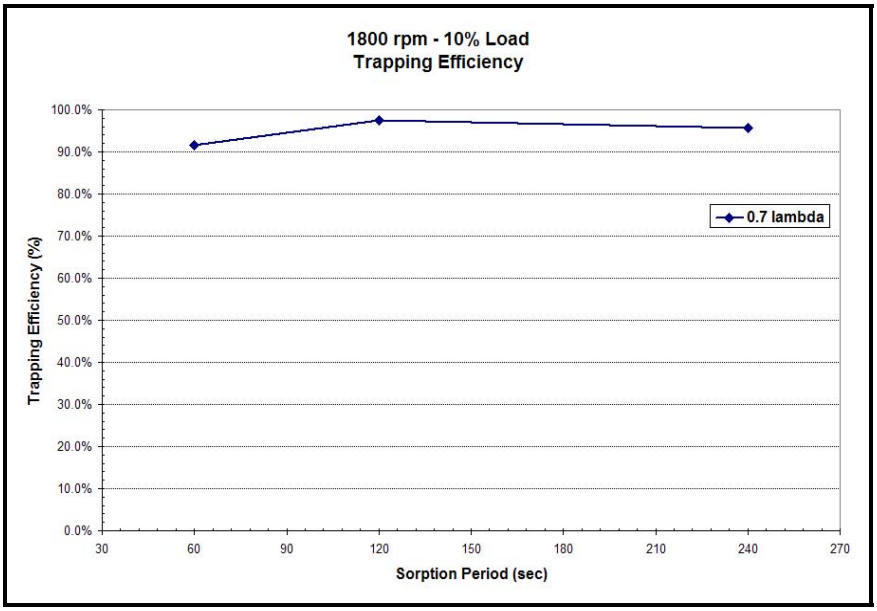


Figure 5.13 – 10% Load NOx Trapping Efficiencies with Full Slip Flow

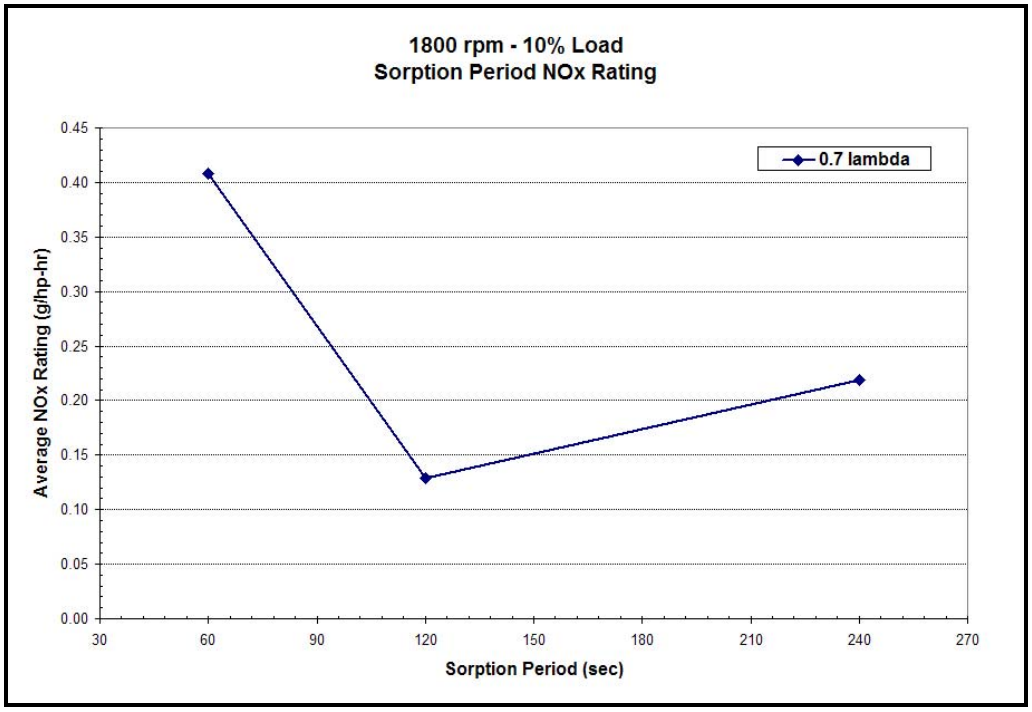


Figure 5.14 – 10% Load NOx Ratings with Full Slip Flow

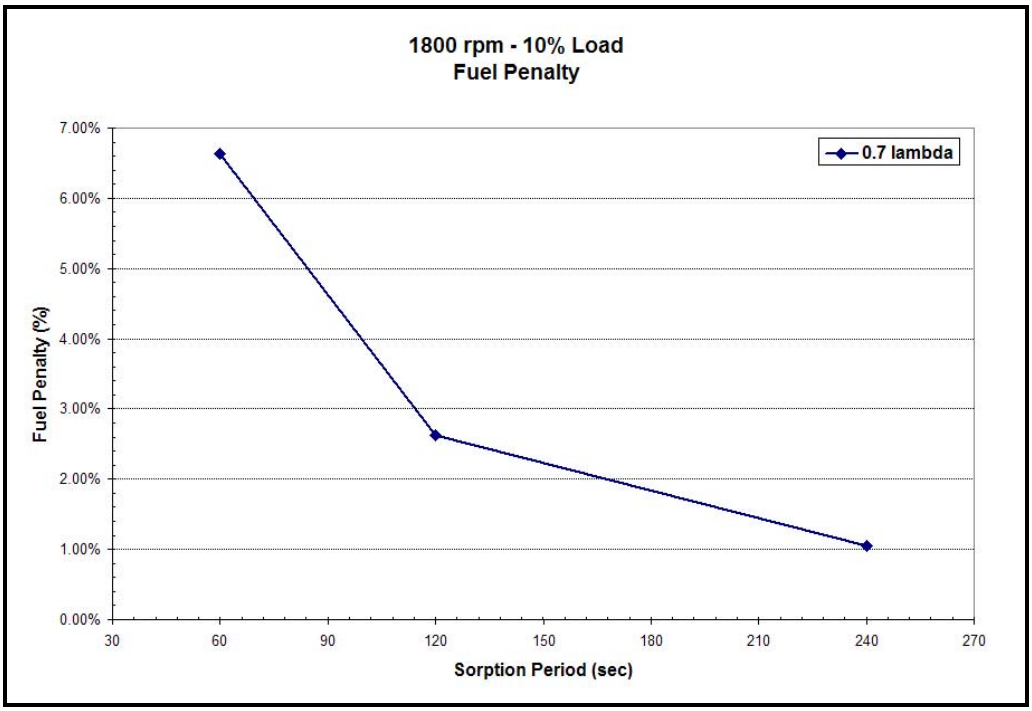


Figure 5.15 – 10% Load Fuel Penalties with Full Slip Flow

NOx STORAGE CAPACITIES

The previous section outlined experiments designed to find the optimal injection rates and sorption periods for catalyst management, and presented an evaluation of the system based on trapping efficiencies and fuel penalties. Another critical characteristic in evaluating a LNT catalyst is its capacity to store NOx. NOx storage capacity is defined as the mass of NOx (as NO_2) stored on the catalyst during the sorption period, until trapping efficiencies fall below 90%. Typically, the capacity is normalized per catalyst volume, giving it units of grams per liter. As stated previously, the storage capacity of a Lean NOx Trap is a function of catalyst temperatures. Thus, thermal management becomes a key factor in optimizing the exhaust aftertreatment system. It is desirable to maximize capacities because this can decrease the catalyst volume required for a particular application, thus reducing capital costs. Higher capacities also result in longer periods between catalyst regeneration thus reducing fuel penalties. This section investigates NOx storage capacities as a function of catalyst temperatures.

For this experiment, the storage capacity of the LNT was tested at three different catalyst temperatures. The aftertreatment system was operated with the optimal regeneration parameters found from the test matrix for 10%, 25% and 50% engine loads until catalyst temperatures stabilized to their respective temperatures; 440° C, 510° C and 560° C. The regeneration sequence was then stopped and the catalyst was allowed to adsorb until trapping efficiencies fell below 90%. Analysis of the results yielded Figure 5.16, which shows the dependence of the NOx storage capacity on catalyst temperatures. The predicted storage capacity from bench flow reactor and baseline engine data, as presented in Chapter 3, are also shown. Because they were extrapolated from experiments with more controlled conditions, results for predicted storage capacities is higher than actual storage capacities. Nevertheless, both show the same general trend of decreasing capacities with increasing temperatures. Comparing the temperature dependence of the LNT for storage capacity (Figure 5.16), with the temperature dependence of the oxidation catalyst for methane oxidation (Figure 4.5), reveals a narrow temperature window for optimizing performance.

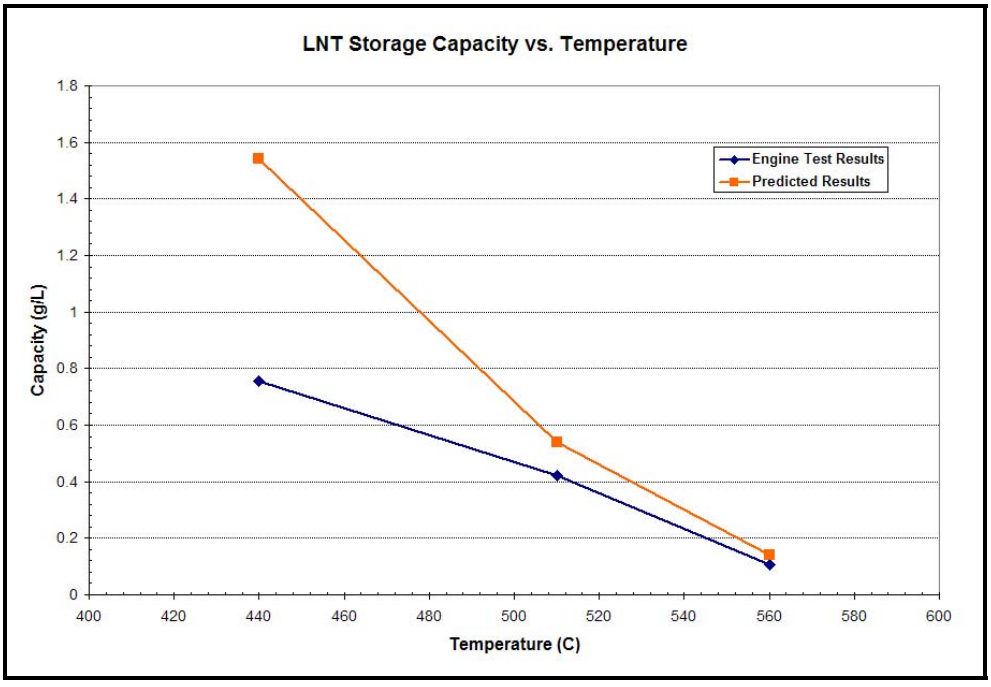


Figure 5.16 – LNT Storage Capacity vs. Temperature

FIXED TEMPERATURE ADSORPTION

Because the LNT and the oxidation catalyst require different temperature ranges for optimal performance, one potential solution would be to physically separate the two catalyst bricks. Placing the oxidation catalyst closer to the outlet of the turbocharger would allow it to be maintained at higher temperatures for methane oxidation. Placing a waste heat recovery system in front of the LNT would allow it to be maintained at a lower temperature for higher NOx storage capacities. Ideally, the LNT would be maintained at a constant temperature regardless of engine load. The following experiment was used to simulate such a scenario. Here, the aftertreatment system is operated with the optimal regeneration parameters for 25% engine load. Once the catalyst temperatures stabilize to 510° C, the engine load is changed to 50%, the regeneration sequence is stopped, and the catalyst immediately begins to adsorb. By doing this, the NOx flux from the engine has been changed to that of the higher load, but the catalyst temperatures have not been given time to change. Thus, the catalyst is adsorbing NOx at the higher engine load but with a constant 510° C. The same procedure was repeated for each engine load. The average NOx rating for the 5 engine modes was calculated until the trapping efficiency fell below 90%. Figure 5.17 shows these average NOx ratings, as well as minimum NOx ratings and NOx flux rates for each engine mode. These results show that when the LNT adsorbs at a constant 510° C, NOx reduction is possible at higher engine loads. Even with the high NOx flow rates an average NOx rating of 0.17 g/hp-hr and instantaneous ratings of 0.06 g/hp-hr are achievable at 75% load. At 100% load average ratings of 0.63 g/hp-hr and instantaneous ratings of 0.17 g/hp-hr are possible. These results demonstrate the potential improvements to be gained by a better thermal management system for the catalyst.

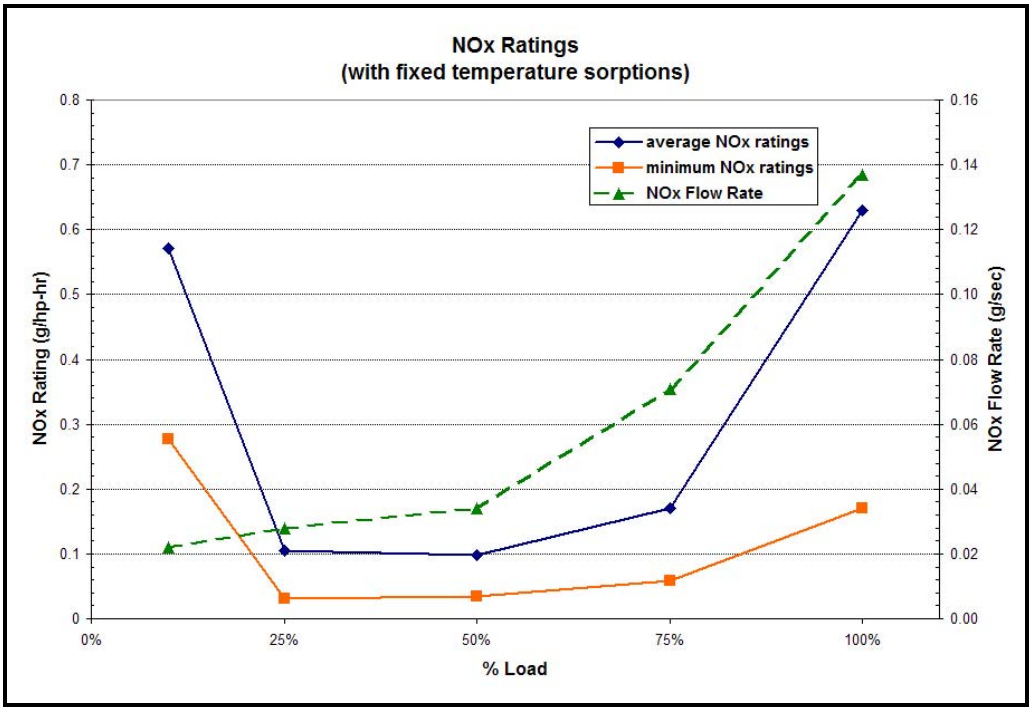


Figure 5.17 – NOx Ratings with Fixed Temperature Adsorption

METHANE UTILIZATION

Experiments in Chapter 4 proved that the oxidation catalyst could successfully combust methane at high enough temperatures. However, in addition to burning out excess oxygen through methane combustion, the rich combustion products CO and H_2 must be formed. The following experiments explored the production and utilization of CO for the range of injection rates used in the test matrix. These experiments were conducted at 25% and 50% engine loads, where catalyst bricks are above their light off temperature. CO levels were measured at three positions along the catalyst chamber during the regeneration sequence; Oxi Cat In, Oxi Cat Out and LNT Out as indicated in Figure 4.4. Figures 5.18 and 5.19 show the grams of CO at each of these positions when injecting for lambda values of 0.5, 0.6, 0.7, 0.8 and 0.9. The results show an increase in CO levels measured at the Oxi Cat Out position as exhaust entering the catalyst becomes richer. For 50% load CO production stabilizes beyond 0.7 lambda. CO levels measured at the LNT Out position are consistently lower than those measured at the Oxi Cat In position. This indicates that the Lean NOx Traps are utilizing some of the CO for regeneration. For 50% engine load, the quantity of CO produced at 0.9 lambda, is small enough that it is entirely consumed by the regeneration mechanism. Similarly, for 25% engine load, all of the CO produced at 0.8 and 0.9 lambda is consumed. Unlike CO levels sampled at the Oxi Cat Out position, CO levels sampled at LNT Out do not taper off beyond 0.7 lambda. This indicates that the reformer catalyst is also producing CO. Because of the catalyst can assembly, it was not possible to access a sample point between the reformer catalyst and the LNT. A more in-depth investigation of methane utilization would require sampling CO levels after the reformer, and is recommended as a next step in methane utilization studies.

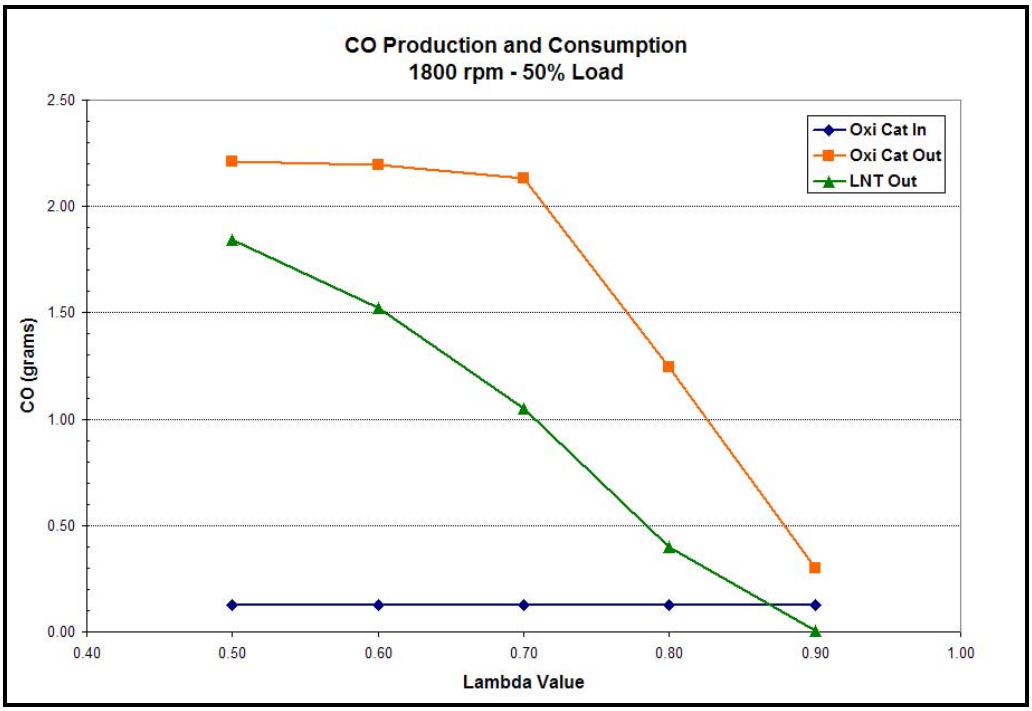


Figure 5.18 – 50% Load CO Production and Consumption

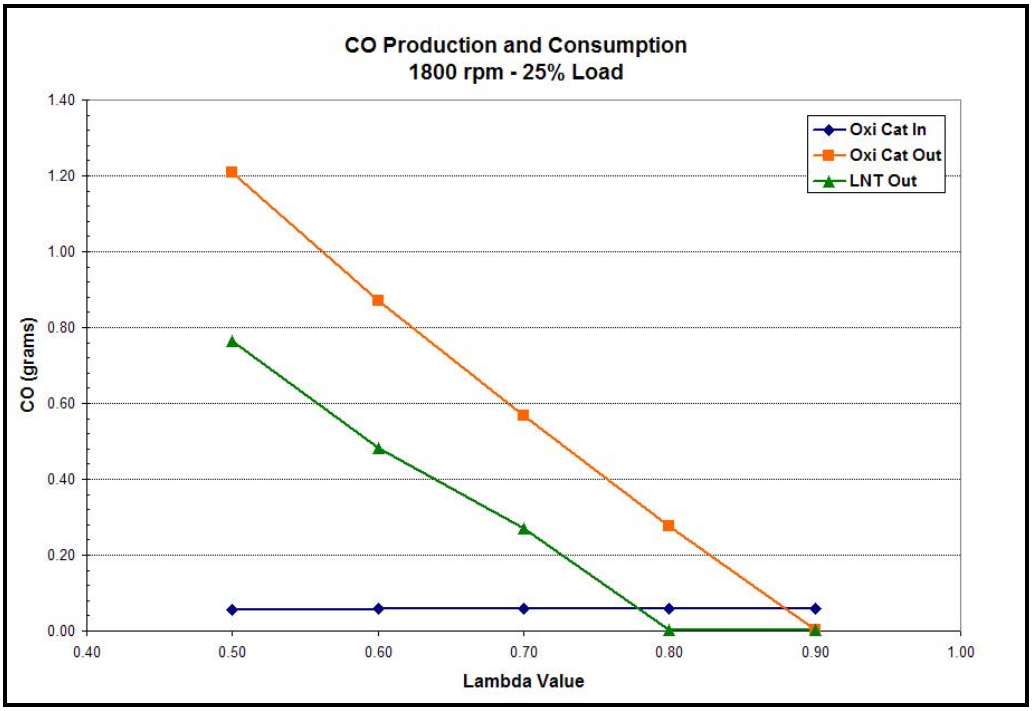


Figure 5.19 – 25% Load CO Production and Consumption

CHAPTER 6 – CONCLUSIONS

The premise of this study was to explore the feasibility of applying a lean NOx trap catalyst to a lean burn natural gas engine. The goal of the research was to optimize the performance of the LNT based on trapping efficiencies and fuel penalties. Additional studies were used to characterize the system's dependence on temperature.

Optimization tests showed the catalyst could trap 97.3% of the NOx at 25% engine load and 91.5% at 50% engine load. These efficiencies achieved respective NOx ratings of 0.05 g/hp-hr and 0.09 g/hp-hr and fuel penalties below 3%. This proves the potential for LNT technology to reach the ARES targeted 0.10 g/hp-hr NOx rating in natural gas applications. However, temperature issues arose at the lower and higher engine loads. Low temperatures at 10% load hindered the oxidation catalyst's ability to break down the methane, while the storage capacity of the LNT falls off at the higher temperatures of 75% and 100% load. Other tests at 10% load showed that the position of the flow control valve during regeneration can play a role in further optimizing the performance.

Methane oxidation tests showed the oxidation catalyst's efficiency versus a sweep of catalyst temperatures. These tests found a light off temperature of around 500° C for the oxidation catalyst. Methane utilization tests showed the production and consumption of CO by the oxidation catalyst and LNT during regeneration. These tests prove that the oxidation catalyst is successfully producing CO for regeneration. However a more in depth analysis of the methane utilization would require sampling after the reformer catalyst. It would also be useful to measure H_2 production and consumption during regenerations.

Capacity tests showed the NOx storage capacity of the LNT versus a sweep of catalyst temperatures. These tests found that any reasonably effective capacity for NOx storage is lost above 560° C. This loss in capacity at higher temperatures

and loss of methane utilization at lower temperatures created a narrow temperature window in which the performance could be optimized. A potential solution to this problem would be to separate the oxidation catalyst from the LNT. Moving the oxidation catalyst closer to the turbocharger would allow it to be maintained at higher temperatures. Placing a waste heat recovery system in front of the LNT would allow it to be maintained at a lower temperature.

BIBLIOGRAPHY

BIBLIOGRAPHY

[1] Zheng, M., Mirosh, E., Liu, B., Checkel, M.D., Hayes, R.E., "Experimental and Modeling Study of Variable Cycle Time for a Reversing Flow Catalytic Converter for Natural Gas/Diesel Dual Fuel Engines", SAE Paper No. 2000-01-0213, Warrendale, Pennsylvania: Society of Automotive Engineers, Inc., 2000.

[2] Fussel, Lori M., Jeffrey W. Hodgson, and David K. Irick. "Automotive Engines and Vehicles" Encyclopedia of Environmental Analysis and Remediation, New York: John Wiley and Sons, Inc., 1998.

[3] Stone, Richard. Introduction to Internal Combustion Engines. Warrendale, Pennsylvania: Society of Automotive Engineers, Inc., 1999.

[4] Turns, Stephen R. An Introduction to Combustion, Concepts and Applications. New York, NY: McGraw-Hill, Inc., 2000.

[5] Rubin, Edward S. Introduction to Engineering and the Environment. New York, NY: McGraw-Hill, Inc., 2001.

[6] Sher, Eran. Handbook of Air Pollution from Internal Combustion Engines, Pollution Formation and Control. Boston: Academic Press, 1998.

[7] Wikipedia, "Acid Rain" http://en.wikipedia.org/wiki/Acid_rain

[8] Boubel, Richard W., Fox, Donald L., Fundamentals of Air Pollution. San Diego: Academic Press, 1994.

[9] Zhang, G., Pflung, A., Raine, R.R., "Comparison of Emissions from Natural Gas and Gasoline Fuelled Engines – Total Hydrocarbon and Methane Emissions and Exhaust Gas Recirculation Effects", SAE Paper No. 970743, Warrendale Pennsylvania: Society of Automotive Engineers, Inc., 1997.

[10] Heywood, John B. Internal Combustion Engine Fundamentals. New York, NY: McGraw-Hill, Inc., 1988.

[11] Amann, A. C., Siegla, C. D., Diesel Particulates-What They Are and Why, Aerosol Science and Technology, Vol. 1, 1982.

[12] Dam, Thang Q., "Nanoparticle Measurement Methods in Internal Combustion Engines", M. Sc. Thesis, Department of Mechanical Engineering, The University of Tennessee – Knoxville, 2001.

[13] Patel, Palak K., "Study of NOx and Loading of a Soot Filter versus EGR for a 2.4-L Diesel Engine", M. Sc. Thesis, Department of Mechanical Engineering, The University of Tennessee – Knoxville, 2001.

[14] Subramanian, S., Kudla, R.J., Chattha, M.S., "Treatment of Natural Gas Vehicle Exhaust", SAE Paper No. 930223, Warrendale, Pennsylvania: Society of Automotive Engineers, Inc., 1993.

[15] Quiros, Edwin N., Yasuhiro Daisho, Turo Yaeo, Takahisa Koseki, Takeshi Saito, Ryoji Kihara. "Combustion and Exhaust Emissions in a Direct-Injection Diesel Engine Dual Fueled with Natural Gas", SAE Paper No. 950465, Warrendale, Pennsylvania: Society of Automotive Engineers, Inc., 2000.

[16] Lisenby, Paul M., "An Experimental Investigation of Natural Gas Catalysts Using a Bench-Flow Reactor", M. Sc. Thesis, Department of Mechanical Engineering, The University of Tennessee – Knoxville, 1995.

[17] Hayes, R.E., Kolaczkowski, S.T., Introduction to Catalytic Combustion. Amsterdam, The Netherlands: Gordon and Breach Science Publishers, 1997.

[18] Helden, R., Verbeek, R., Aken, M., Genderen, M., Patchett, J., Straten, T., Kruithof, J., and Saluneaux, C., 2002, "Engine Dynamometer and Vehicle Performance of a Urea SCR-System for Heavy-Duty Truck Engines", SAE paper 2002-01-0286.

[19] Schmieg, Steven J., Cho, Byong K., Oh, Se H., 2001, "Hydrocarbon Reactivity in a Plasma-Catalyst System: Thermal Versus Plasma-Assisted Lean NoDx Reduction", SAE paper 2001-01-3565

[20] Mital, R., S. C. Huang, B. J. Stroia, Robert C. Yu, and C. Z. Wan 2002, " A Study of Lean NOx Technology for Diesel Emission Control", SAE paper 2002-01-0956.

[21] Duggal, Vinod K., Roy Meyer, David Meyers, Syed M. Shahed. "Development of a Heavy Duty On-Highway Natural Gas-Fueled Engine". SAE Paper No. 922362, Warrendale, Pennsylvania: Society of Automotive Engineers, Inc., 2000.

[22] Clark, Nigel N., Kamel, Mostafa M., 2002, "An Emissions and Performance Comparison of the Natural Gas Cummins Westport Inc. C-Gas Plus Versus Diesel in Heavy-Duty Trucks", SAE paper 2002-01-2737.

VITA

Aaron Michael Williams was born in Dallas, Texas on October 18, 1977. After graduating high school in 1996, he began his pursuit of higher education at Austin College in Sherman, Texas. Here he met his future wife, Sunny Iris, who he dated for seven years before marrying. At Austin College, he studied physics for three years before transferring to Columbia University in New York City, where he began studying mechanical engineering. Two years later, as part of the dual degree program, he received a Bachelors of the Arts in Physics from Austin College and a Bachelors of Science in Mechanical Engineering from Columbia University. Upon completion of his undergraduate studies, Aaron moved to Knoxville and began graduate school at The University of Tennessee. For the first two years of graduate school he participated in the hybrid electric vehicle design project, FutureTruck. In his final year at UT, he conducted his research at the National Transportation Research Center. Aaron received his Masters of Science degree in Mechanical Engineering from the University of Tennessee in December 2004.